

**THE DEVELOPMENT AND STUDY OF TiO₂-
BASED BUOYANT COMPOSITE
PHOTOCATALYSTS FOR ENHANCED
PHOTOCATALYTIC DEGRADATION OF
PHENOL IN AQUEOUS SOLUTIONS**

TU WENTING

NATIONAL UNIVERSITY OF SINGAPORE

2014

**THE DEVELOPMENT AND STUDY OF TiO₂-
BASED BUOYANT COMPOSITE
PHOTOCATALYSTS FOR ENHANCED
PHOTOCATALYTIC DEGRADATION OF
PHENOL IN AQUEOUS SOLUTIONS**

TU WENTING

(B.Eng. (Hons.), NUS)

**A THESIS SUBMITTED
FOR THE DEGREE OF DOCTOR OF PHILOSOPHY**


**DEPARTMENT OF
CIVIL AND ENVIRONMENTAL ENGINEERING
NATIONAL UNIVERSITY OF SINGAPORE**

2014

DECLARATION

I hereby declare that the thesis is my original work and it has been written by me in its entirety. I have duly acknowledged all the sources of information which I have been used in the thesis.

This thesis has also not been submitted for any degree in any university previously.



Tu Wenting

Acknowledgement

First and foremost, I would express my sincere gratitude to my supervisor, Prof. Bai Renbi, for offering me a great chance of carrying out my research work in his laboratory. His kind and continuous support has encouraged me to pursue my research curiosity, and his deep insight in the research area has greatly kept me on the right track of my research work. Through his profound and conscientious discussions offered to me, I have mastered a great deal of knowledge and greatly broadened my views on research. From his valuable and meticulous guidance, I have immensely developed my effective brainstorming, planning and scheduling skills. His logic thinking, research enthusiasm and deep insight has inspired me and will be of great benefits to my life-long study.

My next gratitude goes to Dr. Lin Yi-Pin, who has offered me kind guidance in my research work. His willing to offer his academic help has greatly impressed me.

I would also like to express my appreciation to all the group members in particular Dr. Han Hui, Dr. Liu Changkun, Dr. Wee Kin Ho, Dr. Zhang Linzi, Dr. Zhu Xiaoying, Ms. Li Nan, Ms. Wang Jingjing, and who have provided me with help and suggestions in my research work. Over the past years, we have grown together and I indeed enjoyed working with them. My thanks also go out to all our lab technicians, Susan, Hwee Bee, Suki and Sidek, who had helped me a lot throughout the work. In addition, I would also appreciate the assistance and cooperation of the Final Year Project students

Finally, heartfelt thanks go to my parents and friends for their endless love, support and encouragement!

Table of Contents

DECLARATION	Error! Bookmark not defined.
Acknowledgement	I
Table of Contents	II
Summary	V
List of Tables	XI
List of Figures	XII
List of Symbols	I
Chapter 1: Introduction	1
1.1. Overview	1
1.2. Research objectives and scopes	10
1.3. Organization of thesis	12
Chapter 2: Literature Review	14
2.1. Heterogeneous photocatalysis.....	14
2.1.1. <i>Principle of heterogeneous photocatalysis</i>	14
2.1.2. <i>TiO₂ photocatalysis: mechanisms and kinetics</i>	17
2.1.3. <i>Effect of operation parameters</i>	25
2.2. Immobilized TiO ₂ for environmental photocatalytic degradation applications..	32
2.2.1. <i>Immobilization techniques</i>	33
2.2.2. <i>Types of supports</i>	37
2.2.3. <i>Polymer-supported buoyant photocatalysts</i>	43
2.3. The role of activated carbon in heterogeneous photocatalysis	46
2.4. Some remarks.....	55
Chapter 3: Removal of Phenol in Aqueous Solutions by Novel Buoyant Composite Photocatalysts and the Kinetics	57
3.1. Introduction.....	57
3.2. Experimental	59
3.2.1. <i>Reagents</i>	59

3.2.2. Preparation of buoyant composite photocatalysts.....	59
3.2.3. Characterization of buoyant composite photocatalysts.....	61
3.2.4. Phenol removal experiments with prepared composite photocatalysts.....	61
3.2.5. Phenol adsorption isotherm experiments	62
3.2.6. Phenol photocatalytic degradation kinetics	64
3.3. Results and discussions.....	67
3.3.1. Characteristics of prepared buoyant composite photocatalysts.....	67
3.3.2. Phenol removal by composite photocatalysts of different compositions	70
3.3.3. Adsorption isotherms.....	73
3.3.4. Kinetics of phenol removal in the photocatalytic degradation process.....	74
3.3.5. Effect of experimental conditions on phenol removal	79
3.4. Conclusions.....	85
Chapter 4: A Buoyant Composite Photocatalyst Prepared by a Two-Layered Configuration and Its Enhanced Performances in Phenol Removal from Aqueous Solutions.....	87
4.1. Introduction.....	87
4.2. Experimental	90
4.2.1. Preparation of buoyant composite photocatalyst in two-layered configuration	90
4.2.2. Characterization of prepared composite photocatalysts	91
4.2.3. Stability tests against photocatalytic degradation and mechanical attrition	92
4.2.4. Dark adsorption experiments	93
4.2.5. Phenol removal experiments with prepared composite photocatalysts.....	95
4.2.6. Batch tests on recyclable usage of developed composite photocatalyst.....	96
4.3. Results and discussions.....	98
4.3.1. Characteristics of prepared buoyant composite photocatalysts.....	98
4.3.2. Stability performance against mechanical attrition and photocatalytic degradation	102
4.3.3. Adsorptive property (under dark condition).....	107
4.3.4. Phenol removal performance	109
4.3.5. Recyclability	113
4.4. Conclusions.....	117
Chapter 5: Further Study in Two-Layered Buoyant Composite Photocatalyst for Phenol Removal and In-Situ Regeneration	119
5.1. Introduction.....	119

5.2. Experimental	123
5.2.1. Preparation of buoyant composite photocatalysts.....	123
5.2.2. Characterization	123
5.2.3. Phenol dark adsorption experiments	123
5.2.4. Phenol photocatalytic degradation by the buoyant composite photocatalysts and the effect of some operational parameters	123
5.2.5. In-situ regeneration	124
5.3. Results and discussions.....	127
5.3.1. Characteristics of prepared buoyant composite photocatalysts.....	127
5.3.2. Dark adsorption activity of prepared buoyant composite photocatalysts	130
5.3.3. Photocatalytic degradation of phenol by prepared buoyant composite photocatalysts.....	131
5.3.4. Photocatalytic degradation kinetics of prepared buoyant composite photocatalysts.....	132
5.3.5. Effect of composite photocatalyst dosage.....	138
5.3.6. Effect of suspended solids.....	140
5.3.7. Effect of radical scavengers.....	142
5.3.8. In-situ regeneration effect of PAC layer by the immobilized P25 of the prepared composite photocatalysts.....	145
5.4. Conclusions.....	149
Chapter 6: Conclusions and Recommendations	151
6.1. Conclusions.....	151
6.2. Suggested future studies	156
Reference	159
Publications	184

Summary

In recent years, heterogeneous photocatalytic degradation technology has increasingly gained interest in organic pollutants removal from aqueous solutions, due to the effectiveness to degrade or even completely mineralize a large range of recalcitrant organic compounds under the light irradiation. Hence, the development of efficient photocatalytic degradation water or wastewater purification systems for practical applications has attracted substantial research attention. However, there still have been various challenges to be resolved towards this target. For example, the photocatalytic degradation reactors are commonly operated in the slurry reactor form, which faces the problems such as low UV utilization efficiency and post-treatment photocatalysts recover and reuse. One of the solutions to these problems is to immobilize the photocatalyst micro- or nano-particles onto a suitable substrate support that can maintain or even improve the properties of the used photocatalysts and also make them easily be separated from the treated water after treatment. The use of those macro-supports as the substrate may however result in low photocatalytic performance, due to the limited amount of TiO_2 immobilized on the substrate. Also, the immobilized TiO_2 on larger substrates has faced some mass transfer limitations as compared to the suspended TiO_2 particles in the reactor, due to the reduced surface area and greater transport distance of organic pollutants to be degraded. The detachment of immobilized TiO_2 particles from the substrate may also be a concern for long periods of practical usage.

In this study, a novel buoyant composite photocatalyst, including TiO_2 nanoparticles as the photocatalyst component, powdered activated carbon as the co-adsorbent and polypropylene granules as the immobilization substrate, were

developed to overcome all or some of the above mentioned existing problems. The property and performance of the prepared buoyant composite photocatalysts was examined especially for the removal of phenol from aqueous solutions under various experimental conditions. On a broad prospect, the work included the development of a suitable immobilization system and strategy to immobilize the selected photocatalyst and adsorbent components onto the polypropylene substrate to obtain the desired buoyant composite photocatalyst. Then, the stability and performance of the developed composite photocatalyst was improved. The adsorptivity and photocatalytic degradation activity of the developed materials were investigated in terms of phenol removal from aqueous solutions. Other process parameters, including the effect of turbidity and radical scavengers, were also examined to get a deeper insight of the working mechanism of the composite material and synergistic effect of combining the two different particles onto the same substrate, as well as the recyclability and regeneration performance the composite material. The study may be more specifically described below.

In the first part, novel buoyant composite photocatalysts were prepared by thermally immobilizing titanium dioxide (TiO_2) nanoparticles and powdered activated carbon (PAC) together onto polypropylene granules (PPGs) under properly controlled temperature. All of the prepared composite photocatalysts granules were in millimeter size and truly floating on water surface. The experimental results showed that the developed composite photocatalysts can have high adsorption capacity and good photoactivity for the removal of phenol in aqueous solutions. It was found that the adsorption capacity generally increased with the increase of the PAC content and the photocatalytic degradation performance can be satisfactorily described by a first-order rate law. It was found that the combination of adsorption and photocatalysis

components showed a number of unique advantages over the individual components and especially displayed some distinctive synergistic effect in the removal of phenol. The photocatalytic activity of PAC/TiO₂ mixed composite photocatalysts achieved more than twice of the buoyant photocatalysts with TiO₂ only. The PAC component appeared to help concentrating phenol from aqueous solutions to the vicinity around the TiO₂ nanoparticles, which made the photocatalytic degradation process of phenol more efficient and being less dependent on the phenol concentration in the bulk solutions. The results also showed that different TiO₂/PAC mass ratios induced different extents of the synergistic effect, as reflected by the apparent first-order rate constant values, and a TiO₂/PAC mass ratio of 1:1 achieved better phenol removal performance than other ratios under the experimental conditions tested. In addition, the presence of PAC in the developed composite photocatalyst was found to largely shield the inhibition effect of chloride ions in the solutions on phenol removal.

In the second part, the objective was to improve the physical and photocatalytic degradation stability of the developed buoyant composite photocatalyst. Instead of immobilizing TiO₂ and PAC in a powder mixture together in previous work, a two-layered configuration of immobilizing PAC and TiO₂ respectively on PPGs was developed. Firstly, a thermal bonding method was used to anchor PAC tightly onto the mildly melting surface of PPG substrate. Then, a suspension hydrothermal deposition method was used to load TiO₂ nanoparticles onto the immobilized PAC on PPG substrate. The PAC layer was to act as a barrier layer between the substrate surface and the TiO₂ layer to increase the photocatalytic degradation stability of the prepared composite photocatalyst, as well as to provide it with adsorptive property to enhance its photocatalytic efficiency. The prepared composite photocatalyst was buoyant and can be easily dispersed in solutions with stirring (mechanical, hydraulic

or gaseous bubbling). Experiments demonstrated that the obtained composite photocatalyst was stable against mechanical attrition and photocatalytic degradation, as compared to that prepared by directly immobilizing PAC and TiO_2 together in a mixture on PPG in the previous study. The developed buoyant composite photocatalysts was also found to achieve both good adsorptivity and photocatalytic degradation activity in the removal of phenol and the photocatalytic degradation performance can be satisfactorily described by the Langmuir-Hinshelwood kinetic model. Besides acting as an effective barrier layer, the immobilized PAC intermediate layer also helped concentrating phenol from the aqueous solution to the vicinity of the TiO_2 photocatalyst and thus enhanced the photocatalytic degradation process of phenol. In a batch feed process, the buoyant composite photocatalyst was tested for 20 recycles for its reusability and the results showed that the overall performance in photocatalytic degradation of phenol only decreased at less than 7%, indicating that the prepared buoyant composite photocatalyst has a great prospect for actual applications in the removal of organic pollutants from water or wastewater treatment.

In the final part of this study, the focus was to gain a deeper understanding in how the adsorptive layer prepared in part II enhanced the photocatalytic performance of the composite material. Composite photocatalysts with different ratios of PAC and TiO_2 compositions were prepared by applying a different number of solution depositions of TiO_2 in a soak-dry-cure cycle. All the prepared composite photocatalysts were buoyant and their performances were evaluated from their efficiencies in the removal of phenol in aqueous solutions. The experimental results showed that the photocatalytic degradation performance of the prepared composite photocatalysts had a dependency on the relative ratio of TiO_2 to PAC and the one with the best synergistic effect of adsorption and photocatalytic degradation appeared to be

achieved by that had 2 soak-dry-cure cycles for TiO₂ deposition. It was found that a single coating cycle was not enough to produce good surface coverage of the composite material by TiO₂, whereas excess coating cycles led to over-deposition of TiO₂, which caused more blockage of the immobilized PAC layer and thus significantly decreased the adsorption function of the prepared composite photocatalysts. In addition, the dosage of the composite photocatalysts for a laboratory photocatalytic reactor setup was studied. The in-situ regeneration capability for the PAC layer (its adsorptive capacity) by the TiO₂ layer on the composite photocatalysts was evaluated through the repeated adsorption-light irradiation cycles. It was found that the adsorptive capacity of the PAC layer can be recovered by the photocatalytic degradation function of the composite photocatalysts, but extended irradiation hours may be required for better regeneration performance of the PAC layer, suggesting that there is a need for the proper match of the adsorption and regeneration capability for the composite photocatalyst to achieve sustained long-term performance.

In conclusion, novel buoyant composite photocatalysts with polymeric substrate were successfully developed for the removal of organic pollutants from aqueous solution. The mechanical and photocatalytic degradation stability of the developed composite photocatalysts can be achieved through, for example, the two-layered configuration immobilization method. It was found that the composite material with both adsorption and photocatalysis components showed a number of unique advantages over the individual components and especially displayed some distinctive synergistic effect in the removal of phenol. The study also showed that the proper combination of the adsorbent and photocatalyst components in the composite photocatalyst (both ratio and configuration) was important and had a large impact

on the property and performance of the prepared composite photocatalyst. The developed buoyant composite photocatalyst was demonstrated to effectively remove phenol from aqueous solutions and be less sensitive to process conditions such as turbidity and radical scavenger. Results from the test of repeated uses of up to 20 recycles in a batch reactor showed that the material can be in-situ regenerated and displayed little or only a slight decrease in the overall phenol removal performance, indicating that the developed material has a great potential for practical or long-term applications in water or wastewater treatment.

List of Tables

Table 2-1: The general mechanism of the photocatalytic reaction process on irradiated TiO ₂	18
Table 2-2: Hydroxyl radical attacks of organic compounds in photocatalytic degradation process.....	20
Table 3-1: Actual photocatalysts composition by TGA analysis.....	68
Table 3-2: Adsorption isotherm parameters of phenol on different composite photocatalyst at 25°C	74
Table 3-3: Pseudo-first-order rate constants of phenol photocatalytic degradation by different composite photocatalysts and effect of chloride ions	78
Table 3-4: Effect of pH on the adsorptivity and photocatalytic activity of 50%P25-PPG	81
Table 3-5: Effect of dosage on the adsorptivity and photocatalytic activity of 50%P25-PPG	83
Table 3-6: Effect of initial phenol concentration on the adsorptivity and photocatalytic activity of 50%P25-PPG	83
Table 4-1: Actual compositions of the substrate and the prepared composite materials obtained from the TGA analysis	99
Table 5-1: Actual compositions of the PPG substrate, the intermediate, and the four different composite photocatalysts obtained from the TGA analysis	128
Table 5-2: Effect of initial phenol concentration on different composite photocatalysts	134

List of Figures

Figure 2-1: Simplified schematic diagram of heterogeneous photocatalytic process..	15
Figure 3-1: Schematic diagram of experimental setup for the preparation of composite photocatalysts: (1) 1 L round bottom glass reactor; (2) overhead mechanical mixer; (3) PTFE stirrer shaft; (4) hotplate; (5) 1 L round bottom heating block; and (6) thermal couple.....	60
Figure 3-2: Schematic diagram of the experimental setup for photocatalytic degradation study: (1) feed reservoir (2 L solution); (2) sampling point; (3) overhead mixer; (4) peristaltic pumps; (5) 150 W Xenon lamp; (6) customized jacketed glass reactor (400 mL solution); (7) circulation water to external circulator; (8) circulation water from external circulator; (9) air supply to air diffuser and (10) buoyant composite photocatalysts	65
Figure 3-3: TGA analysis results for base PPG granules and for the prepared composite photocatalysts	67
Figure 3-4: Photographs of the base PPG granules and the prepared composite photocatalysts.....	69
Figure 3-5: A typical FESEM image for 50%P25-PPG, showing PAC and P25 particles on the surface of prepared composite photocatalyst	70
Figure 3-6: Phenol removal by the prepared composite photocatalysts of different compositions: (a) adsorptive removal in dark, and (b) combined adsorptive and photocatalytic degradation removal	71
Figure 3-7: Adsorption isotherm data for phenol by the composite photocatalysts and the fitting results of the Langmuir and Freundlich isotherm models to the experimental data	74
Figure 3-8: Removal of phenol in the two-stage processes with different types of composite photocatalysts	76
Figure 3-9: Kinetic study of phenol removal in the photocatalytic degradation stage by different composite photocatalysts and the fitting of kinetic model to the experimental data under different chloride ion concentrations: (a) 25%P25-PPG, (b) 50%P25-PPG, (c) 75%P25-PPG and (d) 100%P25-PPG	77
Figure 4-1: Results from TGA analysis for the PPG substrate and the prepared various composite photocatalysts or intermediate	100
Figure 4-2: FESEM images for (a) PPG-PAC, (b) 25%P25-PPG, (c) PPG-PAC-P25 (x10000), (d) closer look of PPG-PAC-P25 (x50000) and (d) IPA hydrothermally treated P25	101
Figure 4-3: Effect of mechanical attrition and photocatalytic degradation on the prepared composite photocatalysts: (a) change of total dry weight and (b) change of	

solution turbidity (Data shown by filled marks are for mechanical attrition and those by unfilled marks are for photocatalytic degradation).....	102
Figure 4-4: The changes of solution TOC for different composite photocatalysts during photocatalytic degradation process (the insert shows the enlarged graph in the initial stage).....	104
Figure 4-5: Photos of the PPG substrate, the prepared intermediate and composite photocatalysts before and after 120 hours of photocatalytic degradation test under UV light irradiation.....	107
Figure 4-6: Adsorptive property of various composite materials (under dark condition).....	109
Figure 4-7: Phenol removal by the three types of composite photocatalysts due to both adsorptive and photocatalytic degradation effects ($C_0 = 20 \text{ mg.L}^{-1}$).....	109
Figure 4-8: Kinetic study of phenol removal by photocatalytic degradation by the three types of composite photocatalysts (25%P25-PPG, 100%P25-PPG, and PPG-PAC-P25) and the linear fitting of the data with the pseudo-first order reaction rate model, eq.(2-24).....	112
Figure 4-9: Recyclability of (a) PPG-PAC-P25 and (b) 25%P25-PPG composite photocatalysts, in terms of total phenol and TOC removal percentages.....	115
Figure 5-1: Results from TGA analysis for the PPG substrate, the intermediate, and the four different composite photocatalysts.....	127
Figure 5-2: Photographs of the PPG-PAC and the prepared composite photocatalysts, (a) as freshly prepared and (b) thoroughly washed after preparation, on 5 mm × 5 mm square paper.....	128
Figure 5-3: Dark adsorptive uptakes of phenol by different composite photocatalysts, initial phenol concentration, $C_{in} = 20 \text{ mg.L}^{-1}$	130
Figure 5-4: Photocatalytic degradation of phenol by different composite photocatalysts, initial phenol concentration, $C_{in} = 20 \text{ mg.L}^{-1}$	132
Figure 5-5: Kinetics of phenol photodegradation by different composite photocatalysts and the pseudo-first-order kinetic model fitting for different initial phenol concentrations: (a) $C_{in} = 10 \text{ mg.L}^{-1}$, (b) $C_{in} = 20 \text{ mg.L}^{-1}$, (c) $C_{in} = 50 \text{ mg.L}^{-1}$, (d) $C_{in} = 80 \text{ mg.L}^{-1}$, and (e) $C_{in} = 100 \text{ mg.L}^{-1}$	136
Figure 5-6: Relationship between $1/k_{app}$ and C_0 for different composite photocatalysts.....	137
Figure 5-7: The rate constant of phenol photocatalytic degradation and the adsorption equilibrium constant as a function of coating cycles.....	138
Figure 5-8: The apparent rate constants and amount of phenol adsorbed as a function of PPG-PAC-P25(2) composite photocatalysts dosage.....	139

Figure 5-9: Effect of suspended solids on the photocatalytic degradation performance of PPG-PAC-P25(2) as compared that of P25	140
Figure 5-10: Effect of radical scavengers, a) isopropyl alcohol, IPA and (b) potassium iodine, KI, on the photocatalytic degradation performances of PPG-PAC-P25(2) and 100%P25-PPG	144
Figure 5-11: Effect of irradiation duration on in-situ regeneration efficiencies, (a) phenol adsorption capacity recovered, (b) phenol in solution disappearance kinetics, (c) percentage of total amount of phenol removed from solution and (d) percentage of TOC removal from the solution	147

List of Symbols

AC	activated carbon;
AOPs	advanced oxidation processes;
C_{in}	initial concentration of the reactant (<i>ppm</i>);
C_0	reactant concentration at irradiation time $t=0$ (<i>ppm</i>);
C_t	reactant concentration at irradiation time t (<i>ppm</i>);
CB	conduction band;
CNT	carbon nanotube;
CVD	chemical vapor deposition ;
C60	fullerenes;
E_{bg}	band-gap energy;
FESEM	field emission scanning electron microscopy;
GAC	granular activated carbon;
GC	gas chromatography;
GO	graphene oxide;
$h\nu$	light energy;
h^+	positive hole
IUPAC	International Union of Pure and Applied Chemistry;
k_{app}	apparent rate constant (hr^{-1}), $k_{app}=k_rK$;
k_r	true rate constant;
K	adsorption equilibrium constant of the Langmuir model;
K_C	adsorption equilibrium constant for the primary substance to be photocatalytically degraded
K_i	adsorption equilibrium constant for the various degradation intermediate products
k_2	second-order surface rate constant;
LDPE	low density polyethylene;
LH	Langmuir-Hinshelwood;
MO	methyl orange;
OH•	hydroxyl radical;
OOH•	hydroperoxyl radical;
$O_2^-•$	superoxide radical;

PAC	powdered activated carbon;
PPG-PAC	powdered activated carbon coated polypropylene granules;
PPG-PAC-P25(x)	two-layered configuration composite photocatalysts with x round of soak-dry-cure P25 coating cycles
PANI	polyaniline;
PC	polycarbonate;
PE	polyethylene;
PET	polyethylene terephthalate;
PMMA	poly(methyl methacrylate);
PMTP	previously made titania powder;
PP	polypropylene;
PPGs	polypropylene granules;
PS	polystyrene;
PVC	polyvinyl chloride;
P_{zc}	point of zero charge;
P25	Degussa P25 TiO ₂ nanoparticles;
SGP	sol-gel process
r	rate of reaction
t	the reaction time (<i>hr</i>);
T	irradiation duration (<i>hrs</i>);
TGA	thermogravimetric analyzer;
TOC	total organic carbon;
UV	ultraviolet light
UVA	ultraviolet light in the range of 320 ~ 400 nm;
UVB	ultraviolet light in the range of 280 ~ 320 nm;
UVC	ultraviolet light in the range of 200 ~ 280 nm;
VB	valance band;
λ	light wavelength;
vis	visible light;
VUV	vacuum ultraviolet;
θ	fraction of surface covered by the reactant;
θ_{OH}	fractional surface coverage by hydroxyl radicals ($\bullet OH$);
25%P25-PPG	buoyant composite photocatalysts made from direct thermal

	immobilization method with 25% P25 and 75% PAC in the powder mixture
50%P25-PPG	buoyant composite photocatalysts made from direct thermal immobilization method with 50% P25 and 50% PAC in the powder mixture
75%P25-PPG	buoyant composite photocatalysts made from direct thermal immobilization method with 75% P25 and 25% PAC in the powder mixture
100%P25-PPG	buoyant composite photocatalysts made from direct thermal immobilization method with 100% P25 in the powder mixture

Chapter 1: Introduction

1.1. Overview

The reuse and recycling of wastewater effluent has been recognized as a strategic approach towards sustainable water management around the world to meet the growing water demand in a water-scare environment (Ahmed et al., 2010a; Ahmed et al., 2011; Busca et al., 2008; Zhang et al., 2009). Due to the rapid urban and industrial development worldwide, increasing amounts of chemicals are being used and subsequently released to the natural environment, particularly through wastewater effluent discharge. Many of those chemicals are harmful to both the environment and the human beings. Due to the complex and toxic nature of many of these emerging pollutants, they have been found not being efficiently removed in conventional wastewater treatment processes, remained in the secondary effluents and finally discharged into the receiving water body in the environment (Ahmed et al., 2010a). The presence of toxic organic compounds in storm water and wastewater effluent has been reported to be one of the major impediment to the widespread acceptance for water recycling (Ahmed et al., 2010b). Furthermore, the variety, toxicity and persistence of these chemical can directly impact the health of the eco-systems and present a threat to humans through the contamination of drinking water resources, e.g., surface and ground water (Pirkanniemi and Sillanpää, 2002). As a result, a challenge facing us is how to achieve efficient and cost effective removal of those recalcitrant pollutants from wastewater effluent to minimize their risk of pollution as well as enable wastewater reuse. Towards this direction, scientists and engineers have devoted considerable efforts in developing various new or improved purification methods that can effectively remove or, more preferably, destroy these recalcitrant

organic contaminants. Ideally, the treatment process is able to accomplish complete mineralization of all the toxic organic species without producing any harmful intermediates or by-products, and possibly being cost-effective (Chen et al., 2000b). However, many of the conventional or currently available treatment technologies for wastewater cannot meet the above requirement. Advanced wastewater treatment systems, such as adsorption, filtration, gas stripping, ion exchange, etc., may be used together with the conventional ones, for the further removal of those undesired residual constituents from the waste stream. However, such practice often not only increases system complexity but also provides only an intermediate solution to the problem because these phase separation techniques only transfer contaminants from one phase to another and the removed pollutants do not really disappear ultimately. Even though incineration may be used as a technique to destroy those separated organic pollutants completely, incineration system is expensive to construct and operate and it also can lead to the release of other toxic species into the air, such as dioxin and furan (Benestad et al., 1990). As an alternative, chemical oxidation, such as catalytic wet air oxidation, chlorination and ozonation, has been widely studied for water or wastewater treatment applications. Although chemical oxidation is effective in degrading many organic pollutants, some short chain organic acids have been found to be resistant to the chemical oxidants (Luck, 1999). Beside the process is expensive in operation, the oxidative chemicals may also react with residual pollutants and form even more toxic by-products (Tang et al., 2012).

In more recent years, Advanced Oxidation Processes (AOPs) have attracted the interest as the emerging and promising technology for both effective mineralization of recalcitrant organic pollutants and enhancement of biological treatment effluent, especially in dealing with highly toxic and low biodegradable wastewater (Mijangos

et al., 2006). AOPs usually use a strong oxidant or catalyst with a light source, including those processes of $\text{H}_2\text{O}_2/\text{UV}$, O_3/UV , $\text{H}_2\text{O}_2/\text{O}_3/\text{UV}$ TiO_2/UV and vacuum ultraviolet (VUV), etc. AOPs rely on the in-situ generation of oxygen-based radicals, such as $\text{OH}\cdot$, $\text{OOH}\cdot$, and $\text{O}_2^-\cdot$, and have proven performance in the complete transformation of various organic carbons into CO_2 and H_2O . The reactive radicals are extremely unstable and reactive. They are non-selective oxidizing agents that can virtually destroy almost any organic contaminants present in water. AOPs can therefore destroy pollutants that are not amenable to biological treatments and are characterized by high chemical stability and difficulty for complete mineralization (Esplugas et al., 2002; Gimeno et al., 2005). In spite of the good oxidation capacity to refractory organic pollutants, most AOPs have high chemical consumption and relatively high treatment costs, which constitutes the major barriers for their large scale practical applications (Martinez-Huitle and Ferro, 2006).

Among the various AOPs, heterogeneous photocatalysis that employs semiconductor photocatalysts has gained increasing attention, attributed to its effectiveness in degrading and mineralizing the recalcitrant organic compounds at potentially low cost, with the possibility of utilizing the solar ultraviolet (UV) and visible-lights (vis) as the energy source, and without the necessity of adding additional chemicals. Heterogeneous photocatalysis can be described as the acceleration of photoreaction in the presence of a catalyst. It differs from the other AOPs as it employs a reusable photocatalyst, has no need for additional oxidants and produces no extra sludge residue (Chen et al., 2000b; Vimonses et al., 2010). The history of research in heterogeneous photocatalysis may be traced back to many decades ago when Fujishima and Honda (1972) reported the discovery of photochemical splitting of water into hydrogen and oxygen on titanium dioxide

(TiO₂) electrode under ultraviolet (UV) light irradiation. Since then, photocatalysis has been extensively studied for applications in various areas, especially in the fields of energy and environment (Tanveer and Tezcanli Guyer, 2013). Several features, such as ambient operating conditions, complete destruction of parents and their intermediate compounds, and relatively low operating cost, have promoted the application of heterogeneous photocatalysis to water or wastewater treatment. It has been found that even carbon tetrachloride which was usually considered as being hydroxyl radical resistant could be mineralized by heterogeneous photocatalysis (Hsiao et al., 1983). Among the various semiconductor photocatalysts being investigated, TiO₂ has received the greatest interest (Chen et al., 2000b). TiO₂ is one of the most active semiconductor photocatalysts with activation photon energy in the lower energy UVA wavelength range ($300 \text{ nm} < \lambda < 390 \text{ nm}$) and remains stable after repeated usages in photocatalytic cycles. Because of the low energy band, the process using TiO₂ can be driven by solar UV or possibly even by visible light after some modification of TiO₂. At near the earth's surface, the sun produces about 0.2–0.3 mol photons.m⁻².h⁻¹ in the wavelength range of 300–400 nm, with a typical UV flux of 20–30 W.m⁻², suggesting that sunlight can be an economically and ecologically sensible light source for photocatalysis (Bahnemann, 2004; Goslich et al., 1997; Ljubas, 2005). Besides, the multi-faceted functional properties of TiO₂, such as its chemical and thermal stability or resistance to chemical breakdown and its strong mechanical properties, have promoted its applications in photocatalytic water and wastewater treatment. The first clear recognition and implementation of TiO₂ sensitized photocatalysis as a method of water decontamination may be the work conducted by Bard (1980), and by Pruden and Ollis (1983), in the photo-mineralization of halogenated hydrocarbon contaminants in water, including trichloroethylene,

dichloromethane, chloroform, and carbon tetrachloride. Since then, TiO₂ photocatalysis has been proven to be a process of great potential to eliminate various hazardous pollutants present in air and water (Nakata and Fujishima, 2012), including inorganic compounds (Litter, 1999) such as chromium (VI) (Aarthi and Madras, 2008), lead, arsenic (Fostier et al., 2008) and mercury (Zhang et al., 2004), as well as organic compounds (Ameta et al., 2013) such as surfactants (Lin et al., 2002), pesticides and herbicides (Byrappa et al., 2000; Marin et al., 2011), phenolic compounds (Ahmed et al., 2011), humic substances (Al-Rasheed and Cardin, 2003a, 2003b), organic dyes (Rajeshwar et al., 2008), etc. Meanwhile, TiO₂ based photocatalytic technologies have also been successfully demonstrated in several real wastewater case studies, both for municipal wastewater (Araña et al., 2002; Borges et al., 2013) and industrial waste streams from industries such as textile (Bandala et al., 2008; Garcia et al., 2009), sanitary (Gibbs, 2001), and petroleum refinery (Berry and Mueller, 1994; Diya'uddeen et al., 2011; Malik, 2005; Nair et al., 1993).

Unfortunately, the widespread application and commercialization of the technology in water and wastewater treatment has been hindered by a number of disadvantages, including the costly post separation need for removal and recycling of the TiO₂ nanoparticles used from the treated effluent and the low UV light utilization efficiency due to the high rate of electron/hole pair recombination nature of TiO₂ (Lim et al., 2011; Ochiai and Fujishima, 2012; Shan et al., 2010). TiO₂ photocatalysts are traditionally produced in the form of fine particles, and applied directly into the solution to be treated, forming a slurry system. Especially, with the development of nano-technology, TiO₂ photocatalysts are produced in nanoparticle sizes to provide much higher reaction surface area and hence greatly enhance the photocatalytic activity towards the decontamination of pollutants. However, this has presented a

post-separation problem of the used TiO₂ nanoparticles. Even though the nano-sized TiO₂ is efficient in photocatalytic reaction, the high cost to separate those nanoparticles from the treated effluents has limited the application prospect in engineering practice. To solve this problem, TiO₂ nanoparticles have been immobilized onto various other larger solid substrates, such as ceramics (Teekateerawej et al., 2006), glass microspheres (Balasubramanian et al., 2003; Koopman, 2007), stainless steel plates (Balasubramanian et al., 2003; Chen and Dionysiou, 2006), plastics (Cho and Choi, 2001; Han and Bai, 2009, 2010; Magalhães and Lago, 2009), etc. Among the various supported TiO₂ photocatalytic processes, buoyant composite photocatalysts can be used as a solution to achieve high light utilization efficiency as well as low post separation cost (Han and Bai, 2009). The floating photocatalysts were prepared by immobilizing TiO₂ particles onto substrates of lower density than water, such as hollow glass microsphere (Koopman, 2007; Portjanskaja et al., 2004; Rosenberg et al., 1992), polyethylene sheets (Naskar et al., 1998), polystyrene foam beads (Fabiya and Skelton, 2000; Magalhães and Lago, 2009), polypropylene granules (Han and Bai, 2009), and polypropylene fabrics (Han and Bai, 2010, 2011). Buoyant photocatalysts can float naturally on water surface and thus achieve greater light utilization efficiency because photocatalytic degradation process takes place at the water/air interface and light attenuation is lower in air than that in water (Fabiya and Skelton, 2000; Han and Bai, 2009). Also, enhanced oxygenation of the photocatalysts can be achieved at the water/air interface due to the higher oxygen content than that in water. Meanwhile, buoyant photocatalysts can be easily separated from the water body, eliminating the post treatment problem commonly encountered. However, a major problem associated with the practice of immobilizing TiO₂ on larger substrates is often the lower efficiency than that in the

slurry type reactors, due to the reduced amount of photocatalyst surface area to light for reaction, increased mass-transfer limitation in the process, and the lack of long-term durability of the coated layer of TiO₂ (Choi, 2006).

One of the possible ways to increase the photocatalytic degradation process efficiency was to introduce an inert co-adsorbent, such as silica (Choi, 2006; Kim et al., 2005), alumina (Ding et al., 2001; Lei et al., 1999), zeolites (Xu and Langford, 1995), clays (Balasubramanian et al., 2004), or activated carbon (Foo and Hameed, 2010; Leary and Westwood, 2011; Lim et al., 2011) into the photocatalysis system, either by physical mixing the adsorbent and the photocatalyst together or supporting the photocatalyst onto the adsorbent (Hoffmann et al., 1995). Generally, the removal of organic compounds from aqueous solution may involve at least two major steps: the mass transfer of organic compounds from the bulk solution to the vicinity or surface of the photocatalyst particles, followed by the subsequent photocatalytic degradation of the transferred compounds. The overall performance is therefore dependent on both the mass transfer efficiency and the photocatalytic degradation kinetics. Hence, it is logical to expect that the rate of degradation of the organic pollutants will be a function of the adsorbed content from the solution, and the co-adsorbent can provide more substances to be degraded to the photocatalyst component. Furthermore, organic pollutants in water or wastewater may occur in relatively low concentrations (ppm level or below) and pre-concentration of the pollutants onto the surface where photons are adsorbed is desirable for effective photocatalytic degradation. The co-adsorbent component can usually provide more effective adsorption of the pollutants than the TiO₂ photocatalyst itself (Anderson and Bard, 1995; Takeda et al., 1995), and hence effectively concentrate the free organic molecules in the bulk solution towards the active sites of the photocatalysts and thus

incur better degradation performances (Yoneyama and Torimoto, 2000). For example, TiO₂ and AC combinations were studied for the degradation of a wide spectrum of persistent organic pollutants, including humics (Xue et al., 2011), phenolic compounds (Carpio et al., 2005; Matos et al., 2001; Tryba et al., 2003), pesticides (Kim et al., 2008), chlorinated compounds and dyes (Xue et al., 2011). Matos and co-workers demonstrated the use of different activated carbon and titania combinations for the photocatalytic degradation of aqueous organic pollutants, and showed that the addition of activated carbon to titania slurry under UV irradiation induced a beneficial effect on the photocatalytic degradation efficiency, in terms of the kinetics of pollutant disappearance (Matos et al., 1999; Matos et al., 1998; Matos et al., 2001). Therefore, it may be desirable to develop novel photocatalysts supported on some high surface area substrate with appropriate physical properties, (such as easily recovered, high light utilization efficient, and mechanically strong enough to sustain long-term usages, etc.), and adsorptive property for enhanced photocatalytic degradation efficiency.

Moreover, a number of studies have demonstrated that solution components, such as calcium, magnesium, iron, zinc, copper, bicarbonate, phosphate, nitrate, sulphate, chloride, and dissolved organic matters, etc., can affect the photocatalytic degradation rate of organic pollutants in the solution since these components can be adsorbed onto the surface of photocatalyst, for instance, TiO₂ (Ahmed et al., 2010a; Ahmed et al., 2011; Ahmed et al., 2010b). The inhabitation effect of metal ions may be attributed to the suppression of the production of hydroxyl radicals, due to the trapping of the conduction band electrons by the adsorbed metal ions (Aarthi and Madras, 2006). The inhabitation effect of anions, on the other side, can be attributed to the reaction of the positive holes on and hydroxyl radicals from the photocatalyst

with the anions that behave as the radical scavengers, resulting in slow organic degradation (Parent et al., 1996; Wu et al., 2009; Wu et al., 2010). A major drawback from the high reactivity and non-selectivity of the radicals is that they also react with non-targeted compounds present in the background water matrix. This results in a higher radical demand to accomplish the desired degree of organic pollutant degradation (Ahmed et al., 2011). However, the avoidance of those inorganic salts in the solution is difficult if not impossible, especially when heterogeneous photocatalyst technology is used to treat industrial wastewater. In spite of this, some adsorbents, such as activated carbon, can effectively absorb organic pollutants in water, and its adsorption performance is not greatly affected by the presence of inorganic salts in the solution (Vaccaro, 1971) . Hence, it may be hypothesized that the approach of combination of photocatalyst and adsorbent could also help reduce the inhibition effect of inorganic ions in the solution on the photocatalytic degradation of the organic pollutants. This may be achieved in several ways. Firstly, the effective adsorbent can concentrate and thus increase the amount of organic pollutants around the photocatalysts, hence increasing the competitiveness of organic pollutants to be degraded over the inorganic ions for photoactive sites. Secondly, the higher organic content around the photocatalysts may lead to higher chance of reacting with the positive holes and radicals formed, which reduces the possibility of radicals quenching by the inorganic anions. However, to the extent of our knowledge, the shielding effect of inorganic ions by the photocatalyst-adsorbent combination system has not been well explored. Hence, an effort will also be made to fill this gap in this study.

1.2. Research objectives and scopes

Based on the previous overview, it is clear that the TiO₂-based heterogeneous photocatalysis has a great potential in the decontamination of organic pollutants for water and wastewater treatment applications. However, there are also challenges or difficulties to be solved in the development of economically feasible and efficient photocatalysis processes for practical engineering adoption. Therefore, the overall objective of this research project is to develop a desired composite photocatalyst with both the adsorption and photocatalytic degradation components on a relatively cheap substrate that incurs the composite with buoyant property. This is to be achieved by immobilizing TiO₂ photocatalyst nanoparticles and powdered activated carbon (PAC) microparticles onto polypropylene granules (PPG). Appropriate immobilization conditions for TiO₂ and PAC at different ratios on PPG, degradation kinetic of phenol and the effect of some process operation parameters will be studied in details. The research will try to fill some of the knowledge gap on the synergistic effect of combining and immobilizing adsorbent and photocatalyst components together on the same substrate. Phenol was selected as the target pollutant in this study because phenol and its derivatives are one of the commonly encountered organic pollutants in many types of the industrial effluents that have caused severe environmental problems, and also phenol degradation is one of the research focus areas in our research group. The specific scopes of the study are listed below:

(a) To develop a novel buoyant composite photocatalyst that has both adsorption and photocatalytic degradation functions, and can be used on water surface and easily separated from treated water. This will be done by immobilizing P25 TiO₂ nanoparticles and PAC microparticles on PPG substrate.

(b) To evaluate the adsorptivity and photocatalytic degradation activity of the prepared buoyant composite photocatalyst and the synergistic effect of the adsorbent and photocatalyst components on the prepared composite materials. To understand and study the impact of some operational factors that may affect the performance of prepared buoyant composite photocatalysts, including the effect of P25: PAC ratio, dosage, solution pH, inorganic salts, solution turbidity, etc.

(c) To investigate the role of the added PAC in the prepared buoyant composite photocatalyst and examine its performance improvement, including mechanical stability, photocatalytic degradation stability, synergistic effect, and inhibitory effect towards the presence of inorganic ions and radical scavengers.

(d) To assess the performance in phenol removal and the recyclability and in-situ regeneration capability of the prepared buoyant composite photocatalyst for its potential long-term usage.

1.3. Organization of thesis

Chapter 1 gives a brief overview of the area of research interest for this project, including the background, progress and challenges, and defines the specific research objectives and the scopes of the research project.

Chapter 2 provides a more detailed and comprehensive review on the related subjects, including the principle of heterogeneous photocatalysis, the effect of operation parameters, the kinetics and mechanisms of TiO₂ photocatalysis, the various supporting substrates and immobilization techniques, and the role of co-adsorbent with photocatalyst in the photocatalytic performance. The review is trying to outline the current state of the arts in the relevant area of interest to this study, as well as the challenges or gaps that are faced.

Chapter 3 presents the development of buoyant composite photocatalysts with Degussa P25 TiO₂ nanoparticle as photocatalyst component (P25) and activated carbon fine powder particles (PAC) as adsorbent component on polypropylene granules (PPGs), via a thermal bonding process. The performances of the obtained composite photocatalysts were evaluated according to their phenol removal efficiencies and degradation kinetics. The synergistic effect between the adsorbent component and photocatalyst component in the composite photocatalysts on the degradation kinetics, as well as the effects of experimental conditions, including the saline concentration on phenol removal, is also discussed.

In chapter 4, an improved method of preparing buoyant composite photocatalysts with enhanced mechanical and photocatalytic degradation stabilities is presented. The new development involved in a two-layered configuration for the immobilization of PAC and P25 on the PPG substrate. Firstly, the thermal bonding method was used to

anchor PAC tightly onto the mildly melting surface of PPG substrate. Then, a suspension hydrothermal deposition method was used to load P25 nanoparticles onto the immobilized PAC on the PPG substrate. The PAC layer was to act as a barrier layer between the substrate surface and the P25 layer to increase the photocatalytic degradation stability of the prepared composite photocatalysts, and at the same time, to provide the composite photocatalyst with adsorptive property to enhance its catalytic efficiency. Experiments were carried out to examine how the two-layered configuration approach enhanced the structural and photocatalytic stabilities and improved the photocatalytic degradation performance of the developed buoyant composite photocatalysts. The prepared buoyant composite photocatalyst was also tested in a batch feed process for 20 repeated cycles to exam its recyclability.

In chapter 5, the performance of the prepared buoyant composite photocatalyst from the two-layered configuration approach was examined in more details. Buoyant composite photocatalysts of different compositions (i.e., P25 and PAC ratios) were prepared by varying the loading and curing cycles of P25 up to 6 times, and the obtained composite photocatalysts were examined for their phenol degradation performances, in terms of the modified Langmuir-Hinshelwood kinetic model study. The effect of in-situ regeneration of the PAC layer by the immobilized TiO_2 on the composite photocatalyst was also further examined with repeated batch feed processes at different irradiation durations.

Chapter 6 finally concludes the research project with its findings and makes some recommendations for possible future study and improvement.

Chapter 2: Literature Review

2.1. Heterogeneous photocatalysis

Heterogeneous photocatalysis, according to the definition by International Union of Pure and Applied Chemistry (IUPAC), refers to “*the change in the rate of a chemical reaction or its initiation under the action of ultraviolet, visible, or infrared radiation in the presence of a substance, the photocatalyst, that absorbs light and is involved in the chemical transformation of the reaction partners*” (Braslavsky et al., 2011). The initial interest in the heterogeneous photocatalysis may be traced back to 1972 when Fujishima and Honda discovered the photocatalytic splitting of water on TiO₂ electrodes (Fujishima and Honda, 1972). Since then, extensive research on semiconductor photocatalysis has been carried out for the removal of various organic and inorganic pollutants from air or water medium.

2.1.1. Principle of heterogeneous photocatalysis

The term “photocatalysis” refers to the combination of photochemistry and catalysis which indicates that light and catalyst are necessary to bring about or accelerate a chemical transformation (Chen et al., 2000b). The catalysts used are usually semiconductors that can act as catalysts due to their specific electronic structure characterized by a filled valence band and an empty conduction band (Fox and Dulay, 1993). A heterogeneous photocatalytic system is commonly related to solid semiconductor photocatalysts that are in close contact with a liquid or gaseous medium in which photocatalysis reaction takes place. Exposing the catalyst to light generates reactive species that are able to initiate sequential reactions, such as redox reactions and molecular transformations. These reactive species result from the

photocatalysts absorbing photons with sufficient energy, i.e., equal to or higher than the band-gap energy (E_{bg}) of the photocatalysts. The absorption of light energy leads to a charge separation due to the promotion of an electron (e^-) from the valence band (VB) of the semiconductor to the conduction band (CB), thus generating a positive hole (h^+) in the valence band. A simplified schematic diagram of photocatalytic process initiated by photon action on the semiconductor is presented in *Figure 2-1*, and can be represented by *eq. (2-1)* (Gaya and Abdullah, 2008):

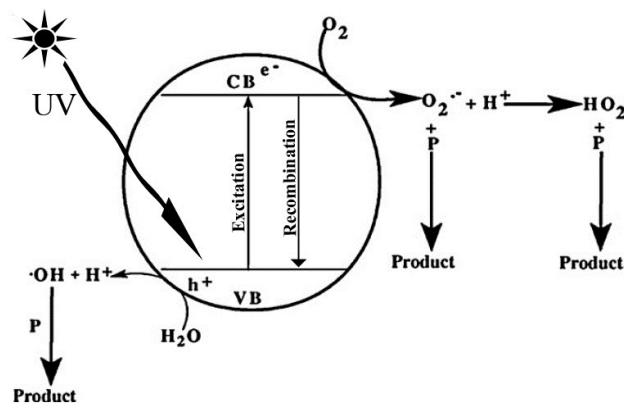
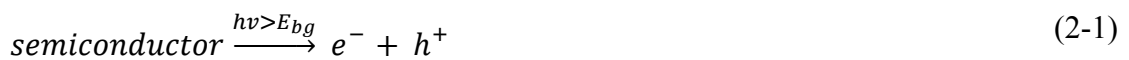


Figure 2-1: Simplified schematic diagram of heterogeneous photocatalytic process



In electrically conducting materials, e.g., metals, the produced charge carriers are immediately recombined. But in semiconductors, a portion of this photo-excited electron-hole pairs diffuse to the surface of catalysts and participate in the chemical reaction. The positive hole (h^+) can oxidize adsorbed donor molecules (such as H_2O in *Figure 2-1*) whereas the electron in conduction band (e^-) can reduce the adsorbed electron acceptor molecules (such as O_2 in *Figure 2-1*). A characteristic feature of semiconducting metal oxides is the strong oxidation power of their holes (h^+). They can react in a one-electron oxidation step with surface-adsorbed water to produce the highly reactive hydroxyl radical ($OH\cdot$). Both the holes and the hydroxyl radicals are

very powerful oxidants that can be used to oxidize most organic contaminants. Moreover, superoxide ions ($O_2^{\bullet-}$), produced from conduction band electron and oxygen, are also highly reactive, which are also able to oxidize organic materials. Some other advantages of heterogeneous photocatalysis include: (1) photocatalytic reaction takes place at room or moderate ambient temperature; (2) organic pollutants can be completely mineralized to non-toxic substances such as CO_2 , H_2O and mineral acids; (3) The possibility of being activated by solar light irradiation could result in low energy cost for practical applications; and (4) the photocatalysts are inexpensive and can be supported on various supporting substrates, allowing their recycling and re-use (Li Puma et al., 2008; Zhang et al., 2009).

2.1.2. TiO₂ photocatalysis: mechanisms and kinetics

An ideal photocatalyst for photocatalytic oxidation is characterized by the following attributes: (1) photo-stability, (2) chemically and biologically inert nature and (3) availability and low cost (Bhatkhande et al., 2002; Carp et al., 2004; Gaya and Abdullah, 2008). Many chalcogenide semiconductors such as TiO₂, ZnO, ZrO₂, CdS, MoS₂, Fe₂O₃ and WO₃ have been examined and used as photocatalysts for the degradation of organic contaminants. Among these metal oxide semiconductors, TiO₂ nanoparticles have proven to be the most promising one, with reported advantages of low cost, non-toxicity, greatly enhanced surface area, tunable properties that can be modified by size reduction, doping, or sensitizer, no substantial loss of photocatalytic activity after repeated process cycles, enhanced photo-induced charge transport, and no depletion layer formation on the surface, etc. (Shan et al., 2010).

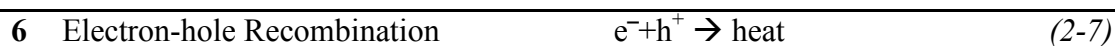
TiO₂ is one of the basic materials in everyday life. It has been widely used as white pigment in paints, cosmetics and foodstuffs. TiO₂ exists in three crystalline modifications: rutile, anatase, and brookite. Anatase type TiO₂ has a crystalline structure that corresponds to the tetragonal system with di-pyramidal habit. Anatase type TiO₂ is commonly recognized as the photoactive phase and mainly used as a photocatalyst under UV irradiation. Rutile type TiO₂ also has a tetragonal crystal structure, but with prismatic habit. Rutile type TiO₂ is commonly known as a low-active or, in some cases, non-active photocatalyst. Hence this type of titania is mainly used as white pigment in paint (Collins-Martinez et al., 2007). Brookite type TiO₂ has an orthorhombic crystalline structure, and is a relatively newcomer to the titania family. It has long been empirically observed that mixed-phase preparation of TiO₂, both anatase and rutile, tends to exhibit higher photocatalytic activities (Linsebigler et

al., 1995). The best known example is Degussa P25, that consists of about 70-80% anatase and the remaining mainly rutile, with a trace amount of brookite and amorphous phase, and has set the standard for photocatalytic activity (Mills and Le Hunte, 1997).

The ability to decontaminate pollutants comes from the redox environment generated from photo-activation of TiO₂ after UV irradiation. The mechanism of the photocatalytic reaction on irradiated TiO₂ has been intensively studied and well understood. A summary of the general process is shown in *Table 2-1*. The photocatalytic process by TiO₂ begins by the absorption of UV light with energy equal to or higher than the band gap energy of 3.2eV for anatase or 3.0eV for rutile on the TiO₂ surface (*eq. (2-2), Table 2-1*). It must be noted that although both anatase and rutile type TiO₂ absorb UV light, rutile type TiO₂ can also absorb light that is nearer to the visible light. However, anatase type TiO₂ exhibits higher photocatalytic activity than rutile type TiO₂ due to its conduction band position that shows stronger reducing power, as compared to that of rutile type TiO₂.

Table 2-1: The general mechanism of the photocatalytic reaction process on irradiated TiO₂

Process Description	Reaction
1 Absorption of efficient photons ($h\nu \geq$ EG=3.2eV) by TiO ₂	$\text{TiO}_2 + h\nu \rightarrow \text{h}^+ + \text{e}^-$ (2-2)
2 Oxygen ion sorption	$\text{O}_2 + \text{e}^- \rightarrow \text{O}_2^{\bullet-}$ (2-3)
3 Neutralization of OH ⁻ groups by photo- holes which produces •OH radicals	$\text{H}_2\text{O} + \text{h}^+ \rightarrow \text{H}^+ + \text{OH}^{\bullet}$ (2-4) ($\text{H}_2\text{O} \leftrightarrow \text{H}^+ + \text{OH}^-$)
4 Oxidation of the organic reactant via successive attacks by OH• radicals	$\text{R} + \text{OH}^{\bullet} \rightarrow \text{R}^{\bullet} + \text{H}_2\text{O}$ (2-5)
5 Direct oxidation by reaction with holes (h ⁺)	$\text{R} + \text{h}^+ \rightarrow \text{R}^{\bullet+} \rightarrow \text{degradation products}$ (2-6)



These energized holes and electrons can either recombine and dissipate the absorbed energy as heat (*eq. (2-7), Table 2-1*) or be available for use in the redox reactions (*eqs.(2-3)–(2-6), Table 2-1*). The solid side at the semiconductor/liquid junction creates an electrical field that separates the energized holes/electrons pairs that fail to recombine, allowing the holes to migrate to the illuminated part of the TiO₂ and the electrons to migrate to the unlit part of TiO₂ particle surface (Heller, 1981). Then, the redox reaction takes place. The electrons (e^-) will react with electron acceptors (*eq. (2-3), Table 2-1*) and the energized holes (h^+) will react with electron donor (*eq. (2-4), Table 2-1*) that adsorbed on or nearby the semiconductor (Bard, 1979).

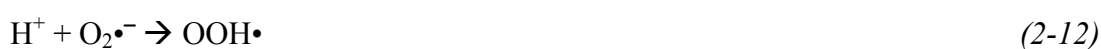
It is well-known that the surface of TiO₂ is readily hydroxylated when it contacts with water. Both dissociated and molecular water are bonded to the surface of TiO₂. Surface coverage of 7-10 OH⁻/nm² at room temperature was reported in literature (Suda and Morimoto, 1987; Takahashi and Yui, 2009). On the other hand, researchers have shown that direct reaction between the organics and the valence holes (*eq. (2-6), Table 2-1*) is not significant (Chen et al., 2000b). Experiments conducted in water-free, aerated organic solvents have shown that only partial oxidation can be achieved. However, complete mineralization was observed in aqueous solutions (Matthews, 1984). Hence, it is generally accepted that hydroxyl radicals are the main responsible oxidizing agent in TiO₂ photocatalytic degradation process (Chen et al., 2000b; Folli et al.). Hydroxyl radical is a very reactive species with an unpaired electron. It has a very high oxidation potential (2.86eV) and can react rapidly and non-selectively to

oxidize almost all organic pollutants in wastewater by hydrogen abstraction (Hoffmann et al., 1995). The four types of OH• attacks have been summarized in *Table 2-2*, as proposed by Turchi and Ollis (1990) (Turchi and Ollis, 1990).

Table 2-2: Hydroxyl radical attacks of organic compounds in photocatalytic degradation process

Process Description	Reaction
(a) Reaction occurs while both species are adsorbed	$\text{OH}_{\text{ads}}\bullet + \text{R}_{1,\text{ads}} \rightarrow \text{R}_{2,\text{ads}}\bullet$ (2-8)
(b) A non-bound radical reacts with an adsorbed organic species	$\text{OH}\bullet + \text{R}_{1,\text{ads}} \rightarrow \text{R}_{2,\text{ads}}\bullet$ (2-9)
(c) An adsorbed radical reacts with a free organic species arriving at the catalyst surface	$\text{OH}_{\text{ads}}\bullet + \text{R}_1 \rightarrow \text{R}_2\bullet$ (2-10)
(d) Reaction occurs between 2 free species in the bulk solution	$\text{OH}\bullet + \text{R}_1 \rightarrow \text{R}_2\bullet$ (2-11)

Photogenerated electrons must be reacted so as to avoid a continuous charge build-up in catalyst particles. At steady state, the rate of h^+ consumption must be equal to the rate of electron consumption. When there is an electron accumulation in the CB, the rate of recombination of e^- and h^+ will be increased. Therefore, electron scavengers or acceptors must be present in the photocatalytic process. Oxygen is the commonly used electron acceptor as it is available at little or no cost. It reacts with CB electrons at the catalyst surface to form superoxide radical anions (*eq.(2-3)*, *Table 2-1*) and participate in the degradation process through the following reactions by forming highly reactive hydroxyl radicals (Jaeger and Bard, 1979):





The kinetics of photocatalytic degradation of organic compounds on TiO_2 usually follows the Langmuir-Hinshelwood model (LH model) (Gaya and Abdullah, 2008; Li et al., 2006; Rajeshwar et al., 2008). According to the recommendations from IUPAC, LH is a mechanism for surface catalysis in which the reaction occurs between species that are adsorbed on the surface (McNaught, 1997). The LH model only considers the macro-scale reaction on the catalysts surfaces, but not the micro-structure on the catalysts surfaces. In this model, the rate of reaction (r) is proportional to the fraction of surface covered by the reactant (θ).

$$r = -\frac{dC}{dt} = k_r\theta \quad (2-20)$$

where k_r is the true rate constant that takes into account of several parameters such as the catalyst's mass, efficient photon flow, and O_2 layer, etc. (Fernández et al., 1995; Valente et al., 2006), and C is the bulk solution concentration of the reactant at time t .

According to the Langmuir's equation for molecules adsorption on a solid surface:

$$\theta = \frac{KC}{1 + KC} \quad (2-21)$$

where K is the adsorption equilibrium constant of the Langmuir model. In photocatalytic studies, the value of K is obtained empirically through a kinetic study in the presence of light, being reported to be better than that obtained under the dark condition (Valente et al., 2006).

Combining eqs. (2-20) and (2-21), one can have:

$$r = k_r \frac{KC}{1 + KC} = \frac{k_r K \cdot C}{1 + KC} \quad (2-22)$$

When the solution is highly dilute, the term KC may become $\ll 1$, eq. (2-22) can then be simplified into:

$$r = -\frac{dC}{dt} = k_r KC = k_{app}C \quad (2-23)$$

where $k_{app}=k_rK$ is the apparent rate constant of a pseudo first order reaction. The solution of eq. (2-23) leads to:

$$\ln\left(\frac{C_0}{C}\right) = k_{app}t \quad (2-24)$$

where C_0 is the reactant bulk solution concentration at UV irradiation time $t=0$, eq. (2-24) indicates that $\ln(C_0/C)$ versus t would show a straight line. By plotting $\ln(C_0/C)$ versus t , one may estimate the apparent rate constant (k_{app}) from the slope of the straight line obtained.

Photocatalytic degradation is assumed to occur on the basis of adsorption, and so it can be expected that the degradation reaction is predominantly between the surface adsorbed substances and the photogenerated oxidants, although other

pathways may exist (Keane et al., 2011; Li et al., 2006). It is therefore reasonable to postulate that photocatalytic degradation follows a modified LH model, where the oxidation of intermediates competes with that of adsorbed primary substance, such as phenol. The reaction rate can then be written as:

$$r = -\frac{dC}{dt} = k_{p,2}\theta_{OH} \times \theta \quad (2-25)$$

where, $k_{p,2}$ is a second-order surface rate constant in terms of the primary substance concentration, θ_{OH} is the fractional site coverage by hydroxyl radicals ($\bullet\text{OH}$), and θ is the fraction of sites covered by the reactant i at any time t . Owing to the fact that water is often the solvent i.e. H_2O and OH^- are in large abundance and the oxygen partial pressure remains the same in a given experiment, the fractional site coverage by $\bullet\text{OH}$ radicals remains constant, and $k_{p,2}\theta_{OH}$ would be constant. Combining eq. (2-25) with eq. (2-20), k_r , the rate constant of the primary substance can be expressed as:

$$k_r = k_{p,2}\theta_{OH} \quad (2-26)$$

On the other hand, the fractional site coverage by the primary substance (θ) can be expressed by Langmuir law as:

$$\theta = \frac{K_C C}{1 + K_C C + \sum_i K_i [I_i]} \quad (2-27)$$

where, K_C is the adsorption equilibrium constant for the primary substance, and K_i refers to the adsorption equilibrium constants for the various degradation intermediate products. If it is assumed that the adsorption coefficients for all organic molecules

present in the reacting mixture are effectively equal, i.e., $K_i=K_C$. Based on the photocatalytic degradation mechanism and mass balance, $C + \Sigma_i[I_i]$ would be equal the initial concentration of the primary substance (C_0), then this assumption can be written as:

$$K_C C + \Sigma_i K_i [I_i] = K_C (C + \Sigma_i [I_i]) = K_C C_0 \quad (2-28)$$

Now, substitution of *eq. (2-26)*, *eq. (2-27)* and *eq. (2-28)* and *eq. (2-20)* results on the expression:

$$r = \frac{k_r K_C C}{1 + K_C C_0} \quad (2-29)$$

The relationship between k_{app} and C_0 can be expressed as a linear equation:

$$\frac{1}{k_{app}} = \frac{1}{k_r K_C} + \frac{C_0}{k_r} \quad (2-30)$$

The values of the adsorption equilibrium constant K_C , and the rate constant k_r were obtained by the linear regression of the $1/k_{app}$ versus C_0 plot, and calculated by *eq. (2-30)*.

2.1.3. Effect of operation parameters

(a). Initial concentration of organic compounds

The influence of initial concentration of organic compounds on photocatalytic degradation rate has been extensively studied (Augugliaro et al., 1991; Chen and Chou, 1993; D'Oliveira et al., 1990; Mills and Morris, 1993). It is believed that adsorption of organic compounds onto the catalyst surface affects the reaction, and usually a high adsorption capacity favors the reaction. For most of the organic pollutants, their adsorption capacities on TiO₂ catalysts are well described by the Langmuir-type equation (*eq. (2-28)*). It means that at high initial concentration all accessible catalytic sites are occupied (Chen et al., 2000b). A further increase in pollutant concentration will not increase the pollutant concentration at the catalyst surface. In photocatalytic processes, generation and migration of the photogenerated electron-hole pair (*eq. (2-2)*, *Table 2-1*), and the reaction between surface-adsorbed organic pollutant and the photogenerated hole, or hydroxyl radical (*eq. (2-5)* and *eq. (2-6)*, *Table 2-1*) are two processes in series. Hence, either of the two steps may become the rate determining factor for the entire process. At low organic concentration, the surface coverage of the photocatalysts by organic pollutants is low; and so second step may dominant the process, which leads to the degradation rate increasing linearly with the organic concentration. On the contrary, the photogeneration of the electron-hole pairs may be limited; and thus the former step, can become the governing step due to the limited adsorption sites occupied by water or oxygen molecules (Wang et al., 1992). Hence, the degradation rate increases slowly with the pollutant concentration, and even a constant degradation rate may be observed at higher concentrations under a certain irradiation light intensity.

(b). Photocatalysts dosage

The rate of photocatalytic reaction is strongly influenced by the concentration of the photocatalyst as well. Several studies have indicated that the photocatalytic rate initially increases with catalyst loading and then decreases at high loading values. Most commonly, a slurry with 0.1~0.2 wt.% TiO₂ is used (Gaya and Abdullah, 2008). Although the number of active sites in solution will increase with increasing the photocatalyst loading, a point appears to be reached where light penetration efficiency is compromised because of excessive catalyst particle concentration. The tradeoff between these two opposing effects results in the need of an optimal photocatalyst loading to be used. The optimal loading concentration range may depend on the reactor geometry, intensity of radiation source, and the properties of TiO₂ such as particle size, phase composite and impurities (Ahmed et al., 2011). Increasing the photocatalysts concentration beyond the optimal range may result in reduced photon flux caused by light scattering and screening effects of the particles on the light. The tendency towards agglomeration also increases at high photocatalyst particle concentrations, resulting in a reduction in effective surface area available for photocatalytic reaction (Ahmed, 2011).

When TiO₂ photocatalysts is immobilized on supports, there exists an optimal thickness for the catalyst film. Obviously, photocatalytic reaction rate reaches a saturation value as the catalysts layer thickness increases. However, if the film is too thick, the strength of the catalyst adhesion is often poor and the film may likely be detached from its support. Photocatalyst film with less than 6 μm thickness was widely accepted in the laboratory studies (Fernández et al., 1995; Naskar et al., 1998), because experimental results indicated that 95% of the incident light has been

absorbed by the catalyst film with a thickness of 4.8 μm of the P25 TiO_2 nanoparticles (Chen et al., 2000a).

(c). Light intensity

The incident light intensity determines the photogenerated electron/hole pair contents and thus the hydroxyl radical formation rate. The nature or form of the light does not affect the reaction pathway (Carp et al., 2004). In other words, the band-gap sensitization mechanism does not affect the photocatalytic degradation. At sufficiently low level of illumination, degradation is of first order intensity. At higher intensity level, on the other hand, the reaction rate increases with the square root of intensity because of the increases of the electron/hole pair recombination during their migration to the catalyst particle surface (Chen and Ray, 1999). As a consequence, strong light may be detrimental to the photocatalysts process as it results in the decrease in quantum efficiency. The optimal light power utilization should be in the domain where degradation rate is proportional to the incident light intensity (Al-Sayyed et al., 1991). The transition points between these regimes, however, will vary with the photo-system (Ahmed et al., 2010b).

(d). Solution pH

Organic compounds in water or wastewater differ greatly in several parameters, particularly in their speciation behavior, solubility in water and hydrophobicity. While some compounds are uncharged at common pH conditions typical of natural water or wastewater, other compounds exhibit a wide variation in speciation (or charge) and physico-chemical properties. At a pH below its pK_a value, an organic compound exists as a neutral species. Above this pK_a value, an organic compound attains a negative charge. Some compounds can exist in positive, neutral, as well as negative

forms in aqueous solution. This variation can also significantly influence their photocatalytic degradation behavior. The pH of an aquatic environment plays an important role in the photocatalytic degradation of organic contaminants. Theoretically, pH value of the solution has strong influence on the surface charge of the solid catalysts particles, the size of the aggregates formed and the band-gap energies of the conductance and valence bands (Singh et al., 2007). The surface charge of a photocatalyst and ionization or speciation (pK_a) of an organic pollutant can be profoundly affected by the solution pH. Electrostatic interaction between semiconductor surface, solvent molecules, organic substance and charged radicals formed during photocatalytic oxidation is strongly dependent on the pH of the solution. In addition, protonation and deprotonation of the organic pollutants can take place depending on the solution pH. Sometimes protonated products are more stable under UV-radiation than their main structures. Therefore the pH of the solution can play a key role in the adsorption and photocatalytic oxidation of pollutants. The ionization state of the surface of the photocatalyst can also be protonated and deprotonated under acidic and alkaline conditions respectively as shown in the following reactions:



The point of zero charge (P_{zc}) of the TiO_2 Degussa P25 is widely accepted at $pH \sim 6.25$ (Ahmed, 2011). While under acidic conditions, the positive charge of the TiO_2 surface increases as the pH decreases (eq. (2-32)); and above pH 6.25, the negative charge at the TiO_2 surface increases with increasing pH. In the literature, the influence of pH on the photocatalytic degradation rate is diversified. Higher reaction

rates for various photocatalytic processes have been reported at both low and high pH values and no general conclusion have been obtained till now (Ochiai and Fujishima, 2012). Typically, reaction rate varies by less than one order of magnitude from one end of the pH range to the other (Fox and Dulay, 1993).

(e).Solution matrix

The amount of UV absorption is influenced by water transmittance over the spectral UV range of interest. Some common constituents that affect water transmittance are suspended solids, dissolved organic matter, nitrate and ferrous/ferric ions. The presence of these components in water can affect adversely the degradation rates of contaminants. Inorganic anions, such as phosphate, sulphate, nitrate, and chloride, have been reported to limit the photocatalytic degradation performance (Calza and Pelizzetti, 2001; Chen et al., 1997; Minero et al., 2000). The main inhibition from these anions is attributed to their adsorption on the surface of TiO₂. Bicarbonate in particular is detrimental to reactor performance as it acts as a hydroxyl radical scavenger (Calza and Pelizzetti, 2001). Long time experience with photocatalytic oxidation systems showed that humic substances in contaminated water can strongly adsorb TiO₂ particles and reduce their activity toward the target pollutant substances (Liu et al., 2013). The observed retardations of humic acids have been related to the inhibition due to chemical adsorption onto the photocatalysts (surface deactivation), competition of active sites on and light attenuation effects (Epling and Lin, 2002). Moreover, the presence of humic acid in the reaction mixture has been reported to significantly reduce light transmission, and therefore the photocatalytic oxidation rate. Humic acid can also compete with organohalides for the active sites on

the TiO₂ surface, leading to a decrease in the overall organic removal efficiency (Schmelling et al., 1997).

Reduction in photocatalytic oxidation reaction rate can also be expected in turbid water due to the shielding (absorption, scattering and/or blocking) of the incident UV light. Giri et al. (2010) investigated the UV shielding effect of 3 different inorganic solids, namely kaolin, bentonite and silica gel, on photocatalytic oxidation of 2,4-dichlorophenoxyacetic acid (2,4-D) in water using TiO₂ fiber. They found that the largest UV shielding effect was observed at 0.5 g.L⁻¹ silica gel, but the effect weakened considerably at 1.0 g.L⁻¹ concentration, due to entrapment of solid particles to jagged TiO₂ surface and/or their settlement.

(f). Oxidants/electron acceptor

The electron/hole recombination is one of the main drawbacks in the application of TiO₂ photocatalysis as it causes a waste of energy. In the absence of suitable electron acceptor or donor, recombination step is predominant and thus it limits the quantum yield. Hence it is crucial to prevent electron-hole pair recombination to ensure efficient photocatalysis. Molecular oxygen is generally used as an electron acceptor in heterogeneous photocatalytic reactions. It was found that the photocatalytic activity nearly completely suppressed in the absence of dissolved oxygen, and the steady state concentration of dissolved oxygen had a profound effect on the rate of photocatalyzed decomposition of organic compounds. The major role of oxygen in the photocatalytic degradation of organic compounds is to act as an electron scavenger for continuous electron removal from the surface of photocatalysts (Ilisz and Dombi, 1999). Therefore, it is important to provide sufficient oxygen in the water or wastewater containing TiO₂ photocatalysts to prevent their electrons

accumulation on the surface of TiO_2 . However, in the photocatalytic removal of dissolved metal ions, oxygen molecule is a strong competitor for metal ions to scavenge the photogenerated electrons. So the presence of dissolved oxygen may significantly inhibit the photoreduction of metal ions (Herrmann, 1999; Litter, 1999; Xu, 2009).

The addition of external oxidant/electron acceptors into a semiconductor suspension has been shown to improve the photocatalytic degradation of organic contaminants by reducing or eliminating the electron-hole pair recombination through accepting the conduction band electrons, increasing the hydroxyl radical concentration and the oxidation rate of intermediate compound and generating more radicals and other oxidizing species to accelerate the degradation efficiency of intermediate compounds (Ahmed et al., 2011). Since hydroxyl radicals appear to play an important role in the photocatalytic degradation, several researchers have investigated the effect of adding commonly encountered electron acceptors such as H_2O_2 , KBrO_3 , and $(\text{NH}_4)_2\text{S}_2\text{O}_8$ on the photocatalytic degradation of various organic compounds, by enhancing the formation of hydroxyl radicals as well as inhibiting the electron-hole pair recombination (Qamar et al., 2006; Singh et al., 2007). In all cases, the addition of these oxidants has been found to result in higher rate of pollutant degradation rates, as compared to that of molecular oxygen.

2.2. Immobilized TiO₂ for environmental photocatalytic degradation applications

In classical heterogeneous photocatalysis, the active material is usually in the form of small particles, typically in the nanometer range. The reason for this small size is simple: the chemistry occurs on the surface of the particles, and for a given mass, the surface area that is provided by a particulate material increases as the particle size decreases (Serpone and Pelizzetti, 1989). Thus, a smaller particle size is beneficial to the chemical activity per unit mass of material. It is also reported that TiO₂ photocatalysts in nano-dimensions can further promote the efficient charge separation and trapping at the physical surface, as well as its high light opaqueness for enhanced oxidation capability (Chong et al., 2010). Unfortunately, some practical and economic challenges, such as the unstable nature of the nanoparticle dispersion, fast photocatalysts deactivation and costly post treatment separation for catalyst recovery practical, largely hindered its applications in large-scale water treatment processes. One of the possible solutions is to immobilize TiO₂ nanoparticles on suitable supports. From the practical point of view, the ideal support for photocatalyst must satisfy several criteria as follows (Pirkanniemi and Sillanpää, 2002; Singh et al., 2013): (a) Strong adherence between catalyst and support, (b) no decrease of the catalyst reactivity by the attachment process, (c) provision of a high specific surface area, (d) with adequate adsorption affinity towards the pollutants, and (e) allowance of fast and easy photocatalyst recovery with good chemical and physical stability. Although the immobilization of TiO₂ onto larger substrates solved the post-treatment recovery problem and possibly enhanced the light utilization efficiencies, the immobilized TiO₂ generally has lower surface area and higher mass transfer limitations for the pollutants than the suspended TiO₂ particles. The photocatalytic

reaction occurs at the liquid–catalyst interface, and therefore when the catalyst is immobilized, both external and internal mass transfer plays significant roles in overall photocatalytic processes. The external mass-transfer resistance could be easily reduced by varying the flow rate (Chen and Ray, 1999). However, the internal mass transfer is an intrinsic property of the catalyst film, and is effected by the nature of the catalyst, coating methods used, and the thickness of the catalyst film (Ballari et al., 2008). The overall rate is sometimes controlled by the internal mass-transfer resistance, which may be difficult to alter.(Chen et al., 2000a, 2001)

2.2.1. Immobilization techniques

A promising alternative strategy for producing a highly active photocatalytic coating is the attachment of stable photocatalytic particles onto a support without any reduction in activity. Generally, two main routes have been explored to fix the titania on suitable supports. One method is to fix the previously made titania powder (PMTP) on to supporting material, which seems to be the simplest starting point to procure a supported coating. There is no clear understanding of the bonding forces acting at the catalyst/support interface when a PMTP is used (Pozzo et al., 1997). Electrostatic interactions (Haarstrick et al., 1996), and van der Waals attractive forces (Siffert and Metzger, 1991), are probably involved but it is also possible that some kind of chemical bonding with suitable binders is applied. Normally, fully inorganic binders should be preferred to prevent any possible long- or even middle-term destroying of the surrounding materials. Polymers and organosilane polymers containing organic functional groups were also used (Robert et al., 2013). Jackson et al. (1991) reported the use of PMTP method with silane coupling and they found that the triethoxysilane would develop bonding bridges between the titania powder and the hollow glass beads, by reacting with hydroxide

groups on both the catalyst and the support surfaces. A thermal binding of PMTP method is probably the simplest immobilizing method by using the in-situ melted polymer as the binding agent for the formation of TiO₂-polymer bridge. For example, Tennakone and co-workers adopted simple hot-pressing method for TiO₂ immobilization on polythene films at 74°C (Tennakone et al., 1995). They found the TiO₂ that was immobilized onto the polythene films being photocatalytically active and suitable for the mineralization of phenols. The main drawback of the binder-through approach exists in the large reduction of the surface of TiO₂ available for adsorption and photocatalytic reaction, due to the partial or even complete encapsulation of the photocatalyst particles in the binder coating (Robert et al., 2013).

The other way for immobilization is based on different alternatives of "in situ" catalyst generation such as the so-called "sol-gel process" (SGP), chemical vapor deposition (CVD), electrophoretic deposition and electrostatic multilayer self-assembly deposition, which may involve a combined series of physical and chemical transformations of a precursor such as a titanium salt (usually an alcoxide) in adequate solvent and under acid or base conditions. This method can produce TiO₂ films with high purity and great homogeneity (Zhang et al., 2005). Among various in-situ generation methods, the SGP has been widely used due to its advantage of a relatively low cost and a flexible applicability to a wide range of sizes and shapes of the substrates. The SGP process generally involves 5 steps: controlled hydrolysis of an alcoxide precursor; condensation to form colloidal particles; gelatin; molding or coating on to a suitable substrate and finally dehydration and densification by calcination at high temperature (Robert et al., 2013). Precursors such as titanium alcoxide, titanium tetrachloride, and titanium halogenide are heated under very high calcinations temperature (over 400°C) to obtain the desired crystal properties and

strong adherence on the support (Aguedach et al., 2005). During heating, dehydration reaction can occur between the OH groups from the catalyst surface and the support, creating an oxygen bridge, thus increasing the adherence of the catalyst to the support (Shan et al., 2010). In general, spread coating and dip coating are the widely used coating methods for this approach. It was found that the spread coating method is suitable for making thick film, whereas the dip coating one is applicable for the production of a thin film on all immersed surfaces of the substrate at the same time. However, the thickness of the film is dependent on the number of times of immersion and the viscosity of the coating solution prepared. A good combination of these factors is important for the preparation of a high-quality thin film photocatalyst. Chemical vapor deposition (CVD) is another interesting method for immobilizing highly pure TiO₂ onto supports. In a typical CVD process, substrates are subjected to a gaseous flow of a single- or multi-component volatile precursor in an inert atmosphere at controlled pressure and controlled temperature, and the decomposition of the volatile precursors takes place at the substrate surface, resulting in the formation of thin films. CVD processes can be implemented in different ways, governed by the type of precursors used, the type of substrates, the operating conditions, and the desired degree of purity, crystallinity, or thin film uniformity (Li Puma et al., 2008). Electrophoretic deposition is based on the application of a potential between two electrodes, and so this method is restricted to conductive supports (Shan et al., 2010). The coating on stainless substrates was reported to be very strong with well controlled thickness by cathodic electrophoretic deposition with Degussa P25 TiO₂ nanoparticles (Dor et al., 2009). A limitation of this method was that it often requires a post-coating annealing at temperatures about 500°C, so that only high temperature tolerant substrate can be used. Besides, the electrostatic

multilayer self-assembly deposition has appeared to be an emerging method for immobilizing photocatalysts on substrates of almost any shapes and sizes, since the early 1990s (Decher et al., 1992). It is based on the concept of multiple weak interactions across the interface between adjacent layers, which are mostly electrostatic interaction in nature. The building of multilayer thin films is achieved by alternative deposition of polyanions and polycations, by dipping or spray, on the surface of a substrate that is previously charged. This method differs from many others by its simplicity of implementation and by benefitting from a fully controlled and homogeneous deposition, from the very good adhesion of the obtained films, and from the ease and versatility of implementation of the technology, whatever the complexity of the substrate geometry is (Decher, 1997). The electrostatic multilayer self-assembly deposition method has been recently successfully adapted with polyelectrolyte multilayers containing commercial Degussa P25 TiO_2 in both wastewater (Krogman et al., 2008) and air treatment (Dontsova et al., 2011). However, maintaining the film porosity during the multilayer building up for preventing complete encapsulation of TiO_2 nanoparticles by the two sandwiching polyelectrolyte layers remains one of the key aspects that need to be improved.

2.2.2. Types of supports

The design of photocatalyst-supported materials is a key aspect in the development of highly efficient photocatalytic processes and reactors, which should take into account of and optimize the interaction between the light, the active catalyst, and the reactants, for maximizing both flow/exposed area contact and utilization of radiated energy. In some cases, the support not only provides its macroscopic structure to the photocatalytic materials but also plays an active role within the reactor, for example, the concentrating effect of pollutants by the adsorptive supports (Zhang et al., 2009).

One of the earliest candidates that emerged as the supporting material was simply the glass reactor wall, probably due to the tenacious sticking capability between titania powder and the lab glassware observed by researchers (Pozzo et al., 1997). Subsequently, all forms of silica based materials have been explored as the photocatalysts support, including glass reactor tube (Ling et al., 2004), glass beads (Qiu and Zheng, 2007; Serpone et al., 1986), glass microspheres (Koopman, 2007; Li et al., 2008), glass plate (Khataee et al., 2011), glass fiber (Brezova et al., 1995), quartz optical fiber (Tromholt et al., 2011), sands (Pozzo et al., 2000), silica gels (Ding et al., 2000; Shironita et al., 2008), etc. The strong adhesion between titania and silica based substrates may be attributed to some sort of sintering effect between the photocatalyst particles and the surface Si-OH groups of the substrates (Pozzo et al., 1997) and the formation of Ti-O-Si linkages (Gao and Wachs, 1999). The advantages of glass as supporting material include the ability to sustain high calcination temperature and ultralow thermal expansion coefficients. Furthermore, the relatively high refraction indices of glass allows better penetration of photons in the reactor system (Gao and Wachs, 1999). However, the glass substrates are fragile and

can easily break, especially in the high temperature calcination process. Unlike the glassy material, silica gel is a porous and amorphous form of silica. It has a large surface area, high thermal stability and good sedimentation ability (López-Muñoz et al., 2005; Shironita et al., 2008). The attainable high surface area of silica can potentially improve catalytic activity by creating more TiO₂ surface readily available for the reactant and thus enhance photocatalytic activity (Choi, 2006; Kim et al., 2005).

Activated carbon (AC), also known as activated charcoal, has also attracted extensive research interest as a potential support in the photochemical processes (Carpio et al., 2005; El-Sheikh et al., 2007; Matos et al., 2007). It is extremely porous and has a very large specific surface area. As a catalyst support, activated carbon can increase the photodegradation rate by progressively allowing an increasing quantity of pollutants to come in contact with the TiO₂ through the means of adsorption (Lim et al., 2011). The synergistic effects between AC and photocatalysts may be incurred by an increased adsorption of the contaminants onto the activated carbon phase followed by a closer transfer through an interphase to the TiO₂ phase, giving a more complete photocatalytic degradation process. In this respect, activated carbon proves to be a valuable support in promoting the photocatalytic degradation process.

A wide variety of polymeric materials have also been tested as supports, for example, polyethylene (PE) film (Tennakone et al., 1995), polyethylene terephthalate (PET) bottles (Fostier et al., 2008; Meichtry et al., 2007), polystyrene (PS) beads (Fabiya and Skelton, 2000), polyvinylchloride (PVC) tube (Damodar and Swaminathan, 2008) and polycarbonate (PC) plates (Fateh et al., 2008), polypropylene (PP) granules (Han and Bai, 2009) and fabrics (Han and Bai, 2010),

poly(methyl methacrylate) spheres (PMMA) (Kamegawa et al., 2011), conductive polyaniline (PANI) thin film (Yu et al., 2012b), and rubber latex sheet (Sriwong et al., 2008). Many polymeric materials are chemically inert, mechanically stable, cheap and very readily available. As compared to other substrates, the cost of the prepared composite photocatalysts can be greatly reduced, making them more economically feasible for possible large scale and wider spread applications. Secondly, the immobilization of TiO₂ onto polymeric materials is often more energy-saving since it is usually done at a temperature below 100-200°C (Singh et al., 2013); as compared to above 400°C or even 500-800°C for other inorganic materials. Being thermoplastic they propose thermo softening properties, which increases the easiness of coating TiO₂ onto them by simple thermal treatment methods.

The 1st reported study on the use of polymer supports for anchoring photocatalyst was perhaps, as known to the authors, by the paper of Tennakone et al. (1995) with a simple thermal treatment method. The anatase form of TiO₂ powder was evenly sprinkled on a commercial polythene film and ironed at a temperature of 74 °C. They reported that the TiO₂ coating was able to achieve more than 50% of phenol degradation in the solution in 2.5 h under non-stirred and non-oxygenated conditions exposed to the solar irradiation. However, the experimental results from photocatalytic mineralization under UV irradiation in 6 h showed 9 mL more CO₂ than the expected theoretical value, suggesting the degradation of the polymer occurred by the embodied TiO₂. Naskar et al. (1998) immobilized Degussa P25 anatase form of TiO₂ nanoparticles on foamed PE sheet by a simple hot pressing method and compared its photocatalytic activity with TiO₂ suspension containing the same amount of titania as the foamed PE sheet. They found that the immobilization of TiO₂ on the polymer led to around 50–60% loss of the catalytic activity. It was

attributed to the largely reduced surface area by partial embedment of TiO₂ particles into the polymer surface. From these two pioneer studies, it can be concluded that the key issue for the embedment of titania particles into the polymer support should be to minimize the degradation of used polymer substrate and the loss of the catalyst activity. A recent method by Velásquez et al. (2012) reported a low-cost controlled-temperature embedding method by dispersing P25 titania particles and PE or PP pellets in glycerin and heating the mixture to the melting point of the polymer, followed by cooling it down to room temperature. The resulted TiO₂-embedded polymer was reported to have strong adherence of P25 on the surface of both substrates, as well as high resistance to UV photodegradation. The simple coating method may lead to the leaching and dissolution of the catalyst due to the lack of proper binding sites and low surface energy on the polymer surface (Singh et al., 2013). In order to overcome this limitation, Dhananjeyan et al. (2000) modified the PE film surface with a PE based anhydride-modified block copolymer to introduce anhydride anchoring groups. Experimental results showed confirmed good adhesion of titania particles and the formation of chemical bond between TiO₂ surface and anhydride groups present on the polymer.

However, the polymer substrate, itself being organic, seems to be equally susceptible to degradation by the TiO₂ photocatalyst as to the organic contaminants under UV light irradiation, apparently through the same reaction mechanisms (Singh et al., 2013). Some researchers tried to introduce a protective layer to prevent the direct contact of the substrate from photocatalytic titania and thus prevent the photodegradation of the substrate (Kasanen et al., 2011a; Kasanen et al., 2011b; Zhou et al., 2011). The protective layer also helped to modify the polymer surface hydrophilicity for better dispersion of hydrophilic TiO₂ powder suspension as

compared to the dispersion of titania directly on hydrophobic polymeric substrate. Multilayer coating approach was adopted for a more complete coverage of the surface without leaving any uncoated spots as observed in single-layer coating (Kasanen et al., 2011b).

Beside the above mentioned and widely explored materials, many other uncommon materials have also been explored, including perlite (Hosseini et al., 2007), pumice stone (Subrahmanyam et al., 2008), cellulose (Aguedach et al., 2005; Neti and Joshi, 2010; Pelton et al., 2006), stainless steel (Chen and Dionysiou, 2006; Gao et al., 1992), quartz sand (Pozzo et al., 2000) and so on. For example, Chen and Dionysiou (2006) reported that an increase in the P25 loading in the sol causes an increase in the amount of crystalline material retained on the support, but at the same time it also increased the micro-cracks in the coated layer and hence decreased mechanical strength of the coated layer. Fernández et al. (1995) investigated the deposition and the characterization of the TiO₂ coatings on several rigid supports (cordierite monolith, stainless steel plates and beta-SiC foam). They found the adherence of the TiO₂ coating decreases with increasing solution viscosity. An intrinsic viscosity leads to thicker coatings which are less resistant and thus, micro-cracks are formed. And the nature of the substrate such as the porosity and the wettability of the substrate play a major role in coatings. Subrahmanyam et al. (2008) showed that the TiO₂ immobilized pumice stone is an easy and efficient method to obtain photocatalytic reactions without the problem of filtration. All these studies suggested that supported TiO₂ could be an economical and efficient process for water and wastewater treatment, if the supporting material and coating technique were properly selected.

2.2.3. Polymer-supported buoyant photocatalysts

In some liquid-phase applications, immobilized TiO_2 led also to the concept of “buoyant photocatalysts” taking advantage of the proximity with the air/water interface for maximizing both the light utilization (especially in solar-light-driven processes) and the oxygenation of the photocatalyst (especially for nonstirred reactions), as well as for facilitating their post use recovery (Robert et al., 2013). To promote photocatalytic oxidation of organic pollutants in water, four components, light, oxygen, the target compound, and the photocatalyst should meet at one place. The water surface appeared to be a good choice. The oxygen demand can be supplied by the oxygen in air through the air-liquid interface and the highest UV intensity can be obtained at the water surface, as compared to anywhere else throughout the water depth in the reactor easily. However, pure titania particles have a density of 3.8g/cm^3 , and it will sink to the bottom of the water in the reactor. Various low density substrates, such as hollow glass microspheres (Portjanskaja et al., 2004; Zaleska et al., 2000), expanded graphite (Modestov et al., 1997; Yaroshenko et al., 2007), pine wood chip (Berry and Mueller, 1994), perlite (Faramarzpour et al., 2009), low density polyethylene (LDPE) (Magalhães et al., 2011), polypropylene (Han and Bai, 2009, 2010, 2011; Tu et al., 2013; Velásquez et al., 2012) and expanded polystyrene (Magalhães and Lago, 2009), have been used for the preparation of buoyant TiO_2 photocatalysts. The polymer-supported buoyant TiO_2 photocatalysts exhibited several advantages, including (Magalhães et al., 2011; Velásquez et al., 2012; Xing et al., 2013):

(a). Maximum light utilization efficiency.

Being floatable, they can utilize solar radiation directly and fully without any light attenuation loss incurred due to traveling through water.

(b). Economical.

The ease with which it can be applied directly to various applications, for example water catchments, natural lakes and contaminated wastewater reservoirs, eliminates the need of any special equipment or installation.

(c). Greater degradation efficiency.

Enriched concentrations of organic contaminants are found to be present on the surface of various water bodies. These catalysts being buoyant are more efficient in destroying suspended insoluble organic contamination, such as accidental oil spills (Rosenberg et al., 1992).

(d). Easy post-treatment recovery.

Buoyant polymer-supported photocatalysts can be recovered by simply using a sieves (Tu et al., 2013).

The first polymer-supported buoyant photocatalyst was reported by Fabiyi and Skelton (2000), using a simple thermal treatment method to coat P25 TiO₂ onto naturally buoyant polystyrene beads. The obtained buoyant PS-P25 buoyant photocatalysts show higher mechanical stability as well as impressive photocatalytic activity. The catalyst activity was found to remain appreciably high for up to 10 successive runs. Han and Bai (2009) prepared a novel buoyant photocatalyst supported on polypropylene (PP) granules using a low temperature hydrothermal method. To make it effective in visible light, the TiO₂ was modified with N-doping with triethylamine. The low melting point of the PP has restricted the preparation method to be carried out at a low temperature. However, the prepared buoyant photocatalyst showed lower photo oxidation activity as compared to powder photocatalyst particles. This was ascribed to the relatively lower loading rate of TiO₂

on PP granules and smaller surface area of the film as compared to the powder particles. Taking their research further, Han and Bai (2010) prepared a highly active buoyant photocatalyst with high loading rate of titania on polypropylene fabric (PPF) by adopting a novel layered-TiO₂ immobilization configurations. The PPF surface was first activated and immobilized with a small flower-like rutile TiO₂ layer using hydrothermal method and further immobilized with N-doped anatase TiO₂. Characterization techniques confirmed that the enhanced hydrophilicity of PPF after pre-treatment was attributed to the formation of hydroxyl or carboxyl groups on its surface. These groups can interact with hydroxyl groups on titania and form hydrogen bonds that can improve the adherence of TiO₂ on PPF. Moreover, the rough surface of rutile TiO₂ provided a large surface area for the subsequent immobilization of N-doped anatase layer. The main highlight of the paper was the enhanced loading amount of titania on the polymer substrate by the flower-like rutile TiO₂ layer, as it was a decisive factor for achieving high photocatalytic activity for the prepared floatable photocatalysts.

2.3. The role of activated carbon in heterogeneous photocatalysis

Although, TiO_2 has been reported as an efficient photocatalyst so far, its poor adsorption property to the pollutants to be degraded often leads to a limitation in the overall process performances, especially when the concentration of the pollutants is low. Some attempts have been made to improve the photocatalytic efficiency of titania by adding an adsorbent as co-component, such as silica, alumina, zeolites, clays, and active carbons (ACs). This addition is to induce a synergistic effect by creating a high organic environment around the TiO_2 photocatalyst through the means of adsorption. Activated carbon has been used as one of the good co-adsorbents with the photocatalysts, attributed to its well established literature references as an adsorbent and its efficiency to adsorb a wide range of organic pollutants with high adsorption capacities.

Activated carbon (AC) is an adsorbent produced from carbonaceous precursors, by either thermal or chemical activation to increase the internal porosity and thus achieve high specific surface area (Bansal and Goyal, 2005). Activated carbon has been the most widely used adsorbent because of its high chemical and mechanical stability, good adsorption capacity and high degree of surface reactivity. Activated carbon adsorption has been recommended by the USEPA as one of the best available technologies (BAT) in the removal of trace amount of organic compounds (Alam et al., 2009). Most of the carbon-rich raw materials can be converted to activated carbon, such as wood, coal, coke, coconut shells, fly ash and even rice husk. Thermal or steam activation requires the oxidation of char in oxidizing environment at a temperature between 800-1000°C. Chemical activation involves heating the carbonaceous precursor and a dehydrating agent to a temperature between 200-650°C. Strong acids, such as phosphoric acid, sulfuric acid and nitric acid, are usually used as dehydrating

agents and may be leached out and reused. Hence, chemically activated carbons typically have a lower pH, due to acidic groups on their surface (Nakhla et al., 1994; Terzyk, 2003). The difference in precursors and activation processes result in activated carbons having varying physical and chemical properties, and displaying different adsorption behaviors.

(a). Surface Area

The highly porous structure of activated carbon is one of the main reasons for its high internal surface area and makes it effective in the adsorption of organic pollutants. Even though properties such as pore size distribution, surface chemistry and adsorbate-adsorbent interactions play a role, surface area is often found to be the limiting factor for adsorption of various target pollutants (Yang, 2003). Hence, a greater surface area of the activated carbon will usually result in a greater adsorption capacity. The typical surface areas of activated carbons are between $500\text{-}1500\text{m}^2\cdot\text{g}^{-1}$ (Marsh, 2006).

(b). Pore Size Distribution

The pores of activated carbon are often classified into three size ranges according to IUPAC recommendations (McNaught, 1997):

- Micropores: Less than 20 \AA (2 nm)
- Mesopores: Between 20 \AA (2 nm) and 500 \AA (50 nm)
- Macropores: Greater than 500 \AA (50 nm)

Micropores in activated carbon are usually comparable to the sizes of the adsorbate molecules. Therefore, all the atoms of the adsorbent can interact with the adsorbate species, which is the main difference between adsorption mechanisms of

micropores and that of mesopores and macropores. Micropore adsorption is hence a pore filling process controlled by the volume of the micropores. Mesopores participate in the transport of the pollutant molecules to the major adsorption sites in the micropores. They are characterized mainly by their specific surface area and pore size distributions. In the case of macropores, the action of adsorption forces does not occur throughout their void volume but at a short distance from their walls. Like mesopores, macropores are also diffusion pores in which they principally transport the pollutant molecules to smaller pores.

During the adsorption process in activated carbon, four main steps occur:

1. Bulk diffusion of the molecule through the bulk liquid towards activated carbon particles.
2. Film diffusion of molecules through the boundary layer surrounding the activated carbon.
3. Pore diffusion through the pores or along the pore walls.
4. Adsorption of the adsorbate on the adsorption sites.

The rate determining step is often step 3 that is the diffusion through the pores of the activated carbon, which is largely influenced by the pore size and the size of the diffusing molecule.

Activated carbon is an excellent adsorbent, especially for systems dealing with organics. It is also well-known that TiO_2 is capable of oxidizing a wide range of organics to water and carbon dioxide. Hence, it can be hypothesized that a combination of these two materials may result in a combined effect of adsorption and degradation, and thus would result in a synergy for the overall process performance. This means that the pollutant is adsorbed and concentrated onto the adsorbent and is

then subsequently degraded by the TiO₂ photocatalysts in the presence of UV at a higher mass transfer rate.

Physical mixing of TiO₂ and AC in aqueous suspensions has been the easiest way of preparing TiO₂-AC combination, as demonstrated by Matos and others (Cordero et al., 2007a; Cordero et al., 2007b; Herrmann et al., 1999; Matos et al., 2010; Matos et al., 1999; Matos et al., 1998; Matos et al., 2001; Matos et al., 2007), and Araña et al. (Araña et al., 2004; Araña et al., 2003a, 2003b; Araña et al., 2002). Mechanical agitation of the TiO₂ and AC particles in aqueous suspension promotes their collisions and subsequently attachment to form a pseudo-TiO₂/AC composite. Matos et al. (1998) tested the mixture of 10mg AC and 50mg TiO₂ in a slurry system on phenol removal and found that the apparent rate constant was 2.5 times higher than that of purely titania. The authors ascribed this result to the adsorption of phenol to the AC that provided a rapid transfer of phenol to the photoactive titania. In view of practical application, production of TiO₂/AC by simple physical mixing involves less chemical consumption and minimizes environmental pollution, which appeared to be a favorable option. However, in such physical mixing, the physical bonding of TiO₂ on the surface of AC is likely to be weak. This may result in appreciable amount of TiO₂ particles to be dislodged from AC in solution, and thus subsequent separation of the TiO₂ nanoparticles from the treated water can be a challenging problem.

Another way of producing TiO₂-AC composite is to immobilize TiO₂ on AC surface by various chemical assisted methods, such as chemical binders (Yuan et al., 2007; Yuan et al., 2005), molecular adsorption-deposition method (Fu et al., 2004), sol-gel (Li and Liu, 2012; Xue et al., 2011; Yao et al., 2010), hydrothermal (Liu et al., 2007; Wang et al., 2009a; Wang et al., 2009b; Yu et al., 2012a), chemical vapor

deposition (Li Puma et al., 2008), etc. According to the optimal catalysts support selection criteria mentioned in *section 2.2*, activated carbon appeared to be a good choice for their high porosity and large specific surface area. Due to its versatility, the sol-gel technique is the most commonly used chemical method for TiO₂/AC preparation. The morphology of TiO₂ on AC may be properly controlled by sol-gel method so that the coating of TiO₂ could be limited to the external surface of AC and the pore structure of AC is largely preserved (Chen and Mao, 2007). Furthermore, the sol-gel technique offers various TiO₂ modification options. For examples, (a) visible light responsive TiO₂/AC (Jamil et al., 2012; Zhang et al., 2010) and (b) TiO₂ coated on Fe₃O₄-loaded AC that allows separation using magnet (Ao et al., 2008). The TiO₂/AC composite was synthesized through CVD method followed by metal-organic CVD technique to deposit the Ti alkoxide precursors on the AC support. Less handling steps were involved in the CVD process, and the integrity of the AC pore structure is better preserved (Zhang and Lei, 2008). However, the requirement for CVD operation environment is much more stringent. The carrier gas must be inert, of high-purity, and completely dry and the gas line must be sufficiently heated to avoid condensation of Ti precursors. TiO₂ nanoparticles can be obtained by hydrothermal treatment of peptized precipitates of a Ti precursor in water, or hydrothermal reaction of titanium alkoxide in an acidic ethanol-water solution (Liu et al., 2007). The sizes of the resulting TiO₂ particles can be controlled by adjusting the concentration of Ti precursor and the composition of the solvent system, while the peptizers and their concentrations can influence the morphology of the obtained TiO₂ particles. TiO₂/AC synthesis using binders was adopted by Yuan et al. (2005). They utilized diglycidyl ether of bisphenol-A epoxy resin as the chemical to bind P25 and AC fiber. Though this technique seems feasible to mount TiO₂ onto AC fiber, it is possible that trace

amounts of binders may still exist after calcination that may cause water contamination by those residues. Besides, if excessively large binder molecules block the AC pores, various sorption sites can be rendered inaccessible to target pollutants and the adsorption capacity of the composite may be considerably compromised. The molecular adsorption-deposition method is another chemical method to produce TiO_2 coating on AC. In this method, a Ti precursor of small molecular size, such as TiCl_4 , is to be absorbed into the micropores of AC in vapor phase. After hydrolysis of the Ti precursor, pyrolysis proceeds at a relatively low temperature to produce TiO_2 anatase (Fu et al., 2004). By changing the vapor pressure of the Ti precursor during adsorption, the molecular adsorption-deposition method can be used to control the final thickness of the TiO_2 layer formed. However, this method may result in a significant amount of TiO_2 embedded into the AC internal pores, thus losing their functionality and resulting in the reduction of the AC sorption capacity.

Apart from simply offering a large space for immobilization, the activated carbon can also increase the photodegradation rate by progressively allowing an increasing quantity of reactants to come in contact with the TiO_2 through instant adsorption (Li Puma et al., 2008; Zhang and Lei, 2008). Minero et al. (1992) have established that the hydroxyl radical generated by the photocatalysts does not migrate very far from the active centers of the photocatalysts and therefore degradation takes place virtually on the catalysts surface. In this respect, activated carbon proves to be an valuable support in promoting the photocatalytic degradation process, by creating a common interface between both the AC phase and TiO_2 particle phase (Li Puma et al., 2008; Zhang and Lei, 2008). The synergistic effect can be explained as an enhanced adsorption of the organic pollutants on to the activated carbon phase, followed closely by a transfer through an interface to TiO_2 surface. The Adsorption-photocatalysis

synergism has also been found to depend on the surface chemistry of AC (Matos et al., 1999). The quantification of the synergistic and inhibitive effects may be determined by the R factor, which is defined as the following:

$$R = \frac{k_{app(TiO_2+AC)}}{k_{app(TiO_2)}} \quad (2-34)$$

where $k_{app(TiO_2+AC)}$ is the apparent rate constant for TiO₂-AC composite and $k_{app(TiO_2)}$ is the apparent rate constant for bare TiO₂.

Synergy factor and inhibition factor are assigned when $R > 1$ and $R < 1$, respectively. The studies based on binary mixture of AC with Degussa P25 TiO₂ nanoparticles by Matos and the others observed both synergistic and antagonistic effects on the removal of phenol, 4-chlorophenol, and 2,4-dichlorophenoxyacetic acid (Cordero et al., 2007b; Matos et al., 2001; Matos et al., 2007). In general, the AC type and its activation process affect its surface functional groups, pH_{pzc} , and topological properties. These properties affect the creation of the TiO₂-AC interface, which has direct impact on interfacial electron transfer rate and thus photocatalytic efficiency of the TiO₂-AC mixture.

Although satisfactory results have been demonstrated with several lab-scale testings of the activated carbon/TiO₂ system for various organic pollutants with different adsorption and photocatalysis rate, there are still some barriers that need to be addressed before photocatalysts-adsorbent system attains practical applications. Firstly, the proper adsorbent selection was one of the important issues that remained non-conclusive at this stage (Zhang et al., 2009). The overall performance of the photocatalyst-adsorbent system would basically depend on three major steps: (1) adsorption of pollutant onto the adsorbent, (2) transfer of the adsorbed pollutant from

the adsorbent to the photocatalyst and (3) photocatalytic decomposition of the pollutant by TiO_2 . Adsorption rate in step 1 was found to be much faster than that of photodecomposition in step 3. Hence, excessive AC adsorption capacity may not be desirable because it may inhibit photocatalytic degradation of target pollutants (Li Puma et al., 2008; Zhang et al., 2009). Thus, choosing a proper adsorbent is critical to the development of the photocatalyst-adsorbent composite system for removal of organic pollutants in wastewater purification. The adsorption capacity needs to be balanced with the organic affinity to the adsorbent to allow adequate diffusion of adsorbed pollutants to the photoactive sites of the photocatalyst. Some studies have shown that the desorption of adsorbed species from adsorbent surface was the major rate limiting step during photocatalytic regeneration of spent activated carbon, and external heat or ultrasonic waves were needed to enhance the desorption for better regeneration of the activated carbon (Crittenden et al., 1997; Liu et al., 1996; Liu et al., 2003; Salvador and Merchán, 1996; Yuen and Hameed, 2009). Some early studies conducted by Torimoto et al. (1996) on propylamide removal by photocatalyst deposited on various adsorbent supports showed that AC/ TiO_2 system had the highest removal due to propylamide adsorption by AC, whereas zeolite/ TiO_2 had the highest photocatalytic decomposition rate due to the moderate adsorption affinity of zeolite. Hence, for possible continuous long-term operation of the photocatalyst-adsorbent composite system, adsorbents of adequate desorption properties or moderate affinity to the pollutants are important in achieving a maximum ultimate degradation of the pollutant by photocatalytic reaction.

To preserve the adsorptive-photocatalytic properties of TiO_2/AC composite for prolonged use, mechanical or adhesion stability of TiO_2/AC is imperative in order to prevent facile dislodgement of TiO_2 from the AC support. Once TiO_2 particles

dislodge from AC, the slurry system becomes essentially a binary mixture of the suspended TiO_2 and AC particles, losing the synergistic function. The strong mounting of TiO_2 on AC may be accomplished through strong chemical bonding at the TiO_2 -AC interface established during chemical synthesis routes such as sol-gel, CVD, and hydrothermal and binders-assisted methods appear to produce mechanically stable composites, while physical binary mixtures of TiO_2 and AC may yield weak entrapment of TiO_2 nanoparticles into AC valleys. Operationally determined mechanical stability can be accomplished through assessing the changes in photocatalytic activities of TiO_2/AC composite over time or cycles of reuse. Other semi-quantitative and qualitative investigations of the TiO_2/AC mechanical stability was also performed, such as visual inspection of the SEM or TEM images of the fresh and reused samples (Araña et al., 2003a), quantifying changes in their surface areas, and analyzing changes in their particle size distributions.

To the best of our knowledge, there is still no engineering-scale demonstration of TiO_2/AC application in real wastewater treatment plants. However, with increasing experience gained in the recent years with applications of solar photocatalysis in water treatment plants, UV/ TiO_2 photocatalysis pilot-scale experiments, and vast experiences with PAC usage in the water industry, the TiO_2/AC application can be conveniently demonstrated in the near future. If the issues discussed in this section can be appropriately addressed, TiO_2/AC presents considerable opportunities for future applications in water treatment and reclamation, as a plug-and-run system integrated into the existing treatment train for water polishing, or for side-stream treatment to enhance overall yield.

2.4. Some remarks

Based on the previous review, it is clear that supported-TiO₂ could be an economical and efficient process for pollutant removal in water and wastewater treatment processes, if the process is carefully designed. Therefore, the objective of this thesis study is to develop a desired composite photocatalyst with both the adsorption and photocatalytic degradation components on a suitable substrate that can resolve problems mentioned in the previous sections, especially the post-treatment separation and mass transfer limitation.

The advantages of floating photocatalysts have already been discussed earlier, including improved separation performance and enhanced light utilization efficiency (Portjanskaja et al., 2004; Zaleska et al., 2000). From the previous discussions, polymeric materials seem to be a good candidate for making buoyant photocatalysts. Polypropylene (PP) is selected in this study, for its physical and chemical stability under normal application conditions, and being cheap and very readily available. Secondly, PP is one of the light polymers that have a density less than that of water; hence the TiO₂ coated polymer could be floating on water surface. Thirdly, the immobilization of TiO₂ onto polymeric materials is often more energy-saving since it is usually done at a temperature below 100-200°C; as compared to above 400°C or even 500-800°C for other inorganic materials. PP is available in the market in various shapes, such as beads, thin sheet, thick plates or flexible fabric. Millimeter-sized granular PP is selected in this study for flexible reactor design and easy post-treatment separation.

In order to minimize the mass transfer limitation in the immobilized TiO₂ system, co-adsorbent is added to enhance the photocatalytic degradation efficiency. From the

previous discussions, PAC appeared to be a good co-adsorbent, as well as a good photocatalysts support. Hence, PAC is selected as the co-component of the buoyant composite photocatalysts. However, greater understanding about the immobilization techniques, photocatalysts compositions, as well as the application parameters, is crucial in developing an optimized buoyant polymer supported photocatalyst technology. Hence, the study will try to fill some of the knowledge gaps on the fabrication of polymer supported buoyant composite photocatalysts, as well as the application performances.

It has also been found from the literature review that the configuration effect of the TiO_2 particles has an impact on the photocatalytic degradation activity. The combination of TiO_2 and PAC has been investigated in several aspects, such as types of PAC, TiO_2 and PAC ratios and the size of the PAC particles, but the configurable effect of the TiO_2/AC combination has not been reported. In order to understand the configurable effect of the TiO_2/AC combination on the photocatalytic reaction and to optimize the material prepared, it is of interest to find a stable and effective TiO_2/AC configuration, that not only provides the desired synergistic effect between photocatalyst and adsorbent components but also provide the photocatalytic degradation stability for the prepared composite because polymeric substrate was suspected to be photocatalytically degraded in some previous studies.

Chapter 3: Removal of Phenol in Aqueous Solutions by Novel Buoyant Composite Photocatalysts and the Kinetics

3.1. Introduction

Recent studies have shown the great potential and advantages of photocatalysis, especially using TiO₂ photocatalysis in water and wastewater treatment. The TiO₂ particles have been immobilized onto macro supports to overcome the post separation issues (Bideau et al., 1995; Lin et al., 2002; Shan et al., 2010). There have been studies in floating photocatalysts prepared by immobilizing TiO₂ particles onto low density substrates, such as hollow glass microsphere (Koopman, 2007), polystyrene beads (Fabiyyi and Skelton, 2000; Magalhães and Lago, 2009), polypropylene granules (Han and Bai, 2009) and polypropylene fabric (Han and Bai, 2010). It has been demonstrated that the floating photocatalysts had the advantages of greater light utilization efficiency because light attenuation is lower in air than in water [20, 21] and enhanced oxygenation of the photocatalyst at the water/air interface (Fabiyyi and Skelton, 2000). The floating or buoyant photocatalysts however still face the problem of low mass transfer rate between the organic pollutants in aqueous solutions and the photocatalysts mostly on the water surface (Lin et al., 2002). On the other hand, some studies investigated the incorporation of inert co-adsorbents with photocatalysts to improve the mass transfer issue. This was usually achieved by either adding adsorbent particles or photocatalyst particles together into the same solution in the reactor, or by depositing photocatalyst nanoparticles into porous adsorbent granules for use together (Lee et al., 2004; Lim et al., 2011). The co-adsorbent was expected to help concentrate organic pollutants in water and create a common interface between the adsorbent phase and photocatalyst phase, which can efficiently provide organic

pollutant to the photocatalyst particles for immediate photocatalytic degradation (Aruldoss et al., 2011; Carpio et al., 2005; Li Puma et al., 2008; Liu et al., 2007; Matos et al., 1998). These practices however did not have the advantages as provided by the buoyant photocatalysts.

In this work, we prepared a novel buoyant composite photocatalyst by immobilizing Degussa P25 TiO₂ nanoparticle photocatalyst (P25) and activated carbon (PAC) fine powder particles on polypropylene granules (PPGs) via a thermal bonding process. The selection of PPG as the substrate is based on the following consideration: (a) a relatively low density (0.86~0.95 g.cm⁻³) that allows the prepared composite photocatalyst to be buoyant in water; (b) the thermo-softening property that makes the immobilization of TiO₂ and PAC particles on the substrate easy under proper heating; (c) the possibility to achieve high resistance to lights, many chemicals, as well as photocatalytic reactions (Han and Bai, 2011), and (d) a material that is cheap and readily available. Phenol was selected as the targeted pollutant to evaluate the performances of the prepared buoyant composite photocatalyst. The objectives of this study were to (a) obtain a novel buoyant composite photocatalyst with both adsorption and photocatalytic degradation functions, (b) evaluate the performance of the composite photocatalyst using phenol as a target pollutant, with an interest in the synergistic effect of the adsorbent component and photocatalyst component and the photocatalytic degradation kinetics, and (c) examine the effects of experimental conditions, including the saline concentration, on phenol removal.

3.2. Experimental

3.2.1. Reagents

Phenol (99.5%, Merck), NaCl (99.5%, Sinopharm), HNO₃ (68%, Fisher Chemicals), NaOH (98%, Sigma-Aldrich) were used as received without further purification. The test solutions were prepared by dissolving the chemicals in ultra-pure water produced by a Milli-Q water purification system.

3.2.2. Preparation of buoyant composite photocatalysts

The photocatalyst component used was Degussa Aeroxide[®] P25 TiO₂ that contained both anatase (70-85%) and rutile (15-30%), with a specific surface area of 50 m².g⁻¹ and an average particle size of 21 nm. The adsorbent component used was Aquasorb[®] CP1-F powdered activated carbon obtained from Jacobi Carbon. The PAC was steam-activated from coconut shells and had a specific surface area of 1050 m².g⁻¹ and a nominal particle size of 325 meshes. The PPGs were purchased from Polyolefin Company (Singapore) with a dimension of 2×3.5 mm (length×diameter). A thermal immobilization method was used to anchor P25 and PAC onto PPGs and the schematic diagram of the experimental setup is shown in *Figure 3-1*. For a typical preparation run, 120 g PPGs were mixed with 60 g of a mixture consisting PAC and P25 at various desired weight ratios in a 1 L custom-made round bottom glass reactor. An overhead mechanical mixer (IKA[®] RW20 Digital, Germany) equipped with a PTFE stirrer shaft (Anchor Propeller, Cowie, UK) was used to provide intense mixing in the glass reactor in the range of 500~900 rpm. A hotplate (Heidolph) equipped with a 1 L round bottom heating block was used as the heating device. The hotplate was set to 250 °C and the temperature in the reactor was monitored with a thermal couple. As the temperature in the reactor gradually raised and reached the softening temperature

(approximately 150 °C) of PPG, P25 and PAC particles started to stick onto the surface of PPGs. Heating was stopped when the temperature in the reactor reached 170°C and the reactor was then quickly removed from the heating block. The content in the reactor was poured into a stainless steel sieve. The PPGs fully immobilized with P25 and PAC particles were collected in the sieve and then washed thoroughly with tap water until no PAC and P25 particles were observed in the washing solution. Finally, the prepared granules were dried in an oven at 90 °C till a constant weight. This final product was taken as the buoyant composite photocatalysts in this work and was named according to the weight percentage of P25 in the mixture for immobilization. For example, 75%P25-PPG will represent the buoyant composite photocatalyst that was prepared using 45 g P25 and 15 g PAC, i.e., 75% P25 and 25% PAC in the powder mixture.

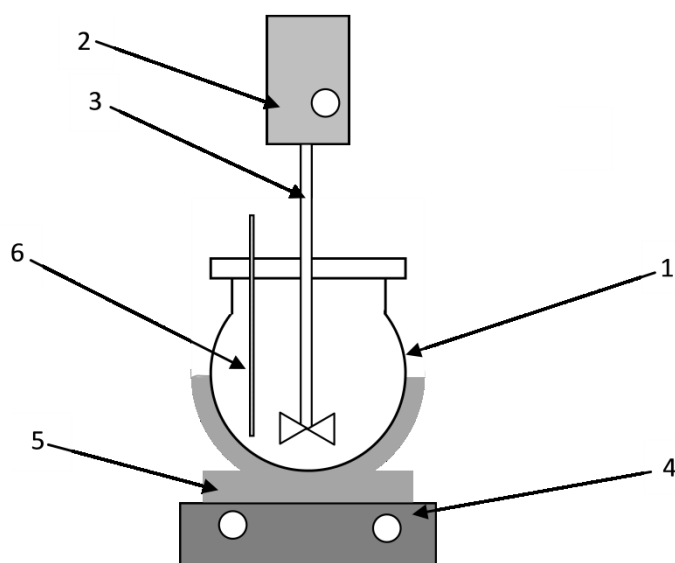


Figure 3-1: Schematic diagram of experimental setup for the preparation of composite photocatalysts: (1) 1 L round bottom glass reactor; (2) overhead mechanical mixer; (3) PTFE stirrer shaft; (4) hotplate; (5) 1 L round bottom heating block; and (6) thermal couple

3.2.3. Characterization of buoyant composite photocatalysts

The actual compositions of the prepared composite photocatalysts were determined using a Thermalgravimetric Analyzer (TGA, TGA2950, DuPont Instruments, USA). A sample of around 7 mg of each type of the prepared composite photocatalysts was tested and the weight variation as a function of furnace temperature was measured by the built-in balance. The TGA furnace was first heated to 400 °C at a rate of 20 °C.min⁻¹ with nitrogen gas as the carrier gas for the decomposition of organic constituents (the polypropylene polymer and possible organic impurities in PPG) (S. H. Abdul Kaleel et al., 2011). The carrier gas was then quickly changed to compressed air and the furnace was continued to heat to 800 °C at the same rate as before for the burn-off of PAC. The remaining part was mainly attributed to P25 and possibly the inert impurities from the PPG substrate (Qourzal et al., 2004; Yu et al., 2005).

The surface morphologies of the prepared composite photocatalysts were observed by a field emission scanning electron microscopy (FESEM, JEOL JSM-6700F, Japan) under 5kV electron beam, following the standard measurement procedures (Han and Bai, 2010).

3.2.4. Phenol removal experiments with prepared composite photocatalysts

Parallel experiments were conducted to investigate the performance of phenol removal with different types of the prepared buoyant composite photocatalysts. Two custom-made glass reactors with jacket for temperature control through a water recirculation system were used. Phenol solution to be tested was placed in the reactors. One reactor was wrapped with an aluminum foil for dark adsorption removal

test and the other one was put under a 150 W Xenon lamp (Newport, USA) for combined adsorption and photocatalytic degradation removal test. The solution temperature in the reactors was controlled at 25 °C in all the experiments. In each reactor, 10 g of a prepared type of composite photocatalysts (except for 100%P25-PPG) was added into 400 mL of phenol solution with a phenol concentration at 20 mg.L⁻¹ and containing NaCl at 3.5wt%. For 100%P25-PPG, only 3.33 g was used in the experiments because it was found to have 2 times more P25 loaded as compared to other types of composite photocatalysts prepared, i.e. 25%P25-PPG, 50%P25-PPG and 75%P25-PPG. The UV light intensity from the Xenon lamp was at around 48 W.m⁻², with a radiation area of 69 mm in diameter. A 0.5 L·min⁻¹ air flow was supplied to each reactor from the bottom for mixing and oxygen supply. The total time monitored for each test run was 12 hrs. About 2 mL sample was taken at a designed time interval and analyzed for phenol concentration using a UV/VIS Spectrophotometer (Jasco V-660, Japan) at $\lambda_{\text{max}} = 270$ nm. All the tests are triplicated to ensure accuracy (n=3).

3.2.5. Phenol adsorption isotherm experiments

The adsorption performance of the prepared composite photocatalysts was evaluated. The experiments were carried out in a number of 500 mL Erlenmeyer flasks, each of which containing 400 mL of a phenol solution was added with 10 g of a prepared composite photocatalyst. The solutions in the flasks had different concentrations of phenol in the range of 10 to 200 mg.L⁻¹ but all contained the same NaCl concentration at 3.5wt% to simulate the salt content in a phenol wastewater. The flasks were covered and then placed in a water bath shaker with the temperature being controlled at 25 °C, shaking at 120 rpm, for 72 hrs to fully reach adsorption

equilibrium. All the tests are triplicated to ensure accuracy ($n=3$). The remaining phenol concentration in the solution in each flask was measured and the adsorbed amount (q) of phenol on the prepared composite photocatalyst was calculated using the following equation:

$$q_e = \frac{V(C_i - C_e)}{M} \quad (3-1)$$

where q_e is the specific adsorption uptake (mg.g^{-1}), V is the volume of the solution (L) in each flask, C_i (mg.L^{-1}) and C_e (mg.L^{-1}) are the phenol concentrations in the solution initially and at the adsorption equilibrium respectively, and M is the mass of the composite photocatalyst added in each flask (g).

The adsorption isotherm data were evaluated with the Langmuir (*eq. (3-2)*) and the Freundlich (*eq. (3-3)*) isotherm models that are commonly used in adsorption studies, as given below (Ho and McKay, 1998).

$$q_e = \frac{q_m b C_e}{1 + b C_e} \quad (3-2)$$

where q_e is the amount of phenol adsorbed per unit weight of the composite photocatalyst at equilibrium (mg.g^{-1}), C_e has the same meaning as defined before, q_m is the maximum adsorption capacity (mg.g^{-1}) and b is the Langmuir model constant (L.mg^{-1}).

$$q_e = K_F C_e^{1/n} \quad (3-3)$$

where K_F is the Freundlich constant that indicates the relative adsorption capacity of the composite photocatalyst ($\text{mg}^{1-(1/n)}\text{L}^{1/n}\cdot\text{g}^{-1}$), n is the model constant representing the intensity of adsorption, and q_e and C_e have the same meaning as defined before.

3.2.6. Phenol photocatalytic degradation kinetics

The photocatalytic degradation performance of the prepared composite photocatalyst was also evaluated. The experiments were conducted with a bench-scale system consisting of a 2 L reservoir and a 400 mL custom-made glass reactor jacketed with water circulation for temperature control by an external water circulator (Julabo, Germany). An overhead mixer was installed on the reservoir to provide mixing and a 150 W Xenon Lamp (Newport, USA) was installed above the reactor to provide the light source. The solution in the reservoir and the reactor was continuously circulated by two peristaltic pumps (Masterflex, UK) at a flow rate of $0.2 \text{ L}\cdot\text{min}^{-1}$. A schematic diagram of the experimental setup is shown in *Figure 3-2*. The use of the large reservoir was to provide a sufficient phenol loading to saturate the PAC adsorption component in the composite photocatalyst before and during the photocatalytic degradation of phenol in the experiment. Therefore the system can be considered as a batch system with a total capacity of 2.4 L. A tracer study showed that there was no concentration gradient between the two compartments (i.e., reservoir and reactor).

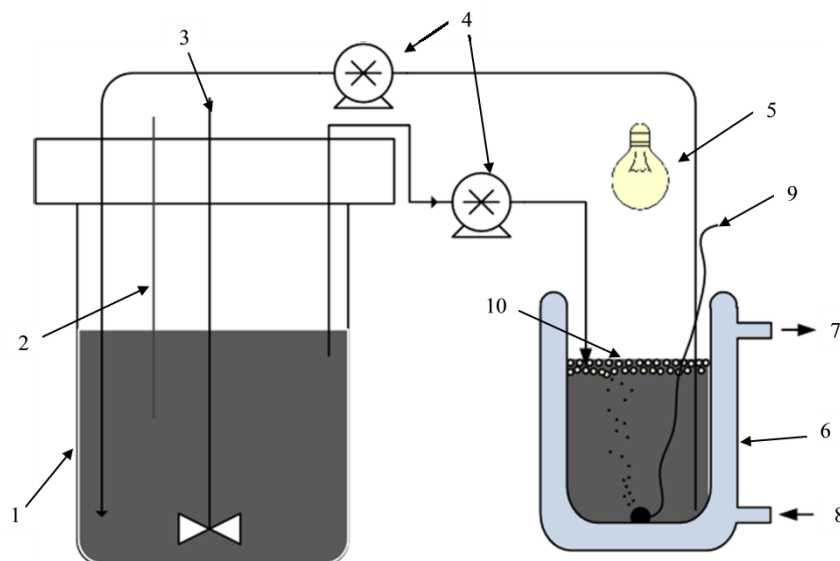


Figure 3-2: Schematic diagram of the experimental setup for photocatalytic degradation study: (1) feed reservoir (2 L solution); (2) sampling point; (3) overhead mixer; (4) peristaltic pumps; (5) 150 W Xenon lamp; (6) customized jacketed glass reactor (400 mL solution); (7) circulation water to external circulator; (8) circulation water from external circulator; (9) air supply to air diffuser and (10) buoyant composite photocatalysts

For a typical experiment, 10 g of a prepared composite photocatalyst was added into the reactor with a phenol concentration of 20 mg.L^{-1} and the system was put in the dark and stirred for the initial adsorption process to reach equilibrium. Then, the Xenon lamp irradiation was turned on for photocatalytic degradation to take place. The concentration of phenol in the reactor was monitored by taking samples at every 15 min interval. Similarly, this set of two-stage process setup was also used for the study on the effect of experimental conditions (i.e. chloride ions, solution pH, photocatalysts dosages, and initial phenol concentrations). All the tests are triplicated to ensure accuracy ($n=3$).

3.3. Results and discussions

3.3.1. Characteristics of prepared buoyant composite photocatalysts

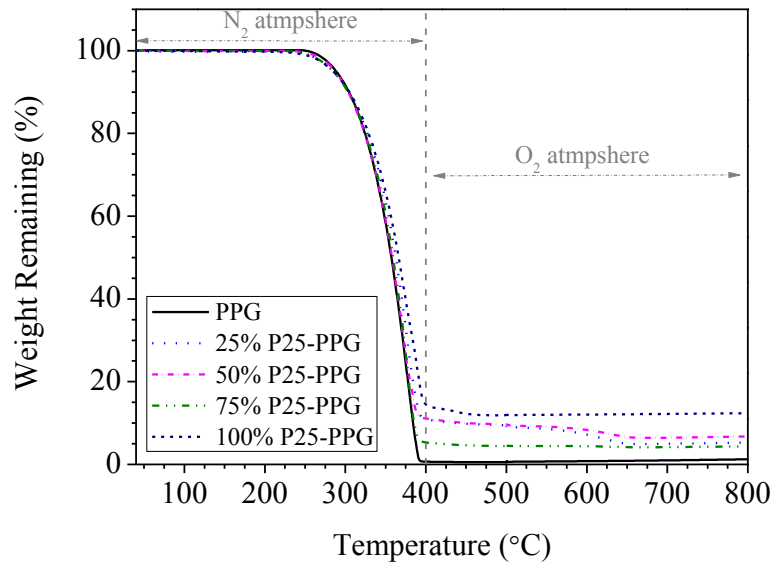


Figure 3-3: TGA analysis results for base PPG granules and for the prepared composite photocatalysts

The TGA results for the PPG granules and the 4 types of prepared composite photocatalysts are shown in *Figure 3-3*, with the analyzed composition information summarized in *Table 3-1*. For the PPG substrate, it was found that about 99.5% of the total mass was lost at 200-400 °C in nitrogen gas and the remaining of 0.5% was stable at 500-800 °C when air was supplied to the furnace. This suggested that the PPG substrate contained about 99.5% of organic content and the remaining 0.5% that cannot be completely burnt off (denoted as “Others” in *Table 3-1*) at 500-800 °C may be attributed to inorganic impurities. For the 4 types of prepared composite photocatalysts, the highest amount of immobilization was achieved by 100%P25-PPG (13.5wt %), which was probably due to the much greater density of P25 particles than that of PAC. For the other 3 types of composite photocatalysts immobilized with both P25 and PAC, higher percentage amounts of PAC immobilization were found to be

achieved with higher PAC percentages in the powder mixture. Whereas for P25 immobilization, the highest percentage amount was observed for 50%P25-PPG (where P25 and PAC were in equal percentage in the powder mixture) and those on 25%P25-PPG and 75%P25-PPG were similar but lower than that on 50%P25-PPG. It seems that the PAC content in the powder mixture had a greater effect on the immobilization amount of P25 on the PPG base granules. The above experimental results provide useful information if the immobilized composition of PAC and P25 on PPGs is to be varied. Moreover, all the calculated densities of the prepared composite photocatalysts from the measured compositions were smaller than 1 g.cm^{-3} , hence, confirmed that all the prepared composite photocatalysts were truly buoyant.

Table 3-1: Actual photocatalysts composition by TGA analysis

<i>Photocatalysts Type</i>	<i>Composition (%)</i>			
	PPG	PAC	P25	Others
PPG	99.5	0.0	0.0	0.5
25%P25-PPG	89.1	6.0	4.4	0.5
50%P25-PPG	88.9	5.2	5.4	0.5
75%P25-PPG	94.3	1.5	4.2	0.5
100%P25-PPG	86.0	0.0	13.5	0.5

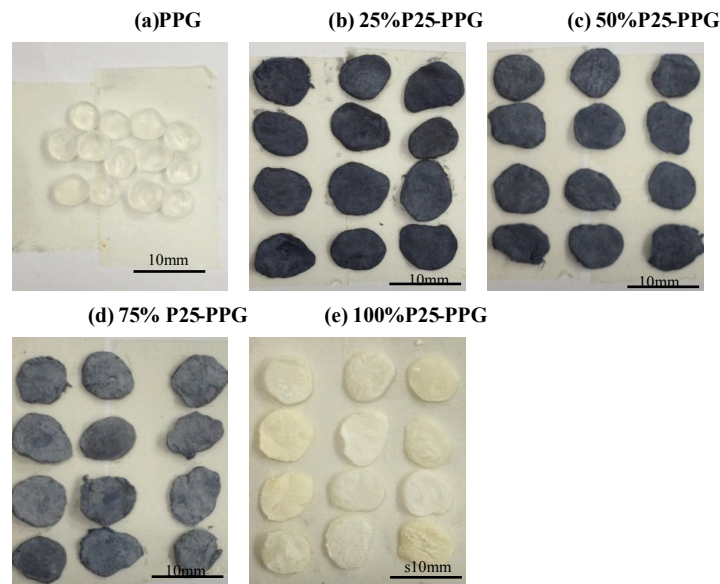


Figure 3-4: Photographs of the base PPG granules and the prepared composite photocatalysts

The photographs of the PPG substrate and the 4 types of prepared composite photocatalysts are shown in *Figure 3-4*. The PPG substrate had a regular round shape and a transparent color. It is observed that the PAC and P25 particles were firmly attached to the PPG substrate in the thermal immobilization process, and the shapes of the granules changed from round to thinner and irregular flat after the immobilization. The surface color of the prepared composite photocatalysts also changed from dark for 25%P25-PPG to whiter and eventually white for 100%P25-PPG, with the decrease of the PAC content. The PAC and P25 components appeared to be uniformly distributed on the surfaces of the PPG granules, suggesting that the immobilization process was effective. A typical FESEM image for 50%P25-PPG is shown in *Figure 3-5*.

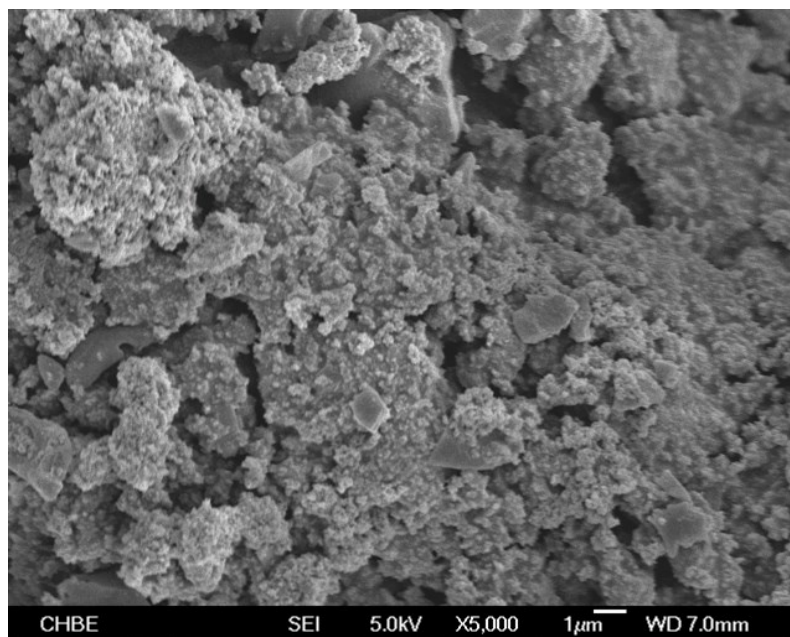


Figure 3-5: A typical FESEM image for 50%P25-PPG, showing PAC and P25 particles on the surface of prepared composite photocatalyst

3.3.2. Phenol removal by composite photocatalysts of different compositions

Blank test using phenol solution with air bubbling confirmed that phenol lost due to evaporation and direct photolysis was negligible (results not shown here). The results in dark adsorption of phenol with the prepared composite photocatalysts of different compositions as a function of adsorption time are shown in *Figure 3-6(a)*. It is clear that the adsorption uptake increased with the amount of PAC immobilized on the PPGs for each type of the composite photocatalysts (referring to *Table 3-1*). The 25%P25-PPG composite photocatalyst showed the highest adsorption uptake and took the longest time to reach the adsorption equilibrium. In contrast, the 100%P25-PPG composite photocatalyst showed almost no phenol adsorption at all. Since the 100%P25-PPG composite photocatalyst had no PAC component, it could be concluded that P25 had little phenol adsorption capacity, which is consistent with a previously reported study (Robert et al., 2000). For the 25%P25-PPG and 50%P25-PPG composite photocatalysts that showed high adsorption uptakes, the absorption

process was observed to be very fast initially and then gradually slowed down, indicating that the process was dependent on the concentration of phenol in the solution.

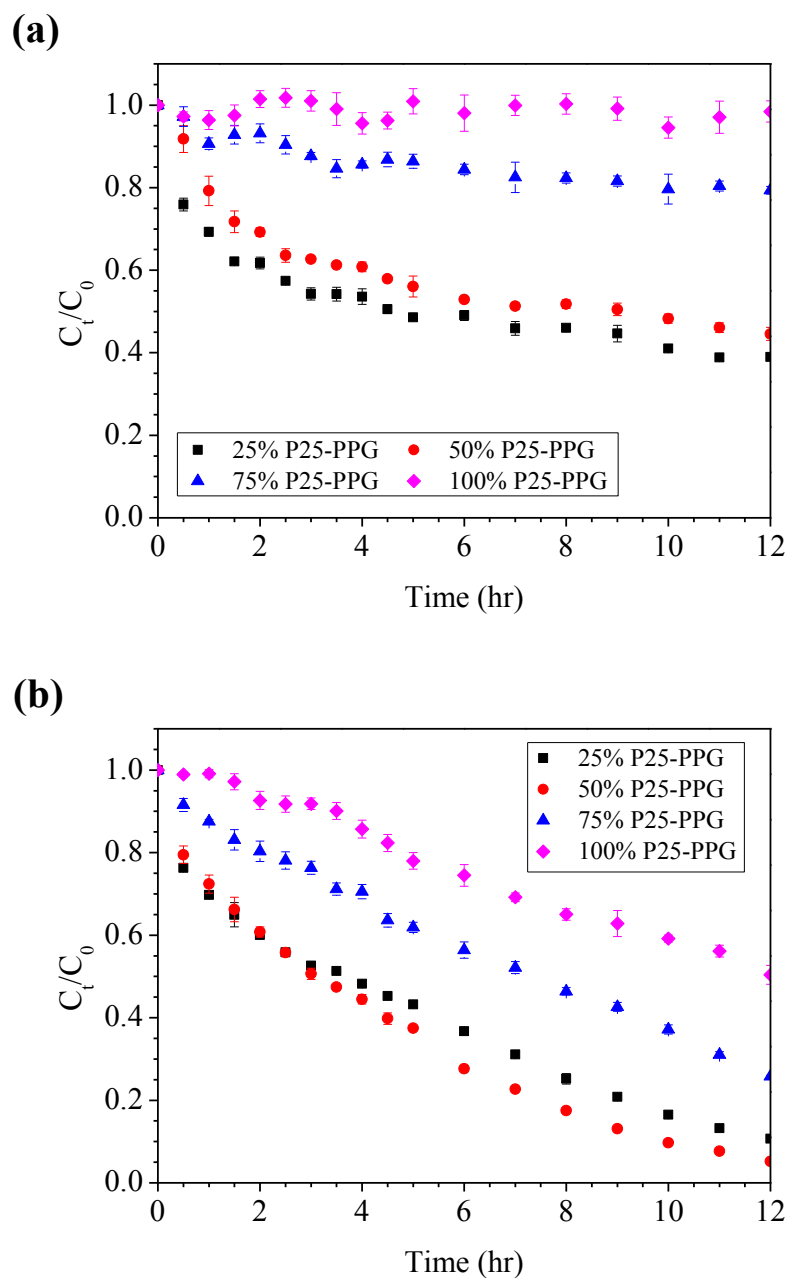


Figure 3-6: Phenol removal by the prepared composite photocatalysts of different compositions: (a) adsorptive removal in dark, and (b) combined adsorptive and photocatalytic degradation removal ($n=3$)

The combined adsorptive and photocatalytic degradation removals of phenol by the composite photocatalysts are shown in Figure 3-6(b). In terms of the total phenol

removal after a period of 12 hrs tested, the 50%P25-PPG composite photocatalyst achieved the highest and almost complete removal of all the phenol in the solution. The next highest removal was achieved by 25%P25-PPG, followed by 75%P25-PPG and 100%P25-PPG. In comparison with the results in *Figure 3-6(a)*, one of the most significant differences in *Figure 3-6(b)* is that the concentration of phenol in the solution was almost linearly decreased (i.e., the lines are straight), especially in the later stage (see from 2 to 12 hrs). Although the phenol concentration in the solution dropped greatly (due to removal) in the later stage, the instantaneous removal rate was still maintained at almost constant. The results suggest that the photocatalytic degradation process by the composite photocatalysts became less dependent on the bulk solution concentration. As compared to ordinary reactions that follows exponential manner, the concentration vs time plots for the composite photocatalysts are almost straight lines (reaction rate kept almost constant), instead of gradually decreased reaction rate with the decreasing bulk concentration. The again confirmed the hypothesis that the PAC component helped concentrate the organic pollutants from the solution and provided to the P25 photocatalyst component, which makes the photocatalytic degradation process less dependent on the concentration in the solution. On the other hand, the photocatalytic degradation removal of phenol by P25 from the PAC component helped the regeneration of the PAC component and thus improved its adsorption uptakes. Therefore, the results suggest that the combination of the photocatalytic component and the adsorbent component in the composite photocatalyst produced synergistic effect. For the 100%P25-PPG composite photocatalyst which did not have the PAC component, although the concentration profile over time also changed almost linearly, the overall removal was smaller, only 49% of total removal as compared to more than 75% of total removals as achieved by

the other composite photocatalysts. Therefore, the concentration of phenol in the solution was not a major controlling factor for the photocatalytic degradation of phenol. Bear in mind that the composite photocatalyst was already saturated with phenol by adsorption before the photocatalytic degradation process started, the decrease of phenol concentration in the solution shown in *Figure 3-6(b)* was completely attributed to a dynamic combination process of photocatalytic degradation and adsorption.

3.3.3. Adsorption isotherms

To have better idea on the contribution of the adsorbent component in the composite photocatalysts, the adsorption isotherm results of the composite photocatalysts in phenol removal are examined. The experimental results for the 3 types of composite photocatalysts with PAC component are shown in *Figure 3-7*. The results are also fitted with the popular Langmuir and Freundlich isotherm models and are included in *Figure 3-7* as well. In general, both models can fit the results satisfactorily, but the Langmuir model appears to give better description than the Freundlich model that tends to slightly overestimate the amount at higher solution concentrations. The determined model constants (q_m and b for the Langmuir model, K_F and n for the Freundlich model, respectively) are given in *Table 3-2*. Both q_m and b are found to increase with the increase of immobilized PAC amount in the composite photocatalysts, indicating that the adsorptive behavior of the composite photocatalysts was indeed mainly controlled by the PAC adsorbent component immobilized, due to the fact that TiO_2 photocatalyst component did not adsorb or had little adsorption effect on phenol. It is found that the K_F value in the Freundlich model decreased with the increase of the P25 composition percentage in the composite photocatalysts,

suggesting a reduced performance in phenol adsorption, agreed with the Langmuir model analysis. The values of n for all the 3 types of composite photocatalysts are greater than 1.0 indicating that phenol adsorption on the composite photocatalysts were favorable and the extent increased with the PAC percentage compositions.

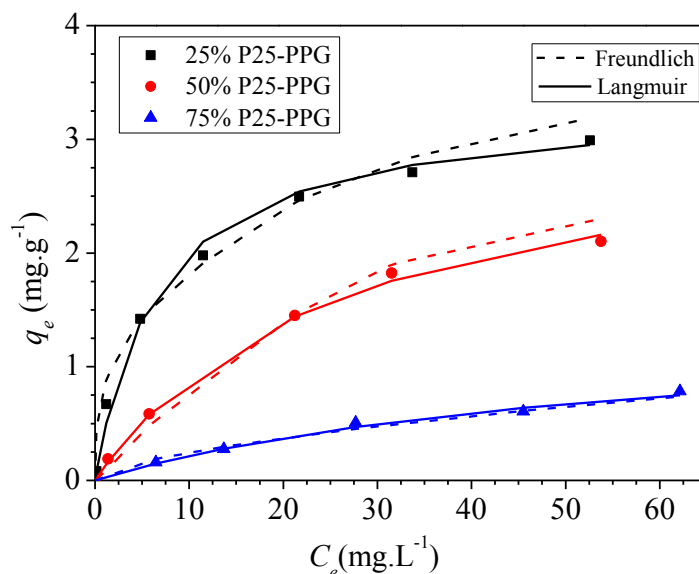


Figure 3-7: Adsorption isotherm data for phenol by the composite photocatalysts and the fitting results of the Langmuir and Freundlich isotherm models to the experimental data

Table 3-2: Adsorption isotherm parameters of phenol on different composite photocatalyst at 25°C

Photocatalysts Type	Langmuir Isotherm			Freundlich Isotherm		
	q_m ($\text{mg}\cdot\text{g}^{-1}$)	b ($\text{L}\cdot\text{mg}^{-1}$)	r^2	K_F ($\text{mg}^{1-(1/n)}\text{L}^{1/n}\cdot\text{g}^{-1}$)	n	r^2
25%P25-PPG	3.326	0.149	0.950	0.841	2.976	0.958
50%P25-PPG	3.204	0.039	0.983	0.311	2.138	0.801
75%P25-PPG	1.428	0.018	0.985	0.062	1.668	0.944

3.3.4. Kinetics of phenol removal in the photocatalytic degradation process

The results on phenol removal in the two-stage process, i.e., a first 2.5 hrs dark adsorption followed by 4 hrs photocatalytic degradation, as described in the experimental section, are shown in *Figure 3-8*. The dash line in *Figure 3-8* at time $t=0$ separates the dark adsorption period from the UV-induced photocatalytic degradation period. It is observed that the 4 types of composite photocatalysts all reached the adsorption equilibrium after the 2.5 hrs adsorption in dark. After the Xenon lamp was turned on at time $t=0$, phenol was further removed by the photocatalytic degradation and this continued for the entire 4 hrs photocatalytic degradation experiment. The net removal of phenol in this process by 25%P25-PPG, 50%P25-PPG, 75%P25-PPG and 100%P25-PPG composite photocatalysts was 6.83%, 6.23%, 1.51%, and 3.07%, respectively. Although 100%P25-PPG composite photocatalyst had the highest amount of P25, it did not achieve the highest removal of phenol in the photocatalytic degradation experiment. In contrast, the 25%P25-PPG and 50%P25-PPG composite photocatalysts had much higher phenol removal than 100%P25-PPG in the photocatalytic degradation experiments, even though they contained similar amounts of the P25 component. These results support the assumption that the addition of PAC with P25 in the composite photocatalyst can greatly enhance the performance of the photocatalytic degradation of phenol by the composite photocatalyst. For the 75%P25-PPG composite photocatalyst, however, the synergistic effect was not obvious. This may be attributed to the fact that the improvement by the inclusion of a small amount PAC was compromised by the reduction in the P25 amount immobilized on the composite photocatalyst. In other words, the ratio of immobilized P25 to PAC may play an important role in the performance of the prepared composite photocatalyst.

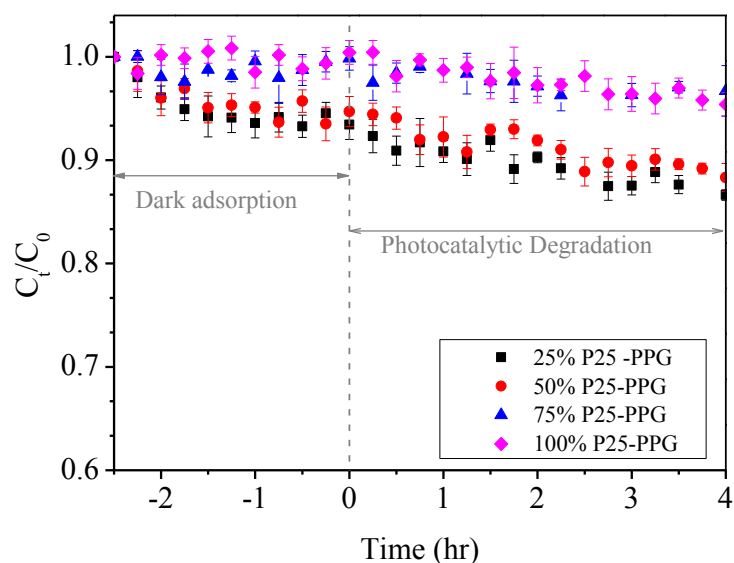


Figure 3-8: Removal of phenol in the two-stage processes with different types of composite photocatalysts ($n=3$)

Similar to the results shown in *Figure 3-5(b)*, the results in *Figure 3-8* for the photocatalytic stage also showed an almost linear decrease of phenol concentration in the solution with reaction time. However, the reaction rate appears to be dependent on the initial concentrations of phenol concentration when the photocatalytic degradation process began (i.e., at $t=0$) and on the type of composite photocatalyst used. Hence, a LH model kinetic analysis (eq. (2-24)) is carried out to provide a better and more quantitative comparison. With the data from the photocatalytic stage, the results from the model fitting analysis are shown in *Figure 3-9*.

The value of k_{app} , which has been proposed to indicate the photocatalytic activity of a composite photocatalyst (Matos et al., 1998), is determined from the slope of the linear plot and is included in *Table 3-3(a)*. In general, it is found that the photocatalytic activities of PAC-containing composite photocatalysts were significantly higher than that without PAC, except for the case of 75% P25-PPG. The results again reveal that the addition of an adequate amount of PAC to the composite

photocatalyst created a synergistic effect in the degradation kinetics, which may be further evaluated using the synergy factor derived from *eq. (2-34)* (da Silva and Faria, 2003; Matos et al., 1998):

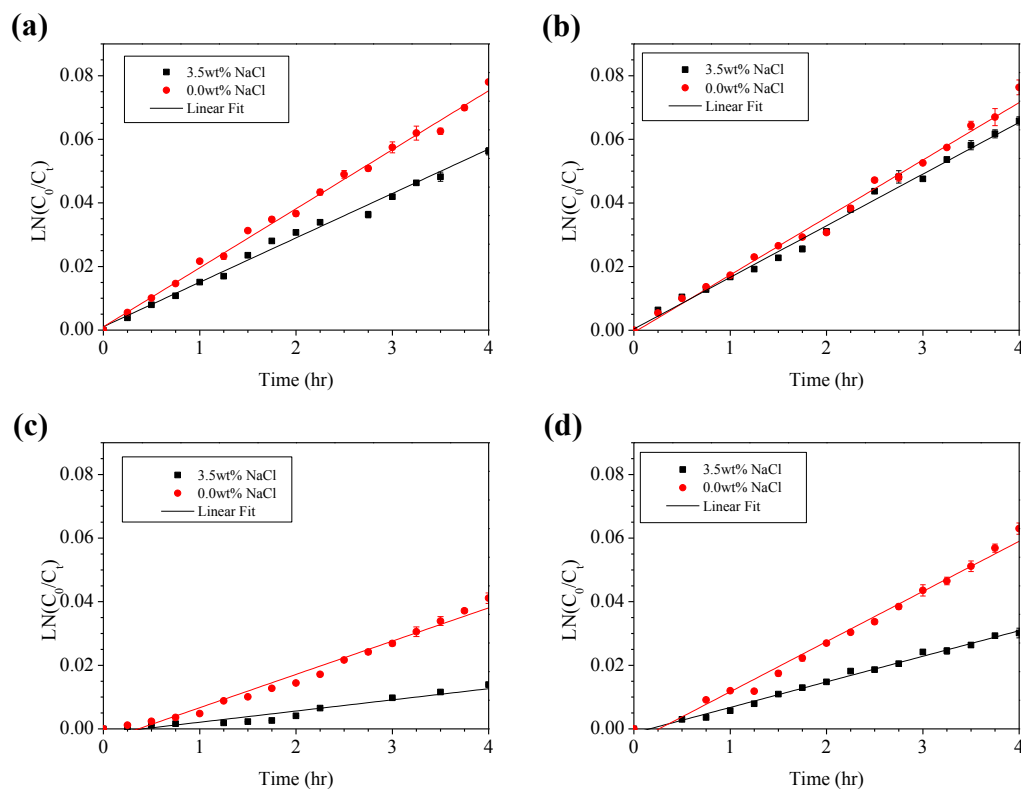


Figure 3-9: Kinetic study of phenol removal in the photocatalytic degradation stage by different composite photocatalysts and the fitting of kinetic model to the experimental data under different chloride ion concentrations: (a) 25%P25-PPG, (b) 50%P25-PPG, (c) 75%P25-PPG and (d) 100%P25-PPG ($n=3$)

The calculated R values are also included in *Table 3-3(a)*. Among the three PAC-containing composite photocatalysts, the 25%P25-PPG possessed the highest R value, followed by the 50%P25-PPG and 75%P25-PPG. A higher PAC loading may induce a better phenol concentrating effect from the solution to the vicinity or surface of the P25 photocatalyst component, thus leading to a faster photocatalytic degradation of phenol. The deviation of 75%P25-PPG in the performance behavior may be attributed to the same reason as discussed early. The overall performance of the composite is controlled by 3 steps, the rate of AC concentrating phenol from solution, the rate of

phenol transfer from AC to TiO₂ and the rate of phenol degradation by TiO₂. The three rates need to be properly balanced to achieve the optimum sustainable performance. In the case of 75%, there may be a greater degradation capability for the immobilized TiO₂, but the rate of phenol from AC may not be enough, due to the less amount of AC in the composite. The results in fact further explains the reason that adding AC component with TiO₂ can result in better performance.

$$R = \frac{k_{app}(\text{composite photocatalysts})}{k_{app}(100\%P25\ PPG)} \quad (3-4)$$

Table 3-3: Pseudo-first-order rate constants of phenol photocatalytic degradation by different composite photocatalysts and effect of chloride ions

(a) Cl⁻ free solutions (0.0wt%NaCl)

Photocatalysts Type	Dark adsorbed (mg)	Pseudo-first order kinetics		Synergy Factor [*]
		k_{app} (hr ⁻¹)	r^2	R
25%P25-PPG	3.06	0.019	0.98	1.18
50%P25-PPG	2.75	0.018	0.99	1.14
75%P25-PPG	0.73	0.011	0.96	0.72
100%P25-PPG	0.012	0.016	0.99	1.00

^{*}: synergistic factor $R = \frac{k_{app}}{k_{app}(100\%P25-PPG)}$

(b) Saline solutions (3.5wt% NaCl)

Photocatalysts Type	Dark adsorbed (mg)	Pseudo-first order kinetics		Synergy Factor ^a	%Reduced [#]
		k_{app} (hr ⁻¹)	r^2	R	
25%P25-PPG	3.00	0.014	0.99	2.27	24.7

50%P25-PPG	2.69	0.016	0.99	2.64	9.10
75%P25-PPG	0.71	0.004	0.97	0.62	67.0
100%P25-PPG	0.013	0.008	0.98	1.00	50.0

$$\#: \%Reduced = \left(1 - \frac{k_{app,saline}}{k_{app,Cl^{-}free}}\right) \times 100$$

3.3.5. Effect of experimental conditions on phenol removal

The effect of experimental conditions, i.e. (a) chloride ions, (b) solution pH, (c) photocatalysts dosages and (d) phenol initial concentration, were studied using the two-stage process setup described in Section 3.2.6.

(a) Effect of chlorine ions.

Phenol wastewater often contains a significant amount of inorganic salts. The presence of the inorganic ions has been shown to influence the kinetics and mechanism of photocatalytic transformation of organic compounds (Calza and Pelizzetti, 2001). Chloride ion is the most commonly found inorganic ions in various wastewaters. Hence the effect of chloride ions was investigated in this study. The photocatalytic activity of phenol degradation by the prepared composite photocatalysts in a saline solution of 3.5wt% NaCl was compared with that in a chloride free solution (i.e., 0.0wt% NaCl). The results are also shown in *Figure 3-9* and the determined pseudo-first-order rate constants included in *Table 3-3(b)*. As shown in the first column of *Table 3-3*, the presence of sodium chloride in the solution almost had no effect on the composite photocatalyst adsorptivity. However, the photocatalytic activity was indeed greatly affected by the presence of Cl^{-} ions, except for the case of 50%P25-PPG which was almost not affected. The photocatalytic activity of 75%P25-PPG, in terms of the k_{app} value, decreased the most, by 67.0% when the concentration of Cl^{-} ions increased from 0.0wt% to 3.5wt%. This

was followed by 100%P25-PPG at about 50.0% reduction, and 25%P25-PPG at 24.7%. Hence, the results suggest that a proper combination ratio of PAC to P25 immobilized on the composite photocatalysts may lead to a shielding effect to the negative influence of Cl^- ions on phenol photocatalytic degradation, as in the case of 50%P25-PPG. The solution pH was monitored with a pH sensor throughout the whole process and only a small pH decreases (from 5.6 to 5.4) were observed after 4 hrs photocatalytic degradation. At pH 5 to 6, the positively charged TiOH_2^+ and TiOH are the main functional groups on the photocatalysts surface, hence, the negatively charged Cl^- compete with organic species for these active sites, and lowered the photocatalytic degradation reaction rate. On the other hand, the presence of strong adsorption force largely increased the organic concentration around the photocatalysts and increased the phenol's competitiveness towards chloride ions. Hence, the photocatalytic activity of 25%P25-PPG and 50%P25-PPG was less affected than the 75%P25-PPG, due to the higher P25 and PAC loading. Besides adsorb onto TiO_2 surface, Cl^- can also recombine with the free radicals, and thus, decrease the reaction between the organic species and free radicals. The 25%P25-PPG had the strongest adsorptivity, but it has the lowest P25 loading on it, so its free radical production was lower and the chloride ions' radical scavenger effect would be more obvious than that of 50%P25-PPG. Hence, 50%P25-PPG was chosen as the optimal composite photocatalyst for further studies described below.

(b) Effect of initial pH.

The pH value of the solution may also be a key factor for the photocatalytic reaction because it would affect the surface charge of the photocatalyst (Liotta et al., 2009; Robert et al., 2000) and the formation of hydroxyl radicals between hydroxyl ions and positive holes on the surface of TiO_2 (Ahmed et al., 2011; Qamar et al.,

2006). The two-stage process performances by the 50%P25-PPG composite photocatalyst was investigated in an initial pH (pH_0) range of 2-10. The experimental results obtained in the dark adsorption stage and photocatalytic degradation stages are summarized in *Table 3-4*. It appears that the solution pH has little effect on the adsorptivity of the composite photocatalyst. On the other hand, the effect of pH on the photocatalytic activity was more significant. The k_{app} value slightly increased first when the solution pH increased from pH 2.0 to 6.0, but decreased when the solution pH was further increased to 10. According to *eq. (3-5)*, the low OH^- concentration in acidic conditions hinders the formation of hydroxyl radicals ($\bullet OH$) with photogenerated positive holes (h^+) and subsequently reduces the degradation rate.



On the other hand, both the TiO_2 surface and phenol molecules are negatively charged under alkaline conditions. Thus, the Columbic repulsion led to the decrease of the photocatalytic activity. Besides, the adsorption of OH^- ions onto TiO_2 surface also created a competition with the phenolate anions, which can also result in a lower photocatalytic activity. Overall, the photocatalytic degradation process appeared to perform better under acidic condition than under alkaline condition.

Table 3-4: Effect of pH on the adsorptivity and photocatalytic activity of 50%P25-PPG

initial pH	2.0	4.0	6.0	8.0	10.0
amount adsorbed ($mg \cdot g^{-1}$)	0.283	0.297	0.299	0.278	0.256
k_{app} (hr^{-1})	0.0151	0.0161	0.0162	0.0128	0.0093

(c) Effect of composite photocatalyst dosage.

The dosage of photocatalyst can be an important parameter in photocatalytic degradation process performance. Several studies reported that an optimal photocatalyst dosage existed for the maximum removal of phenol. This optimum dosage depends on the geometry of the reactor, light source intensity, and properties of TiO_2 such as particles size, phase compositions and impurities (Chen et al., 2000b). This is due to that the increase of the photocatalyst dosage beyond the optimal range may result in unfavorable light scattering and thus reduction of the photon efficiency. In the same two-stage process setup, a variety of dosages ranging from 5 to 30g in 400mL photoreactor were therefore tested. For the dosages greater than 10g, a longer dark adsorption period was allowed to establish the adsorption equilibrium before turning on the Xenon lamp for photocatalytic degradation to start. The experimental results in the effect of the composite photocatalyst dosage on the adsorption uptake and photocatalytic degradation activity of phenol are summarized in *Table 3-5*. When composite photocatalyst dosage increased from 5g to 20g, both phenol adsorption and photocatalytic degradation activity showed linear increases with the increase of the dosage. However, further increases of the photocatalyst dosage to 30g resulted in a decreased photocatalytic degradation activity, even although the adsorptivity continued to increase (due to increased amount of PAC component). Therefore, a proper dosage is indeed desirable. According to the phenol removal results in *Table 3-5*, 10g to 20g composite photocatalysts dosage should be adequate for the photocatalytic degradation system used in this study (400 mL solution in the reactor with a 3.5 inch irradiation diameter), which is equivalent to 25-50 g.L^{-1} composite photocatalysts loadings or 1.35-2.7 g.L^{-1} P25 as calculated according to the measured photocatalyst compositions in section 3.3.1.

Table 3-5: Effect of dosage on the adsorptivity and photocatalytic activity of 50%P25-PPG

dosage (g)	5.0	10.0	15.0	20.0	30.0
amount adsorbed (mg.g ⁻¹)	0.196	0.299	0.668	0.986	1.664
k_{app} (hr ⁻¹)	0.0125	0.0162	0.0198	0.0247	0.0195

(d) Effect of initial phenol concentration

Under the same operation conditions, a variation in the initial concentration of phenol (C_0) will result in different irradiation and reaction time required to complete the degradation process. The adsorption and photocatalytic degradation performances were studied at different initial phenol concentrations ranging from 10-80 mg.L⁻¹. The solution pH value was controlled at 5.6-6.0. The results of the effect of C_0 on phenol adsorption and the determined pseudo-first-order rate constants for phenol photocatalytic degradation are summarized in Table 3-6. Clearly, the amount of phenol adsorbed per unit weight of the composite photocatalyst increased with the increase of C_0 . However, the pseudo-first order rate constant, k_{app} , decreased with the increase of C_0 . This may be expected because only fixed amounts of TiO₂ particles were available to produce hydroxyl radicals for phenol degradation. The fraction of phenol that could be degraded became smaller when the initial phenol concentration increased.

Table 3-6: Effect of initial phenol concentration on the adsorptivity and photocatalytic activity of 50%P25-PPG

initial phenol concentration (mg.L ⁻¹)	$C_0=10.0$	$C_0=20.0$	$C_0=40.0$	$C_0=60.0$	$C_0=80.0$
amount adsorbed (mg.g ⁻¹)	0.253	0.299	0.585	0.609	0.803
k_{app} (hr ⁻¹)	0.0184	0.0162	0.0122	0.0105	0.0076

3.4. Conclusions

The buoyant composite photocatalysts were successfully prepared by thermal immobilization of PAC and P25 onto PPG at temperature slightly higher than its melting temperature. All the prepared photocatalysts had density less than that of water, and can float on water surface. Composite photocatalysts of different compositions were prepared by varying the P25: PAC ratios in the powder mixture. The actual photocatalysts composition was analyzed by TGA. Higher amount of PAC immobilization can be achieved with higher PAC percentage in the powder mixture. Whereas, the dependence of the amount of P25 immobilized on the substrate on the percentage of P25 in the powder mixture was not significant. The FESEM observation confirmed that both P25 and PAC were uniformly distributed on the PPG surface. The adsorptive and photocatalytic performances of the obtained photocatalysts were evaluated for phenol removals in aqueous solutions under various experimental conditions. The higher PAC percentage in the powder mixture lead to better adsorptivity and the adsorption isotherm can be well described by the Langmuir model. Enhanced photocatalytic degradation activity was observed with the composite photocatalysts prepared by P25 and PAC powder mixture, especially at the composition of that for the 50%P25-PPG. The synergistic effect of the P25-PAC combination has been found from the increase in the photocatalytic activity and in the shielding effect on inhibitory inorganic ions, thus, confirming the hypothesis that enhanced photocatalytic activity can be achieved by concentrating organic molecules around the photocatalysts with PAC as the adsorbent. The kinetics of the phenol degradation by the composite photocatalysts fits well with the Langmuir–Hinshelwood model. The operation parameters were further studied with 50%P25-PPG, and it was found to perform better under acidic conditions than alkaline ones,

and has the optimal photocatalysts dosage at 1.35-2.7 g.L⁻¹ P25 under the experimental condition used in this study.

Chapter 4: A Buoyant Composite Photocatalyst Prepared by a Two-Layered Configuration and Its Enhanced Performances in Phenol Removal from Aqueous Solutions

4.1. Introduction

Among the many developments in TiO₂-based photocatalytic degradation processes, buoyant photocatalysts have offered a good solution to achieve high light utilization efficiency and low post separation cost (Han and Bai, 2009). Buoyant photocatalysts can allow photocatalytic degradation to take place on water surface and thus achieve greater utilization efficiency of the light provided because light attenuation is much lower in air than in water medium (Fabiya and Skelton, 2000; Han and Bai, 2009). Enhanced oxygenation of buoyant photocatalysts at the water/air interface is also obtained due to the higher oxygen content at the water/air interface than that in water. Beside, buoyant photocatalysts can be easily separated from the treated water and thus eliminate the post separation issue often concerned. However, the use of those macro-supports as the substrate may result in low photocatalytic performance, due to the limited amount of TiO₂ immobilized on the substrate (Matthews, 1988; Turchi and Ollis, 1988), and the buoyant photocatalysts can reduce the mass transfer rate of organic pollutants in the bulk solution to the photocatalysts on the water surface, attributed to the large transport distance and the non-adsorptive feature of the photocatalysts used (Ahmed et al., 1999; Naskar et al., 1998). The detachment of immobilized TiO₂ particles from the substrate sometimes may also become a concern during long periods of usage (Chen et al., 2000a; Krýsa et al., 2005; Lam et al., 2010). Although hollow glass microspheres as the substrate may

provide excellent stability to photocatalytic degradation for the prepared product, the use of such substrate was generally expensive in the material as well as for the immobilization of TiO_2 , besides their being very fragile in handling. In contrast, low density thermoplastics, such as polypropylene (PP), have been more preferred for TiO_2 immobilization to prepared buoyant photocatalysts. The plastic substrates can offer the advantages of low price, reasonably good mechanical strength, good UV and/or chemical stability, and excellent processing flexibility in the final shape and dimension of the products. To minimize the effect of low mass transfer rate and thus increase the photocatalytic efficiency, co-adsorbents have been used together with the TiO_2 photocatalyst, particularly such as in the case of combining TiO_2 with powdered activated carbon (PAC) (Li Puma et al., 2008; Lim et al., 2011). In the previous chapter, we have successfully prepared buoyant composite photocatalysts through a thermal bonding process, by immobilizing TiO_2 nanoparticles as the photocatalytic component and PAC as the co-adsorbent in a mixture simultaneously onto the polypropylene granule (PPG) substrate (Tu et al., 2013). The study showed that the PAC component in the composite photocatalysts helped concentrating the organic pollutants in the bulk solution to the vicinity of the photocatalyst particles and thus made the photocatalytic degradation process of phenol more efficient and less dependent on its concentration in the bulk solution. However, the buoyant composite photocatalysts prepared by simultaneously immobilizing PAC and P25 together showed some detachment of the P25 nanoparticles and thus unstable performance after extended long periods of usage, attributed to the slow photocatalytic degradation of the PPG substrate immobilized with P25 particles in the process. Therefore, it is of great interest to improve the photocatalytic degradation stability of the developed

buoyant composite photocatalyst for its potential use in long term practical applications for organic pollutant removal.

In this chapter, a new method of preparing buoyant composite photocatalyst with better stability and performance was developed through a novel two-layered configuration, i.e., a PAC layer followed by a P25 layer, on the PPGs. PAC was used in this study not only as a good co-adsorbent, but also as an inert material that can resist radical attack to wrap and therefore protect the PPG substrate. Instead of directly immobilizing a mixture of PAC and P25 onto the PPG surface, an entire PAC layer was first anchored onto the PPG surface in this study through a thermal bonding process similar to that used in chapter 3. Then, another layer of P25 nanoparticles was loaded onto the PAC-immobilized PPG (denoted as PPG-PAC) by a new suspension hydrothermal deposition method. The large specific surface area of the anchored PAC may also help to achieve more P25 nanoparticles being loaded on the prepared buoyant composite photocatalyst (PPG-PAC-P25). Phenol was again selected as a target organic pollutant to evaluate the performances of the developed buoyant composite photocatalyst. A series of characterization analyses and photocatalytic degradation tests were conducted. The primary objectives of this study are to examine how the two-layered configuration, i.e., placed PAC between the PPG substrate and the P25 photocatalytic particles, would enhance the structural stability and the photocatalytic degradation performance of the developed buoyant composite photocatalyst.

4.2. Experimental

4.2.1. Preparation of buoyant composite photocatalyst in two-layered configuration

The raw materials, the PPG substrate, P25 photocatalysts and PAC, are the same as mentioned in *Chapter 3*. The cleaned PPGs were first immobilized with a PAC layer as described in *Section 3.2.2* with entirely the PAC powder. The PAC-immobilized PPGs (denoted as PPG-PAC) were collected and cooled down naturally to the room temperature in a fume hood. Then, the PPG-PAC was washed thoroughly with an ethanol/water (20/80 volume) mixture, followed by tap water for several rounds till no obvious black solids were observed in the washing water. After that, the cleaned PPG-PAC was dried in an oven at 80°C overnight, and then cooled down naturally and stored for further use. To load P25 nanoparticles onto PPG-PAC, a homogeneous P25 nanoparticle suspension was prepared using a hydrothermal reactor (900 mL, Berghof Br900, Germany) with isopropyl alcohol (IPA, AC grade, from Tedia) as the solvent (Han and Bai, 2009). 15 g of P25 and 300 mL of IPA were added into the reactor vessel. The reactor was tightly closed and the contents in the reactor were stirred with a PTFE lined stirrer bar at 500 rpm and heated up to 180 °C on a hotplate stirrer (Heidolph, Germany). The process was continued at 180 °C for 4 hours. After that, the contents in the reactor were slowly cooled down to the room temperature and transferred into a 500 mL amber glass bottle while maintained stirring at 500 rpm all the time. The P25 suspension so prepared in IPA was found to be very stable (Lee et al., 2010), and was also expected to enhance the interaction of P25 with PAC in the following immobilization process (Kusiak-Nejman et al., 2011; Leon y Leon et al., 1992; Rodríguez-reinoso, 1998). Then, 20 grams of the cleaned PPG-PAC were soaked into 50 mL of the above prepared P25 suspension for 30 min in a 250 mL beaker that was stirred at 250 rpm with a PTFE lined magnetic stirrer.

The beaker was covered with a piece of aluminum foil to minimize the evaporation of IPA. After that, the P25-loaded PPG-PAC granules were separated from the solution with a sieve, and then slowly dried in the fume hood with medium ventilation. The loaded P25 layer on PPG-PAC was subsequently cured in an oven, with a programmed heating process from 80 to 145 °C, and stayed at 145 °C for 90 min, before finally cooled down to the room temperature naturally. The curing process was not only to reinforce the P25 TiO₂ deposition layer, but also, at the same time, to remove any adsorbed IPA by the PAC on PPG-PAC. The soak-dry-cure cycle was repeated for another round for more P25 nanoparticles to be loaded onto PPG-PAC. The product so obtained in this study will be referred to as the PPG-PAC-P25 buoyant composite photocatalyst or in short PPG-PAC-P25. The developed composite photocatalyst was also washed with tap water to remove any possible loosely loaded P25 nanoparticles before further use. To compare the performance, composite photocatalyst described in *Chapter 3* by the previous method were also prepared.

4.2.2. Characterization of prepared composite photocatalysts

The actual compositions of the prepared PPG-PAC-P25, 25%P25-PPG and 100%P25-PPG composite photocatalysts, as well as the PPG substrate and the PPG-PAC intermediate, were determined using the thermal gravimetric analyzer (TGA, TGA2950, DuPont Instruments, USA). The detailed procedure was the same as mentioned in *Section 3.2.3* of *Chapter 3*.

The surface morphologies of PPG-PAC, 25%P25-PPG and PPG-PAC-P25 were examined with a field emission scanning electron microscope (FESEM, JEOL JSM-6700F, Japan) under 5kV electron beam, following the standard measurement procedures as mentioned in earlier (*Section 3.2.3*).

4.2.3. Stability tests against photocatalytic degradation and mechanical attrition

The stability of the prepared composite photocatalysts was tested against the photocatalytic degradation and mechanical attrition. The changes of the total dry weight of the composite materials and the solution turbidity and total organic carbon (TOC) content were monitored and analyzed. The tests were conducted in a photocatalytic reactor system consisting of a customized jacketed cylindrical reactor (8.5 cm outer diameter, 7.5 cm inner diameter, 9 cm height, and 400 mL capacity), an external water circulator (Julabo, Germany) for the temperature control (at 25°C), a porous stone diffuser placed at the reactor bottom to provide aeration and mixing for the contents in the reactor, and a 150 W Xenon lamp (Newport, USA) installed 10 cm above the solution surface in the reactor to provide UV light irradiation (69 mm radiation diameter and around 48 W.m⁻² UV light power) when needed. For a specific test in the photocatalytic degradation stability of the materials, a certain amount of each type of the prepared composite photocatalysts (corresponding to a loading amount of 138 mg P25) was suspended in 200 mL ultrapure water in the reactor. The exact dosages for each type of the composite photocatalysts added in the experiments are given in *Table 4-1* under the column title of “5. Dosage (P25)”. For a test run (with UV light irradiation on and air bubbling) reaching a designated time duration, the contents in the reactor were transferred into a 400 mL glass beaker and heated to boiling on a hotplate (Heidolph, Germany) for 3 mins to release any possibly adsorbed organic matters on the PAC component of the composite photocatalyst (Crittenden et al., 1997). The turbidity of the solution was then measured with a portable spectrophotometer (Hach DR/2010, US), and the TOC of the solution was analyzed with a TOC analyzer (Shimadzu TOC-V_{CPH} with ASI-V auto sampler, Japan) after filtering the sample through a 0.45µm membrane filter, which was to give

an indication in the extent of photocatalytic degradation of the composite photocatalyst, if any. In addition, the composite photocatalyst granules in the solution were collected with a sieve, dried in an oven at 80°C overnight, and then re-weighed after cooled down to room temperature to determine whether any weight loss and how much occurred. The composite photocatalyst granules were then re-suspended in a new batch of 200 mL ultra-pure water and another round of the irradiation-boil-dry cycle was conducted. This was continued until a total 120 hours of the photocatalytic degradation time were reached for each type of the prepared composite photocatalysts. Similar tests were also conducted for the PPGs and PPG-PAC that did not have the P25 component (In these cases, the dosages of P25 in the solution were determined according to the PPG and P25 contents in the PPG-PAC-P25 sample, and thus 11.85 g of PPG and 138 mg P25 were added into the solution, the latter was to provide the photocatalytic component and thus incur the photocatalytic degradation capability). In these cases, the solution turbidities were not measured but TOC analyzed. The stability of the prepared composite photocatalysts against mechanical attrition and mixing was also tested with the same procedure as mentioned above, but without the UV light irradiation. This was to examine to what extent the PAC and P25 particles may be detached from the PPG substrate due to operational factors such as mechanical stirring or air bubbling. All the tests are triplicated to ensure accuracy (n=3).

4.2.4. Dark adsorption experiments

The adsorptive property of the various types of prepared buoyant composite photocatalysts was evaluated through adsorption of phenol in aqueous solutions under dark condition. The experiments were carried out in a number of 250 mL Erlenmeyer flasks, each of which, containing 200 mL phenol solution with an initial phenol concentration at 20 mg L^{-1} and an initial solution pH value 5.6, was added with an appropriate amount of a specific type of the prepared buoyant composite photocatalysts that contained the same amount of immobilized PAC component (at around 241 mg). The exact weight dosages for each type of the composite photocatalysts in the experiments are also included in *Table 4-1* under the column title of “4. Dosage (PAC)”. Each flask was sealed and wrapped with an aluminum foil and the contents in all the flasks were stirred on a shaker at 170 rpm under the room temperature ($25 \pm 1^\circ\text{C}$) for 48 hours. All the tests are triplicated to ensure accuracy ($n=3$). The remaining phenol concentration in the solution in each flask was measured at various time intervals and the specific amount of phenol adsorbed per unit gram of the PAC on each type of the buoyant composite photocatalysts was calculated by *eq. (4-1)*:

$$q_t = \frac{V(C_0 - C_t)}{M} \quad (4-1)$$

where q_t is the specific amount of phenol adsorbed (mg.g^{-1} of PAC) at adsorption time t , V is the volume of phenol solution in each flask (0.2 L), C_0 (mg L^{-1}) and C_t (mg L^{-1}) are the phenol concentrations in the solution initially ($t=0$) and at adsorption time t , respectively, and M is the mass of PAC on the composite photocatalysts added in each flask (0.241 g).

The adsorptive performance of the 100%P25-PPG composite photocatalyst was also examined even though they did not contain the PAC component. The

experiments were similarly done as described above but the amount of 100%P25 PPG added into each flask was according to a loading of 138 mg P25, so that the specific amount of phenol adsorbed (q_t) by 100%P25-PPG was calculated according to P25 amount, $M=0.138\text{g}$.

4.2.5. Phenol removal experiments with prepared composite photocatalysts

The behavior and performance of phenol removal by the three types of the buoyant composite photocatalysts (i.e., PPG-PAC-P25, 25%P25-PPG and 100%P25-PPG) was investigated with the same photocatalytic reactor system mentioned before in *Section 4.2.3*. For experiments with combined adsorption and photocatalytic degradation effects in phenol removal, a quantity of each type of the prepared composite photocatalysts, corresponding to an immobilized P25 amount of 138 mg, was suspended in the phenol solution (with a solution volume of 220 mL and initial phenol concentration of $C_{in}=20\text{ mg L}^{-1}$, containing NaCl at 0.5 wt. %) in the reactor that was put under the UV light irradiation. The phenol concentration in the solution was monitored until the complete removal of phenol in the solution or 11 hrs of operation run, whichever was shorter, was reached. During the test runs, about 2 mL sample solution was taken at each of the desired time intervals and used for the analysis of phenol concentration remained in the solution in the reactor by a UV/VIS spectrophotometer (Jasco V-660, Japan) at $\lambda_{\text{max}}=270\text{ nm}$. All the tests are triplicated to ensure accuracy ($n=3$).

Experiments were also conducted on the kinetic removal of phenol by photocatalytic degradation by separating the effect of adsorption on phenol removal in the process. Each type of the prepared composite photocatalysts was first added into the phenol solution (as specified above) in a 250 mL conical flask that was completely

wrapped with an aluminum foil. The flask was placed on a shaker stirred at 170 rpm under the room temperature ($25\pm 1^\circ\text{C}$) for 72 hrs to establish adsorption equilibrium of phenol on the material. The content in the flask was then transferred into the photocatalytic reactor with the UV light irradiation for the photocatalytic degradation process to start. The initial phenol concentration in the solution for the photocatalytic degradation process, C_0 , was determined after the 72 hrs dark adsorption. Other conditions in the experiments were the same as described above and the photocatalytic degradation process continued for 4 hrs. Samples were taken and analyzed for phenol concentration in the solution at various time intervals.

4.2.6. Batch tests on recyclable usage of developed composite photocatalyst

In order to evaluate the possible long-term service potential of the developed composite photocatalyst, a series of repeated batch runs using PPG-PAC-P25 for phenol removal was conducted in the same photocatalytic reactor system as mentioned earlier. A 12.3 g amount of PPG-PAC-P25 was firstly added to 200 mL of the phenol solution with an initial concentration of 20 mgL^{-1} under UV light irradiation for direct phenol removal (i.e., without the 72 hrs dark adsorption equilibrium stage). After a complete phenol removal was achieved (in 10 hrs), the composite photocatalyst was collected and immediately re-suspended into another fresh batch of 200 mL of the phenol solution, without any washing or drying process, for the next round of phenol removal. The concentrations of phenol and TOC in the solution were both measured before and after the 10 hrs run to determine their removal efficiencies achieved in each repeated run. A total of 20 cycles was conducted. For a comparison purpose, the recyclability of 25%P25-PPG was also

similarly tested but only did for 5 cycles, because of its greater change in the performance.

4.3. Results and discussions

4.3.1. Characteristics of prepared buoyant composite photocatalysts

The results from the TGA analysis for the actual compositions of the three types of prepared composite photocatalysts (i.e., PPG-PAC-P25, 25%P25-PPG and 100%P25-PPG), and for the PPG substrate as well as the PPG-PAC intermediate, are shown in *Figure 4-1*, and summarized in *Table 4-1*. For the PPG substrate, about 99.5% of the total mass was lost in the temperature range of 200-400 °C with nitrogen as the carrier gas and the remaining (0.5%) was stable at the temperature up to 800 °C and with air supply to the furnace. This suggests that the PPG substrate contained about 99.5% of easily decomposed organic content and the remaining 0.5% that cannot be completely burnt off (denoted as “Others” in *Table 4-1*) may be attributed to inorganic impurities or additives contained in the PPG substrate. For the PPG-PAC intermediate, the PAC component appeared to be completely burnt off in the temperature range of 400-700 °C with air supply to the furnace, which contributed to about 2.58% of the total weight lost, and the remaining (about 0.5%) remained stable in the temperature range up to 800 °C, indicating those inorganic components contained in PPG. For 100%P25-PPG, weight loss again occurred for PPG in the temperature range of 200-400°C, but no further weight change was observed after 400°C in the air environment in the furnace, suggesting that the P25 component was stable at temperature up to 800°C. Hence, it can be confirmed that the two stage TGA measurements (from room temperature to 400°C with N₂ as carrier gas followed by 400-800°C with air as carrier gas) can clearly distinguish and thus give the composition information contained in the prepared composite photocatalysts (i.e., the PP polymer, PAC and P25 components). For the other two composite photocatalysts of 25%P25-PPG and PPG-PAC-P25 with all components of PPG, PAC and P25, the

weight loss patterns were found to be similar to each of the specific components of PPG, PAC and P25 mentioned above. The analysis also clearly showed, as given in *Table 4-1*, that the composite photocatalyst prepared by the new method (PPG-PAC-P25) achieved much lower amount immobilization for both the PAC and the P25 components than that prepared by the previous method (25%P25-PPG) on the PPG substrate.

Table 4-1: Actual compositions of the substrate and the prepared composite materials obtained from the TGA analysis

1. Photocatalysts <i>Type</i>	2. Composition (%)				3. P25:PAC	4. Dosage (PAC)[*] (g)	5. Dosage (P25)[#] (g)
	PP	PAC	P25	Others			
PPG	99.50	0.00	0.00	0.50	-	-	-
PPG-PAC	96.93	2.58	0.00	0.49	-	9.344	
PPG-PAC-P25	96.43	1.96	1.12	0.48	1 : 1.75	12.30	12.30
25%P25-PPG	89.10	6.00	4.40	0.47	1: 1.35	4.018	3.131
100%P25-PPG	86.00	0.00	13.6	0.46	-	1.013	1.013

^{*}: The dosage is calculated according to 241 mg PAC immobilized on the PAC-PPGs substrates, except 100%P25-PPG that based on 138 mg of P25.

[#]: The dosage is calculated according to 68 mg P25 immobilized on the PAC-PPGs substrates

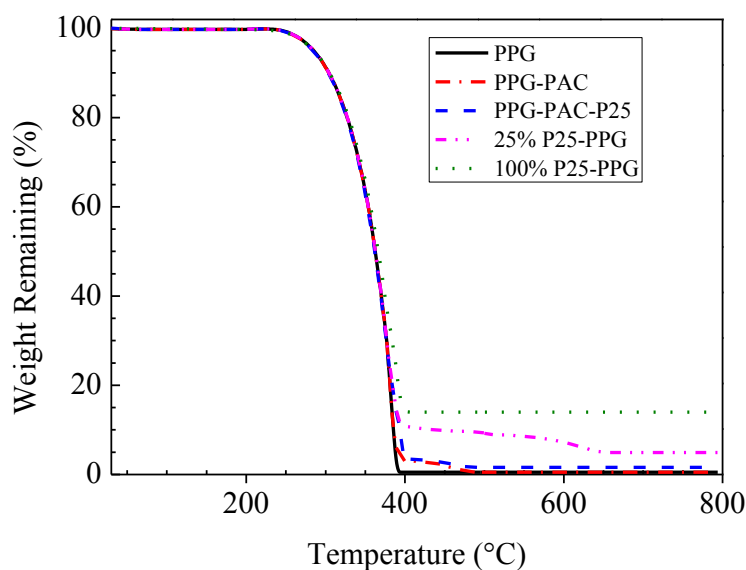


Figure 4-1: Results from TGA analysis for the PPG substrate and the prepared various composite photocatalysts or intermediate

The FESEM images showing the surfaces of PPG-PAC, 25%P25-PPG, PPG-PAC-P25 and P25 after the IPA hydrothermal treatment are shown in *Figure 4-2*. Although PPG had a smooth surface (figure not included), the PPG-PAC was observed to have a PAC layer completely covered or sheltered the PPG surface; as shown in *Figure 4-2(a)*. The P25 nanoparticles, formed aggregates of uneven sizes, were observed on the surface of 25%P25-PPG and did not completely and uniformly cover the surface of the composite (see *Figure 4-2(b)*). As indicated by the blue circles, there are large exposed PAC on 25%P25-PPG. On the other hand, PPG-PAC-P25 showed a much more uniformly distributed P25 nanoparticle porous layer on the PPG-PAC intermediate; see *Figure 4-2(c)* and *Figure 4-2(d)*. The exposed PAC areas on PPG-PAC-P25 were indicated by the red circles in *Figure 4-2(d)*, the exposed areas are generally smaller than that of 25%P25-PPG in *Figure 4-2(b)* and well-distributed on the entire surface. The IPA-hydrothermally treated P25 nanoparticles, as shown in *Figure 4-2(e)*, appeared to experience some extent of agglomeration when they were loaded onto the PAC of the PPG-PAC intermediate,

thus produced a micro-porous P25 layer on the prepared composite photocatalyst of PPG-PAC-P25 in this study, which may be beneficial for the utilization of the immobilized PAC middle layer in the developed composite photocatalyst.

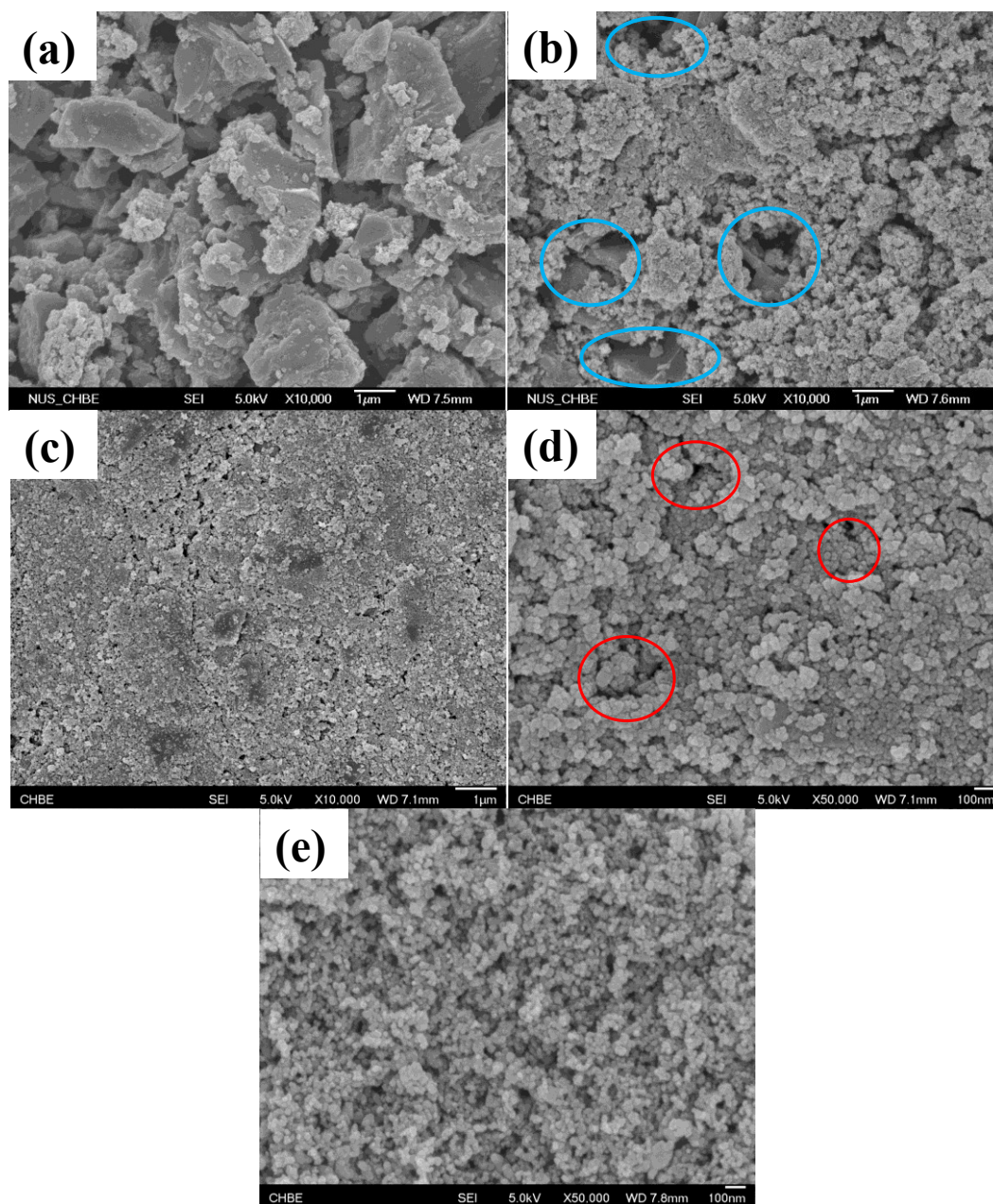


Figure 4-2: FESEM images for (a) PPG-PAC, (b) 25%P25-PPG, (c) PPG-PAC-P25 (x10000), (d) closer look of PPG-PAC-P25 (x50000) and (e) IPA hydrothermally treated P25

4.3.2. Stability performance against mechanical attrition and photocatalytic degradation

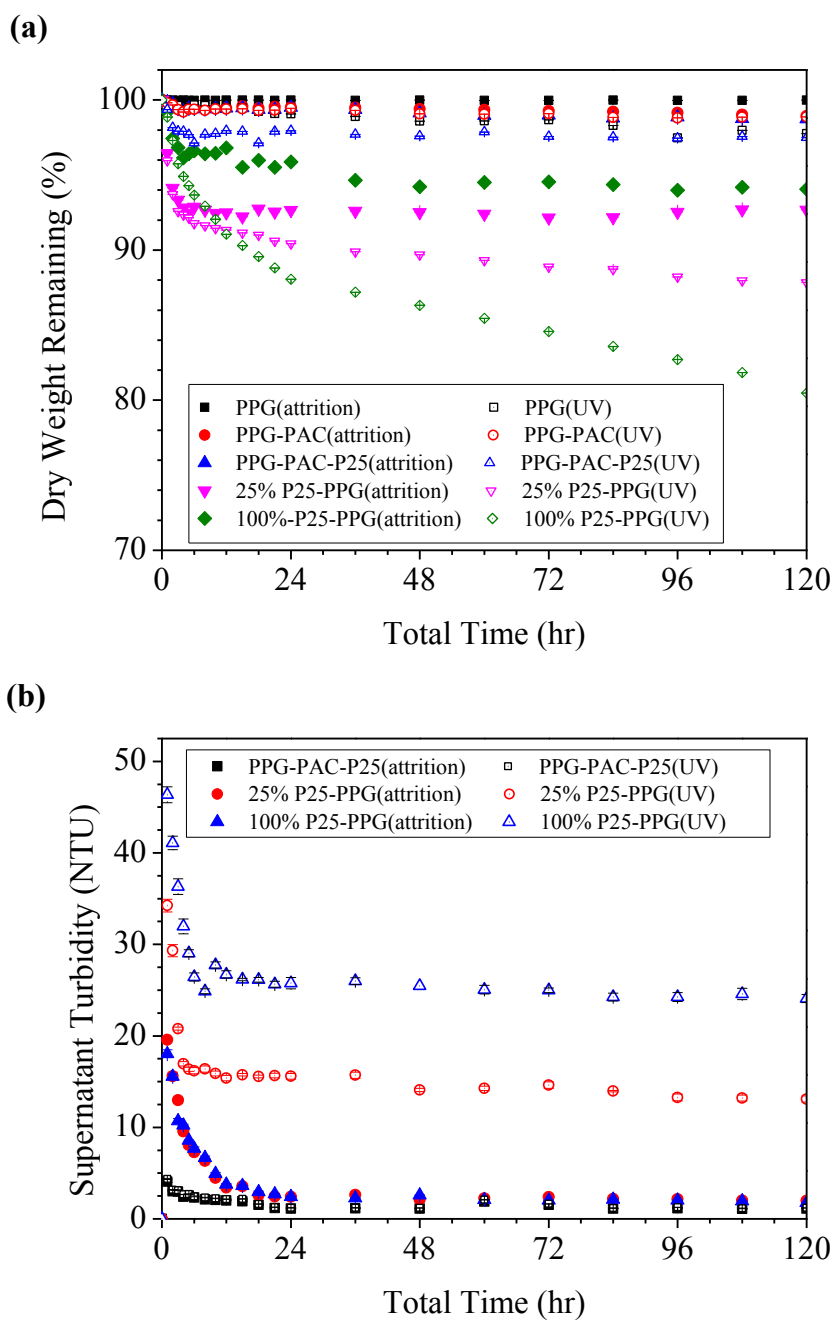


Figure 4-3: Effect of mechanical attrition and photocatalytic degradation on the prepared composite photocatalysts: (a) change of total dry weight and (b) change of

solution turbidity (Data shown by filled marks are for mechanical attrition and those by unfilled marks are for photocatalytic degradation)(n=3)

For practical applications, the mechanical durability and the stability against photocatalytic degradation for the prepared composite photocatalysts are of great interest. The dry weight changes of the prepared various composite photocatalysts due to the mechanical attrition by air bubbling and magnetic stirring and the photocatalytic degradation under UV light irradiation and the corresponding turbidity changes in the solutions are shown in *Figure 4-3*. From *Figure 4-3(a)*, weight losses can be observed for 25%P25-PPG (about 7.33%) and 100%P25-PPG (about 6.00%) during the first 6 hrs due to mechanical attrition, and in the following 114 hrs tested, almost no further changes were found, which suggests that a portion of the P25 and PAC particles that were not firmly attached to the PPG surface can be torn off by the turbulence and collision effect during the initial process life of 25%P25-PPG and 100%P25-PPG. The PPG-PAC also showed a slight dry weight lost in the first 6 hrs (about 1%); possibly due to the drop of some loosely bounded PAC particles, but no further weight change was observed in the following 114 hrs, indicating that the immobilized PAC layer was firmly attached to the PPG substrate. The PPG-PAC-P25 composite photocatalyst showed a similar dry weight change to that of PPG-PAC, confirmed that the P25 layer was also firmly loaded on the PPG-PAC. Hence, the developed PPG-PAC-P25 composite photocatalyst in this study exhibited a reasonably good physical stability. As expected, no dry weight change was observed for the PPG substrate during the entire test period. In *Figure 4-3(b)*, higher solution turbidity values can be observed in the early stages of the test runs and almost negligible solution turbidity was found in all the subsequent period of the test runs during the mechanical attrition experiments. Also, PPG-PAC-P25 showed much lower turbidity than 25%P25-PPG and 100%P25-PPG. The turbidity can be attributed

to some particles detached from the composite photocatalysts and presented in the solutions.

The changes of dry weight of the composite photocatalysts and the solution turbidity due to photocatalytic degradation with the 150W Xenon lamp switched on in the process are also shown in *Figure 4-3(a)* and *4-3(b)*, respectively (indicated by the unfilled marks). More significant weight losses were found for 100%P25-PPG, followed by 25%P25-PPG and PPG, but PPG-PAC-P25 showed only a slight weight loss; see *Figure 4-3(a)*. Similar changes in the solution turbidity to those of dry weight losses are observed for the cases of 100%P25-PPG, 25%P25-PPG, and PPG-PAC-P25; see *Figure 4-3(b)*.

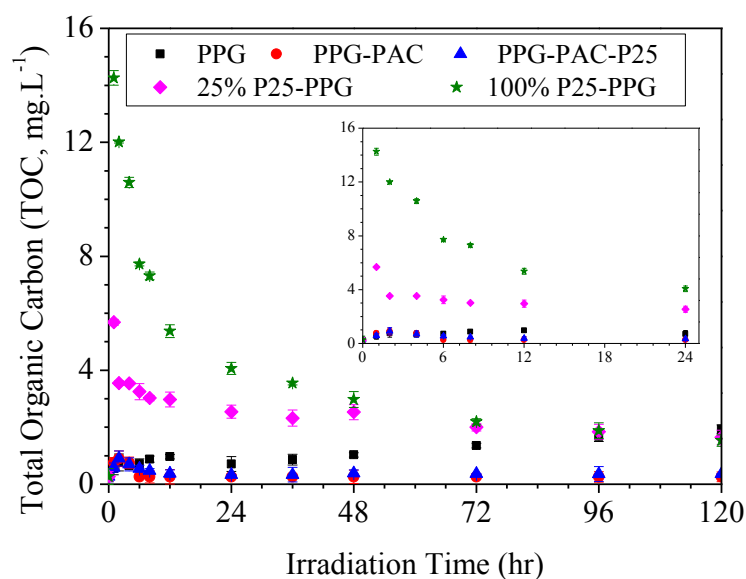


Figure 4-4: The changes of solution TOC for different composite photocatalysts during photocatalytic degradation process (the insert shows the enlarged graph in the initial stage)(n=3)

The possible leaching of organic matters (i.e., PPG) from the composite photocatalysts to the solution due to photocatalytic degradation is shown as TOC values in the solutions in *Figure 4-4*. Although no weight loss of PPG was observed

under mechanic attrition, continuous weight loss of PPG due to photocatalytic degradation under UV light irradiation is observed in *Figure 4-3* and this is converted to the TOC increase in the solution, as shown in *Figure 4-4*. Similar to the changes of turbidity, the increase of solution TOC in the case of 100%P25-PPG and 25%P25-PPG was significant, much greater than that of PPG. The TOC results again confirm that PPG-PAC-P25 was reasonably stable and did not contribute much to the solution TOC.

The results in *Figures 4-3* and *4-4* indicate that the photocatalytic degradation of the PPG substrate, at least partly, contributed to the weight loss and turbidity increase. This may be explained by the photocatalytic degradation of the polymer substrate by the produced radicals at around the P25 aggregates directly attached on the surface of the substrate (Nawi and Zain, 2012). When the exposed polymer molecules around the active photocatalyst component was being degraded, some of the immobilized P25 nanoparticles (perhaps some PAC as well) may drop into the solution, especially for those loosely attached during the first 6 hours, resulting in the observed weight loss and turbidity or TOC increase. The dry weight of 25%P25-PPG and 100%P25-PPG continued to decrease but at a lower rate and seemed never ceased, indicating a continuous degradation of the polymeric substrate by the radicals produced by the immobilized P25 nanoparticles remained on the substrate. Similar observation was also reported by other researchers for directly immobilized TiO₂ nanoparticles on polyethylene film (Thomas et al., 2013) and polyvinyl chloride sheet (Cho and Choi, 2001). The results hence suggest that the composite photocatalysts prepared by the previous direct thermal immobilization method were somewhat prone to or not stable enough to resist the photocatalytic degradation of the PPG substrate. The total weight losses of 25%P25-PPG and 100%P25-PPG under the condition with UV light

irradiation were hence due to both the photocatalytic degradation of the polymeric substrate and the drop-off of some of the immobilized PAC and P25 particles in the process. On the other hand, almost no difference was observed between the weight loss due to mechanical attrition and that of photocatalytic degradation of PPG-PAC, indicated that the PAC layer on the PPG substrate protected the substrate polymer from being degraded in the photocatalytic process (Han and Bai, 2010, 2011; Iketani et al., 2003; Kasanen et al., 2011b; Matsuzawa et al., 2008; Sánchez et al., 2006; Yuranova et al., 2006), which is desired in this study. Slight more weight loss was observed for PPG-PAC-P25 than for PPG-PAC in the UV induced photocatalytic degradation process and a light TOC increase in the first 6 hours, possibly due to the oxidation of PAC, was found (Haarstrick et al., 1996). However, no further weight change was observed with PPG-PAC-P25, nor as well as the solution turbidity and TOC after. Hence, it could be concluded that the PAC and P25 immobilized by the two separate layered configurations on PPG-PAC-P25 provided good strength to resist the mechanical attrition, as well as enhanced chemical stability against the photocatalytic degradation of the prepared composite materials.

The changes in the appearance of the various materials before and after the 120 hours of photocatalytic degradation test with UV irradiation are shown in *Figure 4-5*. The color of the PPG substrate changed from transparent to light yellow and its surface hydrophobicity was also found to be decreased in the P25 suspension in the process. All these evidences indicate that the PPG substrate itself is degradable by the highly reactive radicals produced from the P25 photocatalyst under UV irradiation. For 100%P25-PPG, the P25 layer on it appeared to become much thinner after the 120 hrs of photocatalytic degradation, attributed to the loss of some P25 particles from the composite due to mechanical attrition and the loss of the substrate due to its

photocatalytic degradation. The color of PPG-PAC changed to slight grayish from completely black after the 120 hrs of contact in the P25 suspension, indicating that some P25 nanoparticles may be attached to the PAC surface on PPG-PAC, perhaps by electro-static attractive force (Lim et al., 2011) or due to its rough surface (Matsuzawa et al., 2008). For 25%P25-PPG and PPG-PAC-P25, no distinguishable visual changes by the eyes can be observed for their surface appearance before and after the 120 hrs of photocatalytic degradation test.

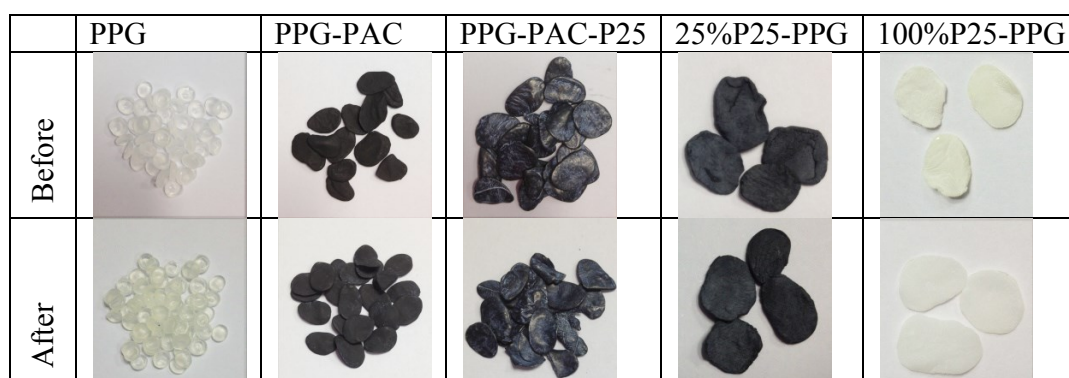


Figure 4-5: Photos of the PPG substrate, the prepared intermediate and composite photocatalysts before and after 120 hours of photocatalytic degradation test under UV light irradiation

4.3.3. Adsorptive property (under dark condition)

The results in the adsorption of phenol under dark condition with the various types of prepared composite materials as a function of the adsorption time are shown in *Figure 4-6*. As expected, the 100%P25-PPG composite which contained no adsorbent component (i.e., PAC) did not show any adsorptive property for phenol. The amount of phenol adsorbed by the PPG-PAC intermediate was the highest, indicating that the PAC component used in the preparation of the composite photocatalyst was a very effective adsorbent for phenol. Although having the same amount of PAC component, PPG-PAC achieved 2.5 times higher phenol adsorption than 25%P25-PPG and 4.5 times higher than PPG-PAC-P25, suggesting that the PAC component on PPG-PAC

was more exposed than that on 25%P25-PPG or PPG-PAC-P25 for phenol adsorption. For 25%P25-PPG which was prepared by the previous method, the P25 nanoparticles and the PAC powder were mixed together before they were simultaneously immobilized on PPG. It was observed that some P25 particles directly loaded on the surface of PAC while both the P25 and PAC components can also be directly loaded on the surface of the PPG substrate side by side. Hence, the adsorptive performance of PAC on 25%P25-PPG became much lower than that of PPG-PAC, but was still significant. For PPG-PAC-P25 prepared by the two-layered configuration new method in this study, the surface of PAC was the only place for the loading of the P25 nanoparticles. Some further block of the PAC surface on PPG-PAC by the P25 nanoparticles was expected and, therefore, the adsorptive performance of PAC on PPG-PAC-P25 became lower than that of 25%P25-PPG (Rodríguez-reinoso, 1998). Nevertheless, the PPG-PAC-P25 composite photocatalyst still displayed a remarkable amount of adsorption for phenol, as compared to 100%P25-PPG. Thus, the adsorptive property of the prepared composite photocatalyst with both the photocatalyst and the adsorbent components can be expected to provide enhanced mass transfer for concentrating organic pollutants from bulk solution and makes them readily available for the photocatalyst component for degradation, possibly leading to more effective photocatalytic degradation performance for phenol. However, it can be arguable that too high adsorption capacity for the composite photocatalyst may not always be desired because it can lead to the coverage of the photocatalyst component by the adsorbed substances and thus reduce its degradation capability or rate. The optimum combination of the adsorbent and photocatalyst components in the prepared composite photocatalyst will form a further research topic in the future.

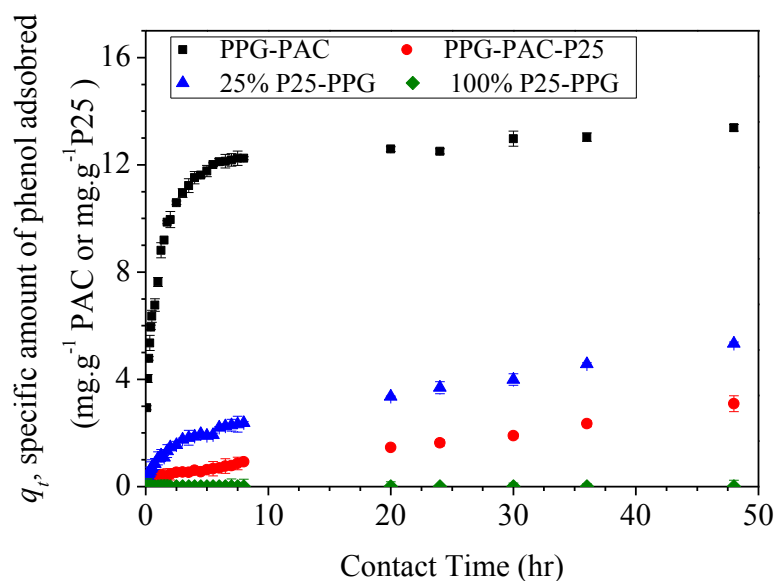


Figure 4-6: Adsorptive property of various composite materials (under dark condition)($n=3$)

4.3.4. Phenol removal performance

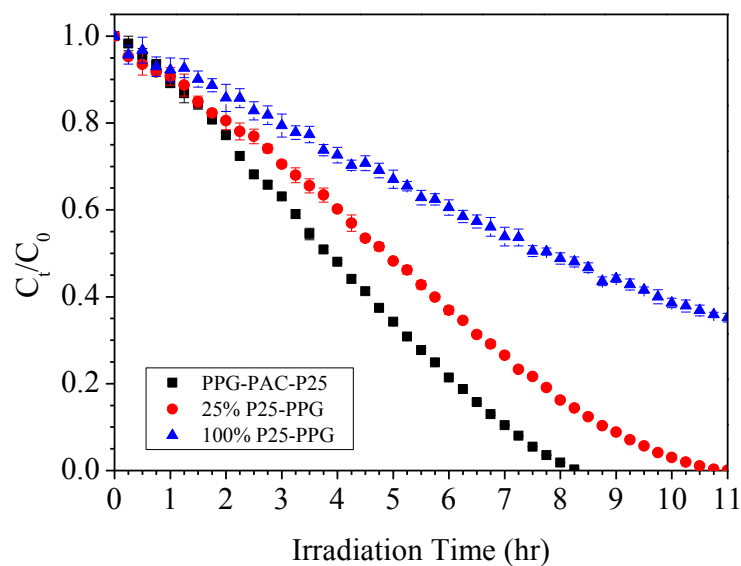


Figure 4-7: Phenol removal by the three types of composite photocatalysts due to both adsorptive and photocatalytic degradation effects ($C_0 = 20 \text{ mg.L}^{-1}$)($n=3$)

The results in the phenol removals by the three types of composite photocatalysts due to their combined adsorption effect and photocatalytic degradation effect are shown *Figure 4-7*. PPG-PAC-P25 is observed to achieve a complete phenol removal

in about 8 hrs, and 25%P25-PPG take around 11 hrs to achieve that. Although 25%P25-PPG showed a faster phenol removal in the first 1 h, possibly due to its better adsorptive property as mentioned in previous section, its total removal efficiency of phenol became lower than that of PPG-PAC-P25 in the rest of the time tested. For 100%P25-PPG that did not have the adsorptive property for phenol, about 64.93% of phenol removal was achieved at the end of the 11 hrs of photocatalytic degradation tested. Since all the three types of composite photocatalysts had the same amount of P25 photocatalyst component, the results in *Figure 4-7* hence suggest that there was a beneficial effect on the phenol removal efficiency with the combination of PAC and P25 on the composite photocatalysts. Moreover, the concentrations of phenol in the solutions were found to decrease almost linearly with the reaction time (i.e., the data lines are somewhat straight) even though the phenol concentration in the solution became lower and lower. This phenomenon suggests that the photocatalytic degradation process by the composite photocatalysts was much less dependent on the concentration in the solutions, confirming the hypothesis that the PAC component helped concentrate the organic pollutants from the solution and provided them to the P25 photocatalyst component for degradation, which leads to the photocatalytic degradation process being less dependent on the concentration in the solution. On the other hand, the photocatalytic degradation of phenol by P25 from the PAC component helped the regeneration of the PAC component on the composite photocatalyst and thus sustained its adsorption uptake. Therefore, it can be concluded that the combination of the photocatalytic component and the adsorbent component in the composite photocatalyst produced some synergistic effect. For the 100%P25-PPG composite photocatalyst, the concentration profile over time also changed almost linearly, but the overall removal was much smaller. Therefore, the concentration of

phenol in the solution may not be the major controlling factor for the photocatalytic degradation of phenol, leading to the observed linearity.

The photocatalytic degradation removal of phenol from the aqueous solution by the three types of composite photocatalysts was further examined by first allowing them to stay in the solution under dark condition to reach adsorption equilibrium and then switching on the UV light irradiation for photocatalytic degradation of phenol to start. This was to separate the adsorption effect from photocatalytic effect in phenol removal in the process. The photocatalytic degradation process was continued for another 4 hrs and the phenol concentration in the solution was monitored. The photocatalytic degradation data has been found to be well fitted by a mono-exponential curve, as shown in *Figure 4-8*, which suggests that a pseudo-first-order kinetic model can be applied to describe the kinetic behavior of photocatalytic degradation of phenol. The pseudo-first-order kinetic model with respect to the instant phenol concentration (C) in the bulk solution may be given as (Matos et al., 1998):

$$r = -\frac{dC}{dt} = k_{app}C \quad (4-2)$$

where k_{app} denotes an apparent pseudo-first-order rate constant.

The integration of Eq. (4-2) with the initial condition of $C=C_0$ at irradiation time $t=0$ hr (the initial bulk solution concentration after the dark adsorption) leads to a linear relationship of $LN(C_0/C_t)$ versus t (eq. (2-24)), which is used to model the data from the photocatalytic degradation process and the results are shown in *Figure 4-8*. The value of k_{app} that is an indication of the photocatalytic activity of a composite photocatalyst is determined from the slope of the linear plot and is also included in *Figure 4-8*.

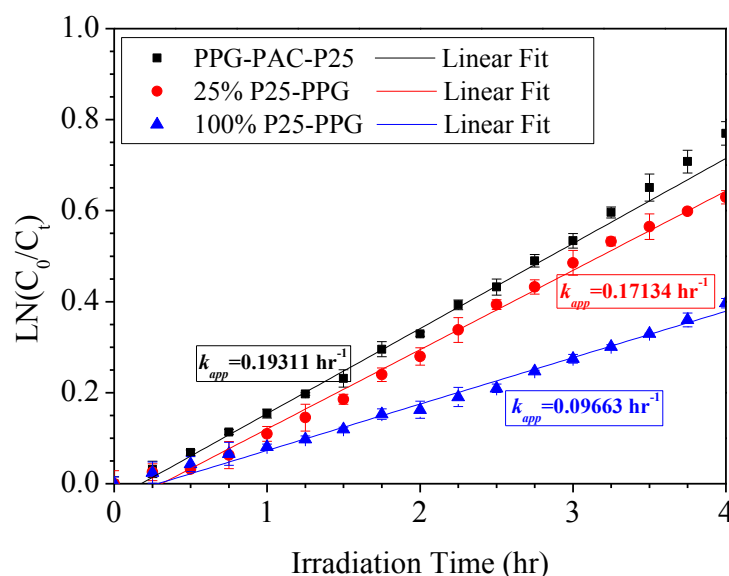


Figure 4-8: Kinetic study of phenol removal by photocatalytic degradation by the three types of composite photocatalysts (25%P25-PPG, 100%P25-PPG, and PPG-PAC-P25) and the linear fitting of the data with the pseudo-first order reaction rate model, eq. (2-24) ($n=3$)

As expected, all the PAC-containing composite photocatalysts (PPG-PAC-P25 and 25%P25-PPG) achieved a much greater photocatalytic activity than that of 100%P25-PPG (as greater k_{app} values). The results again reveal that the addition of PAC as the adsorbent component created a synergistic effect on the photocatalytic degradation performance. In addition, PPG-PAC-P25 also showed higher photoactivity than that of 25%P25-PPG. Two possible explanations may be provided for the improved photocatalytic activity of the PPG-PAC-P25 composite photocatalyst. One reason may involve the good dispersity of P25 and PAC particles on the PPG substrate. For PPG-PAC-P25, the first thermal immobilization step ensured a complete PAC layer to be loaded on PPG and the second solution deposition step ensured a uniform distribution of the segregated (not clustered) P25 nanoparticles to be immobilized on PPG-PAC. In contrast, for 25%P25-PPG, some P25 aggregates loaded directly on the surface of PAC and others directly onto PPG substrate, shoulder to shoulder with PAC particles, being partly blocked. One of the

widely accepted photocatalytic degradation pathway with TiO_2/AC composite involves the first adsorption of organic molecules on the adsorption site, followed by the migration to active sites on the surface of photocatalyst for photocatalytic degradation (Lim et al., 2011). Therefore, the two layered configuration in the preparation of PPG-PAC-P25 in this study seemed to create a combination of P25 and PAC, leading to efficient reversible adsorption of phenol molecules, short traveling distance from adsorbed site to the active centers of photocatalyst and thus a higher degradation capability (Sellappan et al., 2011). Secondly, the PAC layer on PPG-PAC-P25 also acted as a barrier layer to prevent the photocatalytic degradation of the PPG substrate. There was no such barrier on 25%P25-PPG, and it is possible that some of the generated radicals were consumed by the degradation of the polymer substrate around the P25 photocatalyst, rather than for the phenol molecules, and hence reduced its photocatalytic activity towards the removal of phenol.

4.3.5. Recyclability

For practical application, photocatalyst is always expected to have a long lifetime or be recyclable for multi-cycle uses. The results from the recyclability tests on the percentages of total phenol disappearance and TOC removals by the two typical types of composite photocatalysts (PPG-PAC-P25 and 25%P25-PPG) are shown in *Figure 4-9*. Both PPG-PAC-P25 and 25%P25-PPG achieved an almost complete phenol disappearance in the solution in the first round test. For 25%P25-PPG, however, the performance dropped by 12% in the 2nd round and the trend continued in the next 3 consecutive rounds, with only a 72.2% of total phenol disappearance achieved at the end of the 5th round; see *Figure 4-9(b)*. In contrast, the performance in phenol disappearance by PPG-PAC-P25 was quite stable, with only slight decreases in the

efficiency and the percentage of phenol degradation still reached about 93% after the 20th cycle; see Figure 4-9(a). The reduction in the photocatalytic degradation ability may be possibly attributed to the tiny loss of the photocatalyst component (Wang et al., 2009a), as discussed in *Section 4.3.2*. The dark adsorptivity of PPG-PAC-P25 to phenol was also tested in repeated cycles with the same experimental setup but without the UV light irradiation (results not shown here). It was found that only 21.7% of phenol was removed by the dark adsorption during the first adsorption cycle and the dark adsorptivity disappeared completely after only 10 cycles. Considering the difference between the repeated photocatalytic degradation and dark adsorption experiments, one is clear that the only difference was with or without the UV irradiation for photocatalytic degradation. Hence, it could be inferred that the photocatalyst component generated effective radicals during photocatalysis that oxidized and removed phenol or other organic intermediates on the adsorption sites of the PAC layer, which regenerated the PAC that showed sustained adsorptive performance to phenol in the repeated experiments. Thus, the composite configuration of PAC and P25 on PPG-PAC-P25 showed the advantage of concentrating phenol from the solution by the adsorbent component and supplying phenol from the adsorbent component to the photocatalyst component for degradation.

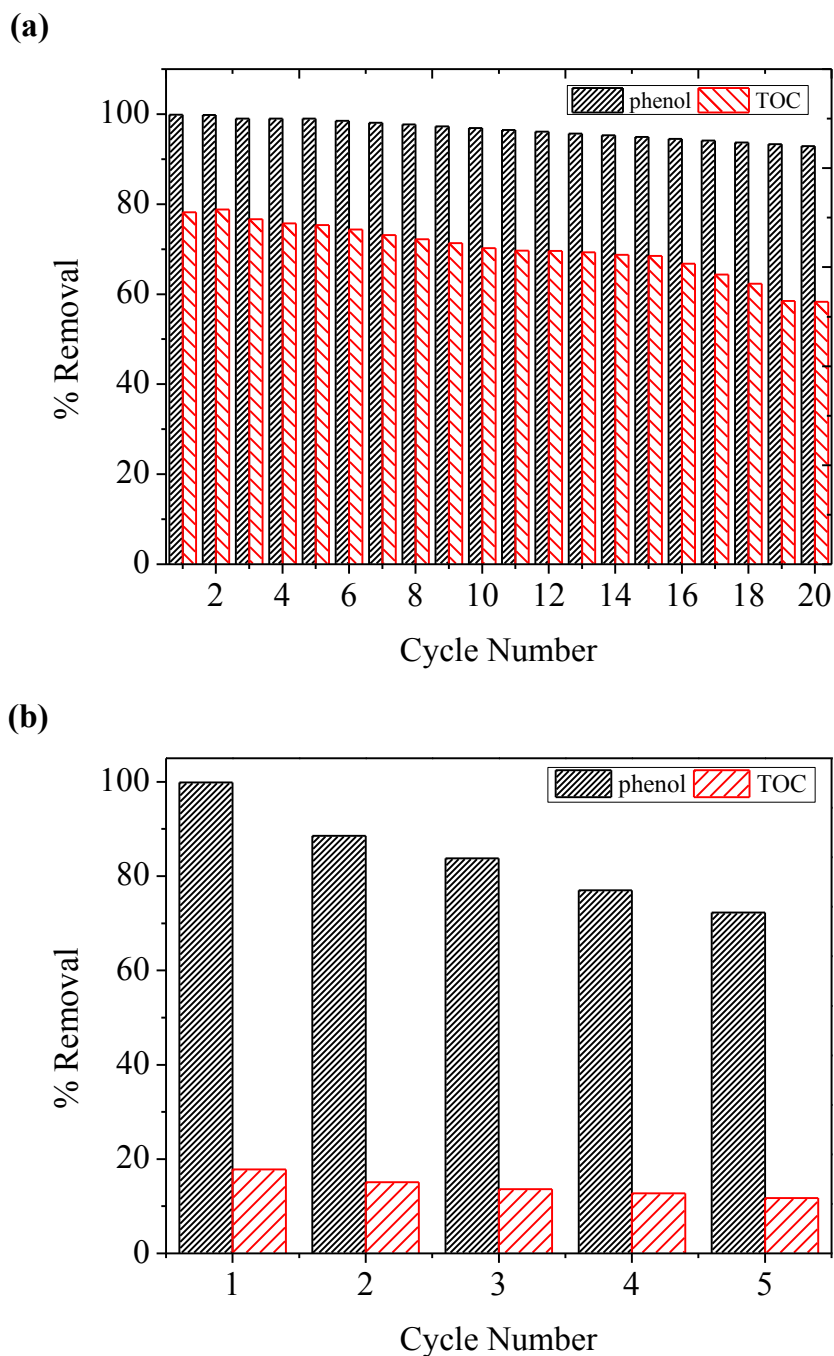


Figure 4-9: Recyclability of (a) PPG-PAC-P25 and (b) 25%P25-PPG composite photocatalysts, in terms of total phenol and TOC removal percentages

The TOC of the phenol solution was analyzed before and after the 10 hours UV irradiation in each repeated cycle. The mineralization efficiency, expressed as the percentage of TOC removal is always lower than that of the total phenol disappearance; see *Figures 4-9(a)* and *4-9(b)*, possibly due to the existence of some

degradation intermediates in the solution. PPG-PAC-P25 achieved 78.2% of TOC removal in the 1st round. However, the mineralization efficiency decreased gradually with the increase of the cycle numbers, and 58.3% of TOC was removed at the end of the 20th cycle. The total weight loss of the photocatalyst component after the 20 cycles was less than 5%, indicating that the P25 particles were well loaded on the PAC layer that wrapped the PPG substrate and the developed composite photocatalyst was very stable. Hence, the decrease in the photocatalytic activity of the composite photocatalyst may be mainly due to the adsorption of the degradation intermediate by-products on the surface of photocatalyst component (Shi et al., 2009), and the loss of P25 photocatalyst component only played minor effect on the decrease of the photocatalytic activity. In contrast, the 25%P25-PPG composite photocatalyst only achieved only 17.8% of mineralization during the 1st round, even though completely phenol disappearance was observed, and the percentage of TOC removed continued to drop in the later repeated cycles. The low TOC removal efficiency of 25%P25-PPG was probably due to the continuously degradation of the polymer substrate that contributed to the TOC content in the solution, as discussed previously in Section 3.2. To further improve the performance of PPG-PAC-P25 developed in this study for better recyclability, it appears necessary to examine the optimum combination of the adsorbent and photocatalyst components, including their relative capacity and strength for its designated function (i.e., adsorption or photocatalysis), which will be further studies in future work.

4.4. Conclusions

A new buoyant composite photocatalyst, PPG-PAC-P25, was successfully prepared through a two-layered configuration method in this study. The thermally immobilized PAC layer was found to be tightly anchored on the PPG substrate, serving as a good platform for the loading of P25 nanoparticles as well as a protection barrier for the PPG substrate from being photocatalytically degraded. The outer P25 layer loaded through a suspension hydrothermal deposition method was well-dispersed on the immobilized PAC of the composite photocatalyst and formed a micro-porous structure that appeared desirable to retain some of the adsorption function of the PAC. Experiments showed that PPG-PAC-P25 had good mechanical and chemical stability against normal mechanical attrition in the process and possible photocatalytic degradation of the prepared composite material (namely the PPG substrate which appeared to be prone to photocatalytic degradation) in the photocatalysis process. PPG-PAC-P25 was also found to have enhanced photocatalytic performance for phenol than 25%P25-PPG or 100%P25-PPG that were developed in a previous study by simultaneously immobilizing PAC and P25 together on PPG by the thermal bonding method. The photocatalytic degradation kinetics of phenol by the composite photocatalysts can be well fitted to a pseudo-first-order kinetic model. The results suggested a synergistic effect in phenol removal for the composite photocatalysts with the PAC and P25 components and the extent of the synergistic effect was greater for PPG-PAC-P25 than for 25%P25-PPG. In the recyclability tests up to 20 cycles in a batch feed process, the photocatalytic degradation performance for phenol disappearance by PPG-PAC-P25 was reasonably good, decreased only by less than 7% after the 20th cycle, although the TOC removal efficiency appeared to be dropped greater by around 20%. There was evidence to

indicate that the performance of PPG-PAC-P25 may be further improved by examining the optimum combination of the adsorbent and the photocatalyst components in the obtained composite photocatalyst. PPG-PAC-P25 hence is a potentially very promising composite photocatalyst for the degradation of organic pollutants in aqueous solutions for practical applications.

Chapter 5: Further Study in Two-Layered Buoyant Composite Photocatalyst for Phenol Removal and In-Situ Regeneration

5.1. Introduction

Since 1993, the idea of immobilizing fine photocatalysts on a larger support has emerged as a method to solve the costly post separation problem (Shan et al., 2010). However, the immobilized system often suffered from a mass transfer limitation due to the reduced available surface area for reaction, as compared to the commonly used slurry system (Ahmed et al., 1999). A possible way to increase the mass transfer is to add inert co-adsorbent to the system, such as activated carbon (AC). The effect of co-adsorbent has been explained by the formation of a common contact interface between the two solid phases of adsorbent and photocatalyst, in which the AC acts as the adsorption center to bring the organic pollutants in the solution closer to the surface of photocatalyst, such as TiO_2 , and thus an enhancement of the photocatalytic degradation efficiency (Lim et al., 2011; Matos et al., 1998; Matos et al., 2001). Furthermore, AC also appeared to be a good TiO_2 supporting substrate due to the high porosity and large specific surface area (Shan et al., 2010). Various synthesis or preparation protocols have been adopted to produce TiO_2/AC combination or composite photocatalysts. Most of the prepared composites showed preserved AC pore structure, and the TiO_2 coating was limited to the external surface of AC, which was demonstrated to have much better photocatalytic performance than that of the titania alone. However, there are still various practical issues remained for the practical applications of the TiO_2/AC composite photocatalysts. Especially, particle

dispersibility and separation are two main engineering issues to be dealt with for the TiO₂-based photocatalysis systems. The density of TiO₂/AC composite is larger than that of AC skeletal density, which is usually greater than 1400 kg.cm⁻³, and makes the composite particles easily settled to the bottom of the reactors. Although they can be separated and recovered by gravity separation methods, as compared to the more energy-intensive filtration method required to separate the submicrometer-sized titania (Liu et al., 2007), extensive mixing, by air bubbling or mechanical mixing, for those heavy composite particles is required to ensure the particles to be uniformly distributed throughout the reactor. However, excess air bubbling for example, also leads to light scattering by the large air bubbles and thus limits the photon transmission through the whole photocatalytic reactor and lower the UV utilization efficiency. Beside the scattering issue, UV light also attenuates significantly in water with traveling distance (the attenuation coefficient in water is more than 100 times greater than that of air). As a result, most of the supplied UV light was lost before it reached the surface of the photocatalysts to incur photocatalytic reaction. Among the various TiO₂-based photocatalytic processes, buoyant composite photocatalysts can be used as a solution to achieve high light utilization efficiency as well as low post separation cost (Han and Bai, 2009). Buoyant photocatalysts can float naturally on water surface and thus achieve greater light utilization efficiency by avoiding light attenuation in water medium (Fabiya and Skelton, 2000; Han and Bai, 2009) and enhanced oxygenation of the photocatalysts at the water/air interface. Meanwhile, buoyant photocatalysts can be easily separated from the water body, avoided the post separation concern.

In recent years, polymer-supported nanocomposites, which incorporate advantages of both nanoparticles and the polymers, have received increasing attention

in both the academia and industry. The polymer-based nanocomposites retain the inherent properties of nanoparticles, while the polymer substrate provides better mechanical strength for long-term usage (Zhao et al., 2011). Despite the attractive advantages of the polymer substrates, such as chemically inert, mechanically stable, cheap and readily available (Shan et al., 2010), it has been uncommon to see TiO₂ or other photocatalysts directly immobilized on polymeric substrates. This was due to the fact that most polymers are not resistant to photogenerated active oxygen species (such as OH• and O₂^{-•}) (Tennakone and Kottegoda, 1996; Tennakone et al., 1995). It has been shown that appropriate intermediate layers between TiO₂ and the organic substrate can be provided to protect the polymeric substrate from being attacked by the reactive radicals generated by the photocatalysts (Kasanen et al., 2011b). In practice, one intermediate layer may be found not enough to achieve long term sustainability and good affinity with the TiO₂ particles. As a result, multi-intermediate layers were also employed, which made the preparation processes complicated (Iketani et al., 2003). Activated carbon is well-known for its high chemical stability, excellent mechanical strength and good UV adsorbing characteristics. The inertness of the carbon surface on the carbon/metal heterogeneous catalysts has been explained by the weak chemical interactions of the active species in photocatalysis with the carbon surface (Rodríguez-reinoso, 1998). In our previous work, we have successfully prepared a two-layered buoyant composite photocatalyst from polypropylene granule substrate, by a two-step immobilization method. A PAC layer was fixed onto the PPG substrate by a direct thermal-bonding method, followed by a suspension hydrothermal deposition method to load the P25 TiO₂ nanoparticles on the surface of the immobilized PAC layer. Both good adsorptivity and photocatalytic activity were observed in the experiments for the removal of phenol,

suggesting that the developed buoyant composite photocatalyst is a promising photocatalyst for the application of the degradation of organic pollutants in aqueous solutions.

On the above background, the primary aim of this work is to make some further study in the investigation of the photocatalytic performance of the buoyant composite photocatalyst with proper composition (PAC and P25 ratio) and various operational parameters. The composite photocatalysts with different adsorptivities were prepared with different number of the soak-dry-cure cycles, described in *Chapter 4*, from 1 cycle up to 6 cycles. The photocatalytic activities of the obtained composite photocatalysts were evaluated by phenol removals from aqueous solutions. The effect was examined with the modified Langmuir-Hinshelwood kinetic model so as to find the desired photocatalyst composition that provides both good adsorptivity and photocatalytic activity. Then, some operation parameters, such as photocatalyst dosage, suspended solids, and radical scavengers, were tested to find out their impact and possible ranges for appropriate operational performance. The in-situ regeneration efficiency of the PAC layer by the P25 layer of the composite photocatalyst was investigated through repeated adsorption-photocatalytic degradation cycles.

5.2. Experimental

5.2.1. Preparation of buoyant composite photocatalysts

The two-layered configuration composite photocatalysts were prepared with the method described in *Section 4.2.1*. The soak-dry-cure cycle were repeated and the products after 1, 2, 4 and 6 times of the process were obtained and for test (denoted as PPG-PAC-P25(1), PPG-PAC-P25(2), PPG-PAC-P25(4) and PPG-PAC-P25(6), respectively). After the final cure step for each type of the products, the granules were washed with tap water to remove any possible loosely loaded P25 nanoparticles, then dried in an oven at 80°C overnight and stored in a desiccator for further use.

5.2.2. Characterization

The actual compositions of the prepared different types of the buoyant composite photocatalysts, as well as PPG substrate and PPG-PAC intermediate, were analyzed using the Thermalgravimetric Analyzer (TGA, TGA2950, DuPont Instruments, USA), similarly to that described in *Section 3.2.3*.

5.2.3. Phenol dark adsorption experiments

The adsorption performances of the prepared buoyant composite photocatalysts were evaluated, according to the procedure described in section 4.2.4. The exact weight dosages for each type of the composite photocatalysts in the experiments are calculated according to the same amount of immobilized PAC component (around 166 mg), and also included in *Table 5-1* under the column title of “4. Dosage (PAC)”.

5.2.4. Phenol photocatalytic degradation by the buoyant composite photocatalysts and the effect of some operational parameters

For the experiments in phenol photocatalytic degradation with the prepared buoyant composite photocatalysts, the initial phenol concentration (C_{in}) was varied from 10 mg.L⁻¹ to 100 mg.L⁻¹. The photocatalytic degradation experiments were carried out in the same photocatalytic reaction system as mentioned in *Section 4.2.3*. The composite photocatalysts were first dispersed into 200 mL phenol solution with 0.5wt% NaCl in a 250 mL conical flask wrapped with aluminum foil and placed on the shaker for 72 hrs to reach the adsorption equilibrium. The contents in the conical flask were then transferred to the jacketed reactor and placed under the Xenon lamp UV irradiation for the photocatalytic degradation process. About 2 mL sample solution was taken every 15 min and analyzed for the phenol concentration with a UV/VIS spectrophotometer (Jasco V-660, Japan) at $\lambda_{max}=270\text{nm}$. The first sample was taken at the end of the 72 hrs dark adsorption, just before the light was turned on, in order to determine the initial phenol concentration for photocatalytic degradation (C_0). Preliminary trials found that 7.45g PPG-PAC-P25(1) composite photocatalyst was adequate enough to cover the entire irradiation area in the reactor, and hence, the dosages for the other 3 types of the composite photocatalysts were determined based on 69 mg P25 loading on each type of the composite photocatalysts. The respective dosages for each type of the composite photocatalysts in the experiments are given in *Table 5-1*, under the title of “5. Dosage (P25)”. The time duration monitored for each photocatalytic degradation test run was 4 hrs. Similarly, the effects of composite photocatalysts dosage, suspended solids and radical scavengers in the solution were studied with the same photocatalytic reactor setup.

5.2.5. In-situ regeneration

The experimental protocol for the in-situ regeneration of the composite photocatalysts involved three major aspects, namely, phenol molecules loading to the composite by adsorption, photocatalytic regeneration of the saturated composite and subsequent re-adsorption capacity of phenol by the regenerated composite that evaluated the recovery capability. The fully loaded composite photocatalysts were prepared by repeated adsorption cycles. 12.3 g of PPG-PAC-P25(2) composite photocatalysts was suspended in 0.22 L phenol solution (20 mg.L⁻¹ with 0.5wt% NaCl) and placed in a 250 mL conical flask wrapped with aluminum foil and placed on the shaker at 170 rpm and the phenol solution were replaced with a new batch of the phenol solution after every 72 hours. This long dark adsorption contact time was to ensure that phenol molecules migrated into the internal PAC sorption sites and achieved a full saturation of the PAC component. The phenol adsorption eventually stopped after 10 repeated adsorption cycles, because no more adsorption of phenol molecules can occur. After that, the phenol suspension was transferred to the photocatalytic reactor for photocatalytic degradation of adsorbed phenol. The irradiation was done with phenol solution instead of pure water, which was to minimize the instant concentration gradient change between the phenol-loaded composite photocatalysts and the liquid phases so as to minimize the effect of desorption at the initial stage. After irradiated for certain duration, the composite photocatalysts were separated from the solution and re-suspended in 0.22 L fresh phenol solution in the conical flask and placed on the shaker for another 72 hours dark adsorption. The photocatalytic degradation-adsorption cycle was evaluated for 4 cycles. Pure oxygen was supplied to the solution at a rate of 12 L.hr⁻¹ during the UV irradiation so as to maintain a high dissolved oxygen level. The phenol concentrations were measured before and after the 72 hours dark adsorption to evaluate the recovery

of the composite photocatalysts' adsorption capacity. Solution phenol concentrations were monitored during the UV irradiation period by periodic sampling for analysis and the total organic carbon (TOC) in solution was measured before and after the UV irradiation, by a Shimadzu TOC-V_{CPH} analyzer with the ASI-V autosampler.

5.3. Results and discussions

5.3.1. Characteristics of prepared buoyant composite photocatalysts

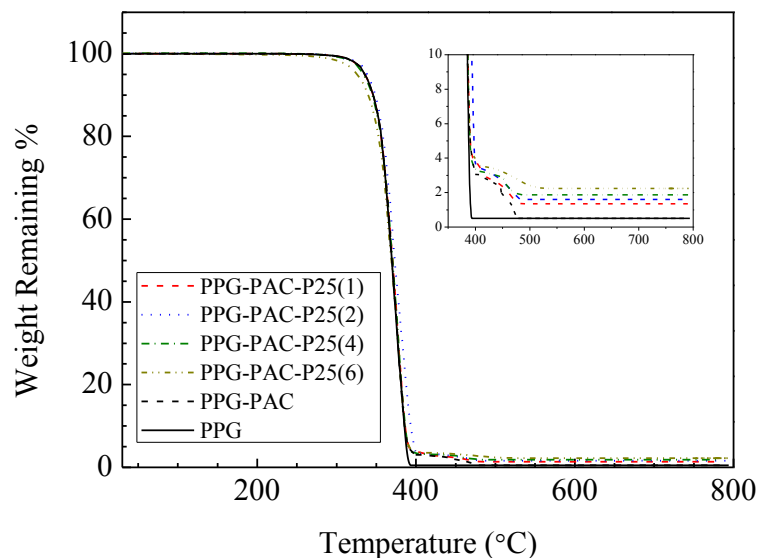


Figure 5-1: Results from TGA analysis for the PPG substrate, the intermediate, and the four different composite photocatalysts

The TGA analysis results for the PPG substrate and the 4 prepared composite photocatalysts are shown in *Figure 5-1*. For the PPG substrate, about 99.5% of the total mass was lost at 200 °C-400 °C in nitrogen gas and the remaining of 0.5% was stable at temperature increased up to 800 °C when air was supplied to the furnace. The results are the same as obtained previously in *Chapter 3* and *Chapter 4*, and are included in *Table 5-1*. For the PPG-PAC intermediate, about 2.58% of the weight loss for PAC was observed at the temperature range of 400-600 °C in air atmosphere and the impurities (about 0.49%) remained stable at 600 °C-800 °C. For the 4 composite photocatalysts prepared by different numbers of coating cycles, the more coating cycles resulted in a higher amount of P25 deposited on the prepared composite photocatalyst. For PPG-PAC-P25(1) and PPG-PAC-P25(2) , the total amount of P25 fixed was less than that of PAC on the PPGs. As the number of coating cycles

increased to 4, the amount of P25 immobilized was comparable to that of PAC, and the amount of P25 loaded exceeded the PAC loading for PPG-PAC-P25(6). The respective composition ratios of PAC and P25 on the PPGs are also summarized in *Table 5-1*. Besides, all the prepared composite photocatalysts were found to have an average density smaller than 1 g.cm^{-3} , and tests confirmed that they were all truly buoyant in water.

Table 5-1: Actual compositions of the PPG substrate, the intermediate, and the four different composite photocatalysts obtained from the TGA analysis

1. Photocatalysts Type	2. Composition (%)				3. P25:PAC	4. Dosage (PAC)* (g)	5. Dosage (P25)# (g)
	PPG	PAC	P25	Others			
PPG	99.5	0.00	0.00	0.50	-	-	-
PPG-PAC	96.93	2.58	0.00	0.49	-	6.43	-
PPG-PAC-P25(1)	96.36	2.23	0.92	0.48	1 : 2.42	7.45	7.45
PPG-PAC-P25(2)	96.43	1.96	1.12	0.48	1 : 1.75	8.47	6.15
PPG-PAC-P25(4)	96.40	1.50	1.62	0.48	1 : 0.93	11.07	4.26
PPG-PAC-P25(6)	96.42	1.18	1.91	0.48	1 : 0.62	14.07	3.60

*: The dosage is calculated according to 166 mg of immobilized PAC component

#: The dosage is calculated according to 69 mg of immobilized P25 component

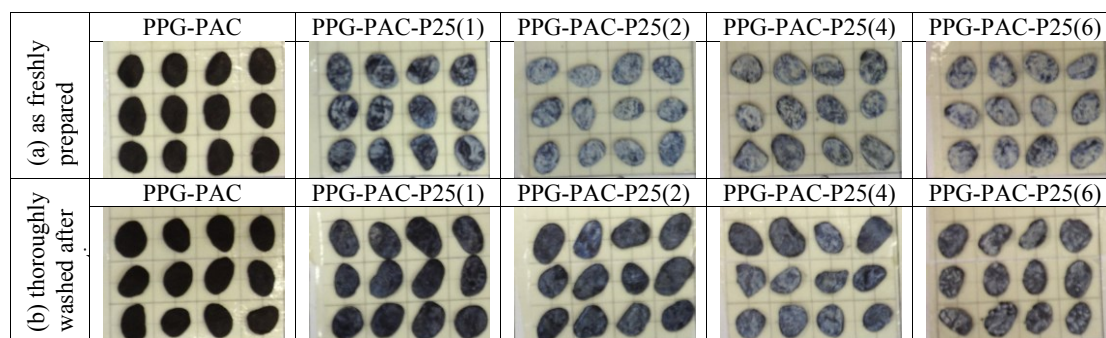


Figure 5-2: Photographs of the PPG-PAC and the prepared composite photocatalysts, (a) as freshly prepared and (b) thoroughly washed after preparation, on $5 \text{ mm} \times 5 \text{ mm}$ square paper

The photographs of the freshly prepared PPG-PAC and the four types of the composite photocatalysts are shown in *Figure 5-2*. Although the PPG substrate had a regular round shape and a semi-transparent color (see *Figure 3-4*), after the thermal immobilization process for the PAC coatings, a thin layer of black PAC was observed to cover the PPG surface and the shape of PPG-PAC changed from round to thinner and irregular flat shape. The shapes of PPG-PAC-P25(x , $x=1, 2, 4$ or 6) were found to be similar to that of the PPG-PAC, and the shape was not changed by the soak-dry-cure cycles. As shown in the “(a) as freshly prepared” photos in *Figure 5-2*, single coating cycle was not enough to cover the entire surface of PAC-PPG. As the number of coating cycles increased, more and more PPG-PAC surface was covered with the white P25 nanoparticles. However, when the number of coating cycles increased to 4 and above, the P25 coating layer seemed to become too thick and cracks were observed, for example, on PPG-PAC-P25(6). Nevertheless, not all the P25 were firmly immobilized onto the PPG-PAC after the soak-dry-cure process. As shown in the “(b) thoroughly washed after preparation” photos, the amount of immobilization for all the 4 composite photocatalysts became less than those for “(a) as freshly prepared”, indicating that some of the immobilized P25 nanoparticles were washed off during the washing process. A thin and uniform P25 layer was left on the PPG-PAC-P25(2), and a slightly thicker layer was observed on PPG-PAC-P25(4). However, due to the cracks formed after curing, a non-uniform thick P25 layer was observed on PPG-PAC-P25(6). Although the percentage of P25 loading increased with the increasing number of coating cycles, excessive coating cycles may affect the P25 nanoparticle distribution on the PPG-PAC intermediate surface, and hence possibly affect the adsorptivity and photocatalytic activity of the composite photocatalysts.

5.3.2. Dark adsorption activity of prepared buoyant composite photocatalysts

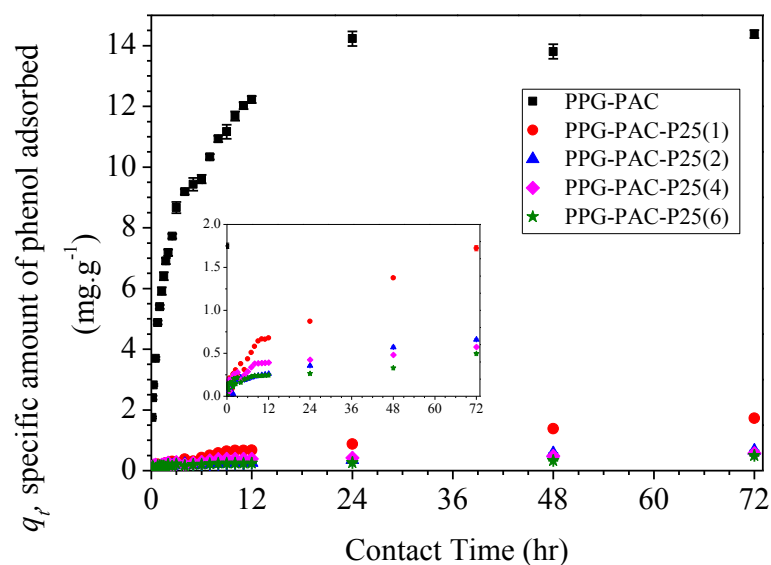


Figure 5-3: Dark adsorptive uptakes of phenol by different composite photocatalysts, initial phenol concentration, $C_{in} = 20 \text{ mg.L}^{-1}$ ($n=3$)

The specific adsorption uptakes of phenol by different types of the buoyant composite photocatalysts are shown in *Figure 5-3*. When the PPG-PAC was added to 20 mg.L^{-1} phenol solution, 14.38 mg.g^{-1} phenol adsorption by the PAC was found after 72 hours contact time, and the value is very near to the 14.49 mg.g^{-1} equilibrium uptake amount achieved by the original PAC component in the dark adsorption study. Hence, it could be concluded that the thermal immobilization process of PAC did not significantly affect the adsorption capacity of PAC. However, less than 1 hr was taken to reach the adsorption steady state for PAC, as compared to more than 24 hrs required for PAC on PPG-PAC. The adsorption rate seems to be greatly reduced by the immobilization process, possibly due to the reduced carbon surface in contact with phenol molecules in the bulk solution and thus limited mass transfer. The relatively high adsorption capacity achieved by PPG-PAC indicated that a great adsorption capacity of the immobilized PAC layer was retained. However, a large decrease in the adsorption uptake amount was observed after the coating of P25 on PPG-PAC and the

adsorption uptake decreased by almost 90% on PPG-PAC-P25(1) and further decreased with more coating cycles, indicating that the amount of adsorption sites on the buoyant composite photocatalysts was controlled not only by the PAC layer, but also the amount of P25 immobilized on the PAC layer (Torimoto et al., 1997). Hence, it could be concluded that the coverage of P25 on PAC layer affected its adsorption capacity, perhaps due to the physical blockages of the adsorption sites of PAC.

5.3.3. Photocatalytic degradation of phenol by prepared buoyant composite photocatalysts

The photocatalytic removal of phenol from its aqueous solution by different types of the composite photocatalysts is plotted against the UV irradiation time after they reached adsorption equilibrium and is shown in *Figure 5-4*. Blank test using phenol solution with air bubbling and UV irradiation confirmed that phenol loss due to evaporation and direct photolysis was negligible (results not shown here). The differences in the starting concentrations (C_0) in *Figure 5-4* for photocatalytic degradation were due to the different amount of phenol adsorbed during the 72 hours dark adsorption period before the photocatalytic degradation process began. It can be found that the PPG-PAC-P25(2) composite photocatalyst achieved the highest photocatalytic removal; and 1.303 mg of phenol was degraded during the 4 hrs experiment, followed by PPG-PAC-P25(4) (1.185 mg), PPG-PAC-P25(6) (1.079 mg) and PPG-PAC-P25(1) (0.958 mg). Only about 0.330 mg phenol was removed by the entirely P25 coated PPG composite photocatalysts, i.e., 100%P25-PPG, as prepared by the direct thermal immobilization method in the early study (Tu et al., 2013). The results confirmed again that the PAC layer has enhancing effect on the photocatalytic activity of the immobilized P25, attributed to the effectiveness of PAC as adsorbent to

provide high phenol concentration to the P25 photocatalysts. In addition, as shown in the TGA results in *Table 5-1*, the amount of P25 immobilized on was very limited on the prepared composite photocatalysts, less than 2% by weight, as compared to 13.5 wt. % P25 loading on 100%P25-PPG. Hence, the P25 nanoparticles are closely packed on the PPG surface, and only around 15 granules of 100%P25-PPG were needed to achieve the 69 mg P25 dosage. But more than 100 composite granules were required to achieve the same P25 dosage, making the P25 photocatalysts more dispersed on the new composite photocatalysts surface, providing larger surface area and encourage photocatalysts-pollutant interaction.

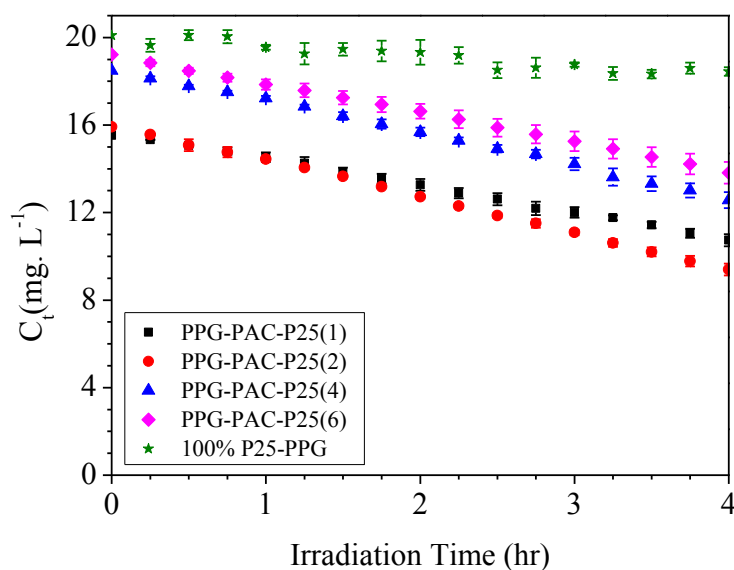


Figure 5-4: Photocatalytic degradation of phenol by different composite photocatalysts, initial phenol concentration, $C_{in} = 20 \text{ mg.L}^{-1}$ ($n=3$)

5.3.4. Photocatalytic degradation kinetics of prepared buoyant composite photocatalysts

The degradation curves in *Figure 5-4* can be well fitted by a mono-exponential curve, shown in *Figure 5-5(b)*, suggesting that a pseudo-first-order kinetic model can be applied for describing the kinetic behavior (*eq. (2-23)*). As discussed in early chapters, k_{app} is the pseudo-first-order rate constant and its k_{app} value has been proposed to indicate the photocatalytic activity of a composite photocatalysts (Matos et al., 1998). The values of k_{app} determined from the slope of the linear plots in *Figure 5-5* are summarized in *Table 5-2*, together with the amount of phenol adsorbed by each type of the composite photocatalysts during the 72 hours dark adsorption.

In general, it is found that the photocatalytic activity of the composite photocatalysts with PAC was significantly higher than that of 100%P25-PPG, without PAC, especially for the PPG-PAC-P25(2). The results again reveal that the addition of PAC as the adsorbent component could create a synergistic effect on the photocatalytic degradation performance of the prepared composite photocatalysts, which may be further evaluated using the synergistic factor according to *eq. (2-34)*. The calculated R values are also included in *Table 5-2*.

Among the 4 prepared composite photocatalysts, the PPG-PAC-P25(2) always achieved the highest R value. It seems that the synergism is related to the composite adsorptivity of the photocatalysts, because the PPG-PAC-P25(2) composite photocatalyst also showed the highest amount of phenol adsorption per unit g of PAC. A higher adsorptivity may induce a better phenol concentrating effect from the solution to the vicinity or surface of the P25 photocatalysts, and thus leading to a better photocatalytic activity. On the other hand, it is also noticed that, for all the 4 composite photocatalysts, the R value remained constant or slightly decreased when the initial phenol concentration exceeded 20 mg. L⁻¹. This can be explained that when

the bulk solution concentration is high enough, $> 20 \text{ mgL}^{-1}$ in this case, there were plenty of phenol molecules around the photocatalysts and were readily available for photocatalytic degradation. Hence, the P25 nanoparticles may be always fully in contact with the organic pollutants, and thus more organic pollutants to the P25 photocatalysts by the high adsorptivity would not further improve the photocatalytic degradation activity. Whereas at low organic concentrations, the P25 photocatalysts surfaces may only be partially in contact with the organic pollutants, and so the concentrating effect by PAC would bring more phenol towards the photocatalysts for degradation and thus enhanced synergism can be observed at low phenol concentrations.

Table 5-2: Effect of initial phenol concentration on different composite photocatalysts

		$C_{in}=10.0$ (mg.L^{-1})	$C_{in}=20.0$ (mg.L^{-1})	$C_{in}=50.0$ (mg.L^{-1})	$C_{in}=80.0$ (mg.L^{-1})	$C_{in}=100.0$ (mg.L^{-1})
PPG-PAC-P25(1)	<i>adsorbed</i> (mg.g^{-1}) [^]	1.894	2.465	4.649	6.297	10.219
	k_{app} (hr^{-1})	0.172	0.093	0.052	0.032	0.027
	$R^{\#}$	1.345	3.781	3.263	3.240	3.325
PPG-PAC-P25(2)	<i>adsorbed</i> (mg.g^{-1}) [^]	3.346	7.870	8.923	10.567	19.718
	k_{app} (hr^{-1})	0.365	0.133	0.067	0.042	0.029
	$R^{\#}$	2.858	5.385	4.206	4.245	3.625
PPG-PAC-P25(4)	<i>adsorbed</i> (mg.g^{-1}) [^]	1.266	5.566	6.718	6.006	16.292
	k_{app} (hr^{-1})	0.163	0.088	0.045	0.027	0.022
	$R^{\#}$	1.274	3.567	2.813	2.700	2.750
PPG-PAC-P25(6)	<i>adsorbed</i>	0.436	4.713	5.021	5.372	15.264

	$(\text{mg.g}^{-1})^{\wedge}$					
	$k_{app} (\text{hr}^{-1})$	0.192	0.074	0.043	0.025	0.021
	$R^{\#}$	1.504	2.992	2.706	2.500	2.613
100%P25-PPG	$adsorbed$					
	$(\text{mg.g}^{-1})^{\wedge}$	0.000	0.000	0.000	0.000	0.000
	$k_{app} (\text{hr}^{-1})$	0.128	0.025	0.016	0.010	0.008
	$R^{\#}$	1.000	1.000	1.000	1.000	1.000

$$\wedge: adsorbed = \frac{\text{amount of phenol disappeared during 72 hrs adsorption (mg)}}{\text{weight of PAC on the composite photocatalysts (g)}} = \frac{0.2 \times (C_{in} - C_0)}{\text{dosage} \times \text{PAC}\%}$$

$$\#: Synergistic factor, R = \frac{k_{app}}{k_{app(100\%P25 PPG)}}$$

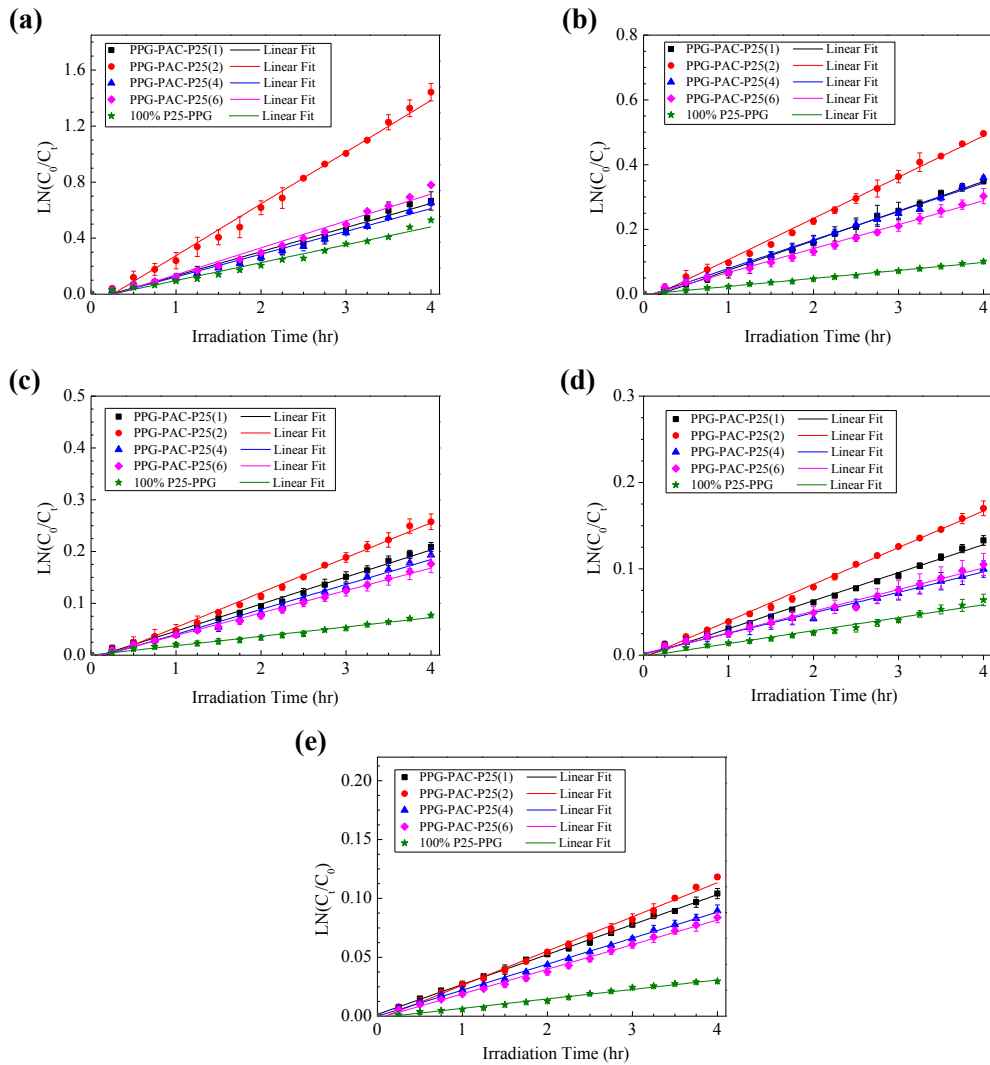


Figure 5-5: Kinetics of phenol photodegradation by different composite photocatalysts and the pseudo-first-order kinetic model fitting for different initial phenol concentrations: (a) $C_{in} = 10 \text{ mg.L}^{-1}$, (b) $C_{in} = 20 \text{ mg.L}^{-1}$, (c) $C_{in} = 50 \text{ mg.L}^{-1}$, (d) $C_{in} = 80 \text{ mg.L}^{-1}$, and (e) $C_{in} = 100 \text{ mg.L}^{-1}$ ($n=3$)

Figure 5-6 shows a plot of $1/k_{app}$ versus C_0 for different composite photocatalysts. The values of the adsorption equilibrium constant K_C , and the rate constant k_r were obtained by the linear regression of the data points calculated by eq. (2-31). Figure 5-7 shows the dependence of the rate constant k_r and adsorption equilibrium constant K_C determined in this way on the different composite photocatalysts. The adsorption equilibrium constant, K_C , first increased sharply when the coating cycle increased from 1 to 2, but then decreased when the number of coating cycles further increased. The PPG-PAC-P25(1) composite photocatalysts has the highest PAC loading, but achieved relatively low adsorptivity. It was found that the PPG-PAC surface was only partially covered by the P25 nanoparticles, which is not enough to change the surface hydrophobicity of the PAC layer. Poor liquid phase contact was observed during the experiments for the PPG-PAC-P25(1) composite photocatalysts, and perhaps resulted in the low adsorptivity. The decreases in the adsorptivity for the 4 coatings and 6 coatings composite photocatalysts may be considered to be due to the decrease in the exposed amount of PAC, as well as the increased pore blockage by the P25 particles immobilized. On the other hand, only slight variations were observed for the rate constant, k_r , probably due to the same immobilized amount of P25 being used in the test of the different types of the composite photocatalysts and the phenol decomposition process is mostly determined by the amount of TiO_2 particles. But the adsorption strength seems to be an important factor affecting the photocatalytic activity of the composite photocatalysts. The highest rate constant was observed for the 2 coatings composite photocatalysts, which also has the highest adsorptivity. After that, the rate constant decreased with increasing coating cycles, which may be due to

the decrease in the amount of adsorbed phenol. It is obvious that a decrease in the amount of adsorbed compounds caused a decrease in the photodegradation rate (Li et al., 2006). Secondly, it is also observed that the P25 coatings on PPG-PAC-P25(4) and PPG-PAC-P25(6) were much thicker and packed than that on PPG-PAC-P25(1) and PPG-PAC-P25(2) photocatalysts. The surface active site of the photocatalysts would be reduced when large aggregates were formed and hence reduced the accessibility of phenol molecules to these sites, thus leading to the decrease in the photocatalytic activity. Therefore, for the composite photocatalysts to show high photocatalytic activity, they should have enough and well dispersed TiO_2 particles on the surface, but at the same time, retain the adsorption strength of the PAC as much as possible to bring the organic molecules sufficiently to the vicinity of the composite photocatalysts. In the present case, the PPG-PAC-P25(2) composite photocatalyst appeared to exhibit both high adsorptivity and high photocatalytic activity and hence it was chosen for the following further studies discussed.

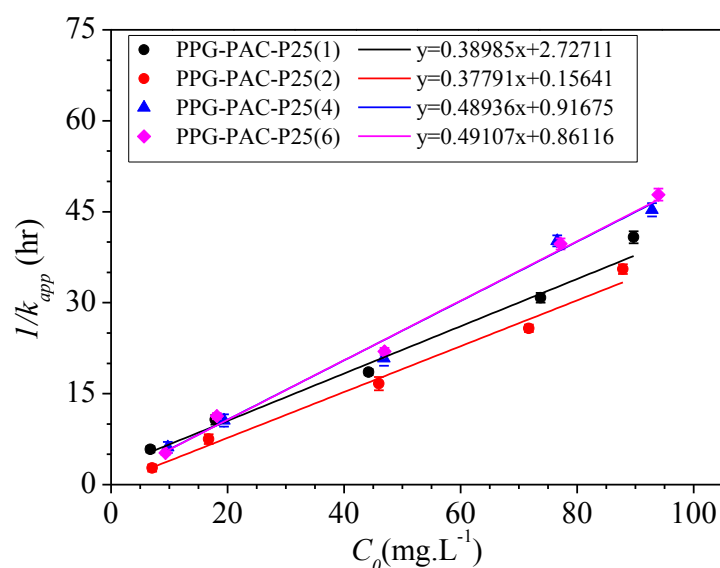


Figure 5-6: Relationship between $1/k_{app}$ and C_0 for different composite photocatalysts ($n=3$)

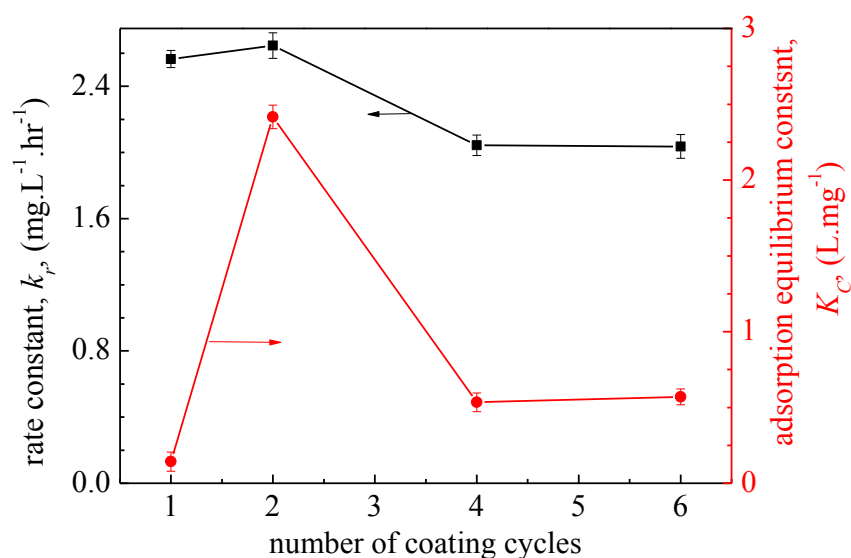


Figure 5-7: The rate constant of phenol photocatalytic degradation and the adsorption equilibrium constant as a function of coating cycles ($n=3$)

5.3.5. Effect of composite photocatalyst dosage

The dosage of composite photocatalysts can be an important parameter in the performance of photocatalytic degradation process. Several studies reported an optimal photocatalyst dosage existed for the maximum removal of phenol (Tu et al., 2013). The optimum dosage depends on the geometry of the reactor, light source intensity, and properties of TiO_2 such as particles size, phase compositions and impurities (Chen et al., 2000b). This is due to that the increase of the photocatalyst dosage beyond the optimal range may result in unfavorable light scattering and thus reduction of the photon efficiency.

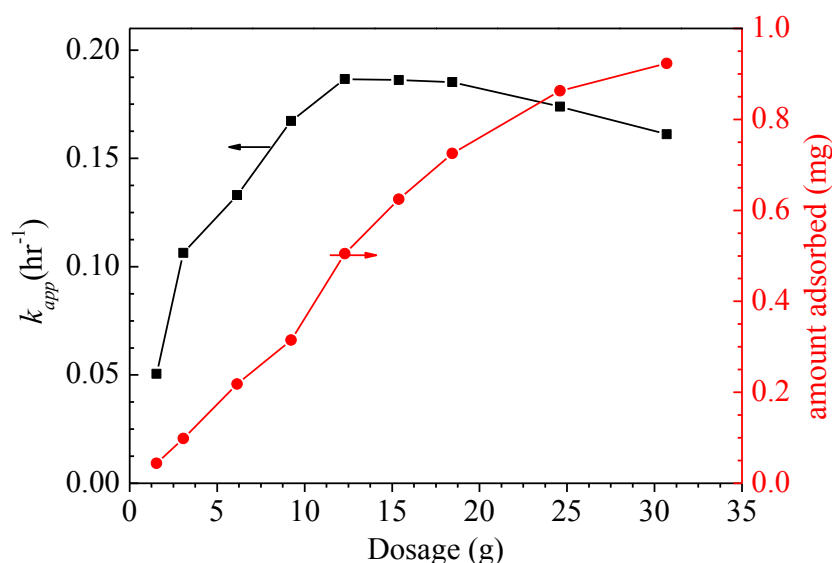


Figure 5-8: The apparent rate constants and amount of phenol adsorbed as a function of PPG-PAC-P25(2) composite photocatalysts dosage

In the same photocatalytic process setup, a variety of PPG-PAC-P25(2) dosages ranging from 1.53 g to 30.75 g was tested with the 200 mL phenol solution (20 mg.L^{-1} with 0.5 wt.% NaCl) in the photocatalytic reactor. The experimental results are shown in Figure 5-8. When the composite photocatalysts dosage increased from 1.53 g to 12.3 g, both phenol adsorption and photocatalytic degradation in terms of k_{app} showed linear increases with the increase of the dosage. However, further increases of the photocatalyst dosage to 30.75 g resulted in a decreased photocatalytic degradation activity, even although the adsorptivity continued to increase, due to the increased amount of PAC component in the photocatalyst. Therefore, a proper dosage is indeed desirable. As for the jacketed reactor used in this setup, about 7.5g composite photocatalysts were just enough to cover the entire irradiation area. Hence, the dosages lower than 7.5 g would reduce the UV efficiency as the irradiation area was not fully utilized. The photocatalytic activity continued to increase when increasing the dosage to 12.3 g. The aeration by air diffuser at the reactor bottom also provided mixing effect in the reactor, resulting in the photocatalyst granules with localized

movements, turning up and down in the surface zone, and hence fully utilizes the available UV irradiation. However, further increasing the dosage beyond 12.3g would cause a thick photocatalyst layer on the water surface, and the air bubbling was not strong enough to turn all the granules moving up and down, so only the granules laying on the very top surface can receive the UV irradiation, and the others lying below would not be effectively used, reducing the overall photocatalytic activity. According to Figure 8, 12.3 g composite photocatalysts dosage should be adequate for the photocatalytic degradation setup used in this study, which is equivalent to a dosage loading of 61.5 g L^{-1} of PPG-PAC-P25(2), or 0.689 g L^{-1} in terms of P25 amount, or 3.29 kg.m^{-2} , taking into account of the 69 mm irradiation diameter provided by the Xenon lamp used in the photocatalytic reactor.

5.3.6. Effect of suspended solids

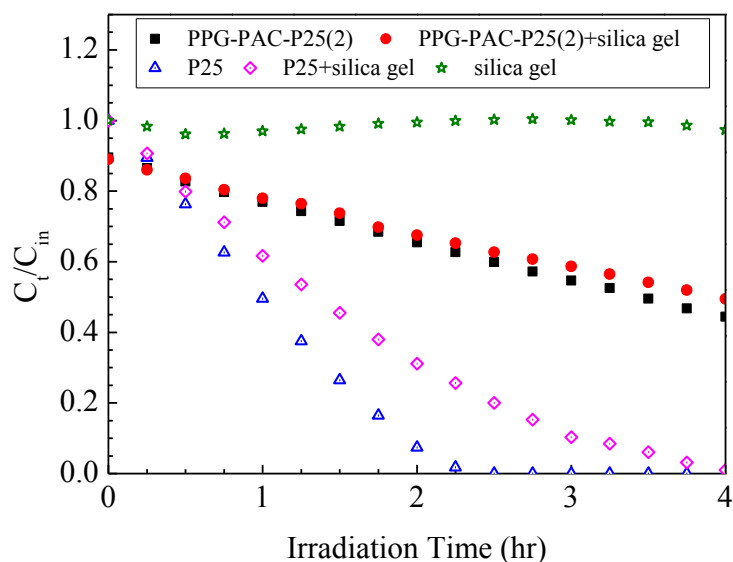


Figure 5-9: Effect of suspended solids on the photocatalytic degradation performance of PPG-PAC-P25(2) as compared that of P25

The negative impact of water turbidity on UV transmission is well-known in water and wastewater industries. Reduction in photocatalytic oxidation reaction rate can be

expected in turbid water due to shielding (absorption, scattering and/or blocking) of the incident UV. During the preliminary screening of inorganic solids, including kaolin, bentonite and silica gel, only silica gel exhibited no significant impact on solution pH and dark adsorption. As solution pH is a very sensitive parameter for photocatalytic reaction, 0.5 g.L⁻¹ silica gel was selected to evaluate the UV shielding effect of the inorganic solids on the photocatalytic degradation performance of PPG-PAC-P25(2), as compared to that of the P25 suspension. The concentration profiles from the photocatalytic degradation experiments are shown in *Figure 5-9*. The addition of 0.5 g.L⁻¹ silica gel particles into the P25 slurry photocatalytic degradation system resulted in reduced initial photocatalytic degradation rate and about 1.5 hours more to reach complete phenol removal. Since no other operational parameter was changed, the reduction of the photocatalytic activity of P25 can solely be attributed to the UV shielding effect by the silica gel particles (Giri et al., 2010). However, only small decrease in the photocatalytic activity was observed with the PPG-PAC-P25(2), and the final phenol removal was decreased by only 5% in the presence of the silica gel. This can be explained by the “floating” mechanism of the prepared composite photocatalysts. In the slurry system, silica gel particles have equal chance to absorb the incident light as the P25 photocatalysts and thus reduced the UV light efficiency of the photocatalyst. But in the case of buoyant photocatalysts, the active photocatalysts were floating on the water surface, formed a thick blanked to conceal the shielding effect of suspended solids lying below. Therefore, only a few of the silica gel particles that happened to be on the water surface and lying above the buoyant composite photocatalysts would result in the light scattering and most of the other particles lying below would have no effect on the composite photocatalysts’ photocatalytic activity. It thus can be concluded that the buoyant composite

photocatalysts can largely avoid the shielding effect by the suspended solids presented in water to be treated.

5.3.7. Effect of radical scavengers

Two scavengers, IPA and KI, were added to the reaction solution to capture the reactive species during the photocatalytic reaction. Preliminary adsorption experiments for different scavenger concentrations of IPA and KI show that no interference was noticed for the applied IPA or KI concentrations up to 21.28 mmol.L⁻¹ ($\alpha(\text{KI})=100$ or $\alpha(\text{IPA})=100$). Further increasing the concentration of the scavengers would result in interference with phenol adsorption. Hence, in order to compare the photocatalytic activity changes due to radical scavengers, the degradation experiments were only performed within the scavengers concentration limit that no adsorption interference with the phenol adsorption was noticed (i.e., $\alpha(\text{IPA})$ and $\alpha(\text{KI})$ up to 100). In order to evaluate the effect of PAC layer, the photocatalytic activity of 100%P25-PPG were also measured and compared as the base buoyant composite without co-adsorbent component.

Isopropyl alcohol (IPA) is known to be a good hydroxyl radical (OH•) scavenger and is used to discriminate between direct oxidation with positive holes (h⁺) and the degradation with hydroxyl radicals in solution (Chen et al., 2005). The rate constant of reaction between OH• radical and IPA is $1.9 \times 10^9 \text{ M}^{-1} \text{ S}^{-1}$, which is close to the diffusion limit. That is, the reaction between these two reactants would occur as fast as the reagents encounter each other (Pantopoulos and Schipper, 2011; Zhang et al., 2008). Though direct oxidation of short aliphatic alcohols by photogenerated holes occurs, it was considered negligible because they have a very weak adsorption on TiO₂ surface in aqueous media (Palominos et al., 2008). Different concentrations of

IPA were dosed, and its inhibitory effects on the photocatalytic activities (k_{app}) are shown in *Figure 5-10(a)*. It can be observed that the degradation of phenol suppressed in the presence of IPA. The apparent rate constant of 100%P25-PPG decreased by 24% after adding only 0.21 mmol L⁻¹ IPA into the solution. However, further increasing the IPA concentration did not result in further decrease in the photocatalytic activity. At $\alpha(\text{IPA})=100$, only 33% drop in the initial degradation rate constant was noticed. This is a relatively small increase with a high scavenger concentration, indicating that the hydroxyl radicals in the solution have a moderate contribution in the photocatalytic degradation of phenol by 100%P25-PPG (Chen et al., 2005). However, the quenching effect of IPA on the PPG-PAC-P25(2) composite photocatalysts was much more obvious. Similar scavenging effect on the photocatalytic activity of PPG-PAC-P25(2) towards phenol removal was observed only at low IPA concentrations, the apparent rate constant (k_{app}) decreased significantly as the IPA concentration increased. The photocatalytic activity dropped by more than 57% at $\alpha(\text{IPA})=100$. This is due to the fact that PAC is a good organic adsorbent that can absorb various organics. Its concentrating effect not only brought phenol molecules to the vicinity of the immobilized P25 nanoparticles, but at the same time, it also brought IPA molecules near to the photocatalyst surface. Especially at high IPA concentrations, the adsorptive force made much more IPA molecules around the photocatalysts' active sites and fewer places for phenol molecules, hence greatly reduced the photocatalytic degradation of phenol molecules.

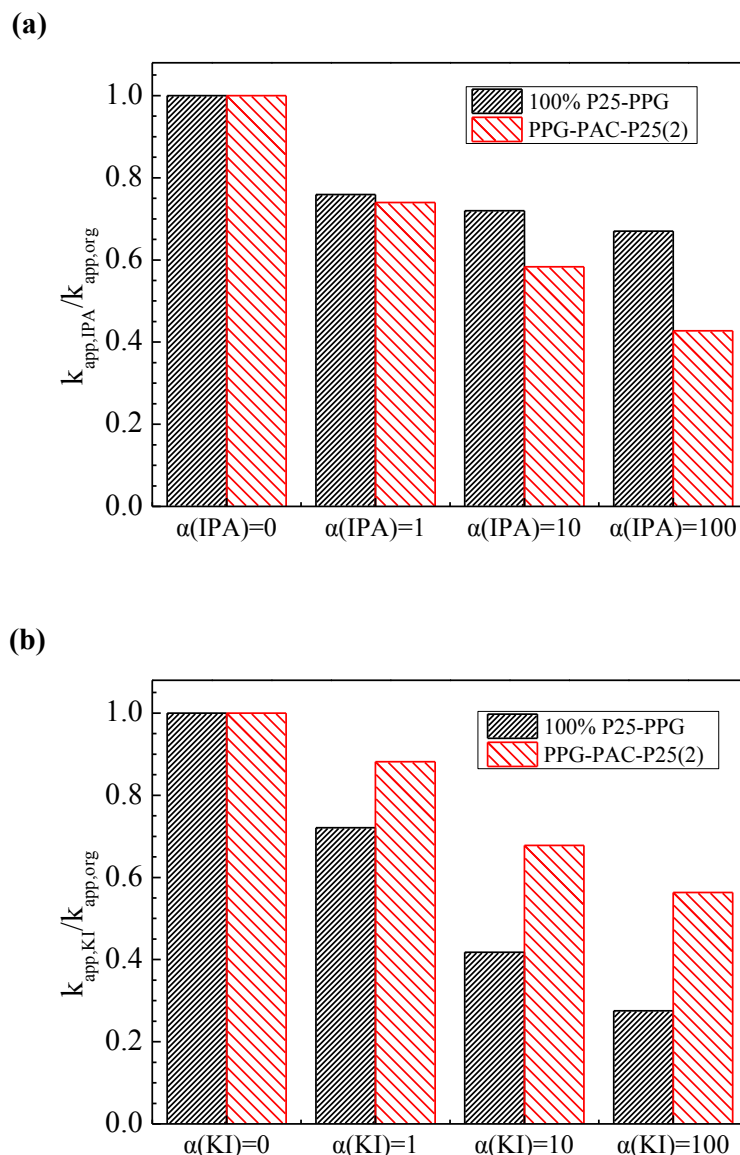


Figure 5-10: Effect of radical scavengers, a) isopropyl alcohol, IPA and (b) potassium iodine, KI, on the photocatalytic degradation performances of PPG-PAC-P25(2) and 100%P25-PPG

$\alpha(\text{IPA}) = \frac{C_{0,\text{IPA}}}{C_{0,\text{phenol}}}$, the molar ratio of IPA over phenol concentration;

$\alpha(\text{KI}) = \frac{C_{0,\text{KI}}}{C_{0,\text{phenol}}}$, the molar ratio of KI over phenol concentration;

Iodide ion is an excellent scavenger which reacts with photogenerated positive holes and hydroxyl radicals. Valence band holes and hydroxyl radicals are easily captured by I^- (Chen et al., 2005). Different concentrations of KI were dosed, and its inhibitory effects on the photocatalytic activity (k_{app}) of two types of composite

photocatalysts photoactivities (k_{app}) are shown in *Figure 5-10(b)*. Applying a $\alpha(KI)=100$ showed more than 72% decrease in the apparent rate constant of 100%P25-PPG. The greater inhibition of the reaction through KI compared to that of IPA at lower scavenger concentrations gives an indication that the photogenerated positive holes play a more important role in the photocatalytic degradation of phenol by 100%P25-PPG than hydroxyl radicals (Van Doorslaer et al., 2012). However, the KI scavenging effect was less obvious on the PPG-PAC-P25(2) composite photocatalysts. Although its apparent rate constant continued to decrease with increasing KI concentrations, the reduction in k_{app} was smaller than that of 100%P25-PPG. PAC is a good organic adsorbent, and it has negligible adsorptivity towards inorganic ions in the aqueous solution. Hence, this shielding effect on inorganic radical scavenger was due to the PAC layer. The presence of adsorption force from the PAC layer would largely increase the phenol concentration around the photocatalysts and hence increased the competitiveness of phenol over iodide ions towards the active sites for photocatalytic degradation. A similar shielding effect by the composite photocatalysts on the negative influence of chloride ions on phenol photocatalytic degradation was also noticed in our previous study (Tu et al., 2013).

5.3.8. In-situ regeneration effect of PAC layer by the immobilized P25 of the prepared composite photocatalysts

In the previous study of the composite photocatalysts' recyclability with 20 repeated photodegradation cycles, it was noticed that the adsorptive sites on the PAC layer were continuously in-situ regenerated during the photocatalytic degradation process. Therefore, the aim of this section is to better understand the in-situ regeneration capability of the deposited P25 layer for the adsorption capacity and

photocatalytic recovery of PPG-PAC-P25(2) composite photocatalyst with different UV irradiation durations (T). The preliminary study showed that when 12.3 g saturated PPG-PAC-P25(2) composite photocatalysts were suspended in 20 mg.L⁻¹ phenol solution with 0.5wt% NaCl, it required 8 hours to reach 95% phenol removal from the solution under the experimental condition of 25°C and 0.2 L.min⁻¹ O₂ supply, and full phenol removal could be achieved within 12 hours. Hence, 5 different irradiation durations were selected. $T=1$ hr and $T=4$ hrs were not enough to degrade all the free phenol molecules in the solution, $T=8$ hrs was almost enough to remove the free phenol molecules in the solution, and $T=12$ hrs and $T=16$ hrs irradiation were more than enough to degrade all the free phenol molecules in the solution. The in-situ regeneration efficiencies were evaluated according to 4 aspects shown in *Figure 5-11*, (a) the re-adsorption capacities of PPG-PAC-P25(2) composite photocatalysts, (b) the apparent rate constant changes against the apparent rate constant in the first UV irradiation cycle ($k_{app,1}$) when the PAC particles were fully loaded with phenol molecules, (c) total percentage of phenol removed from the solution and (d) total percentage of TOC removed from the solution.

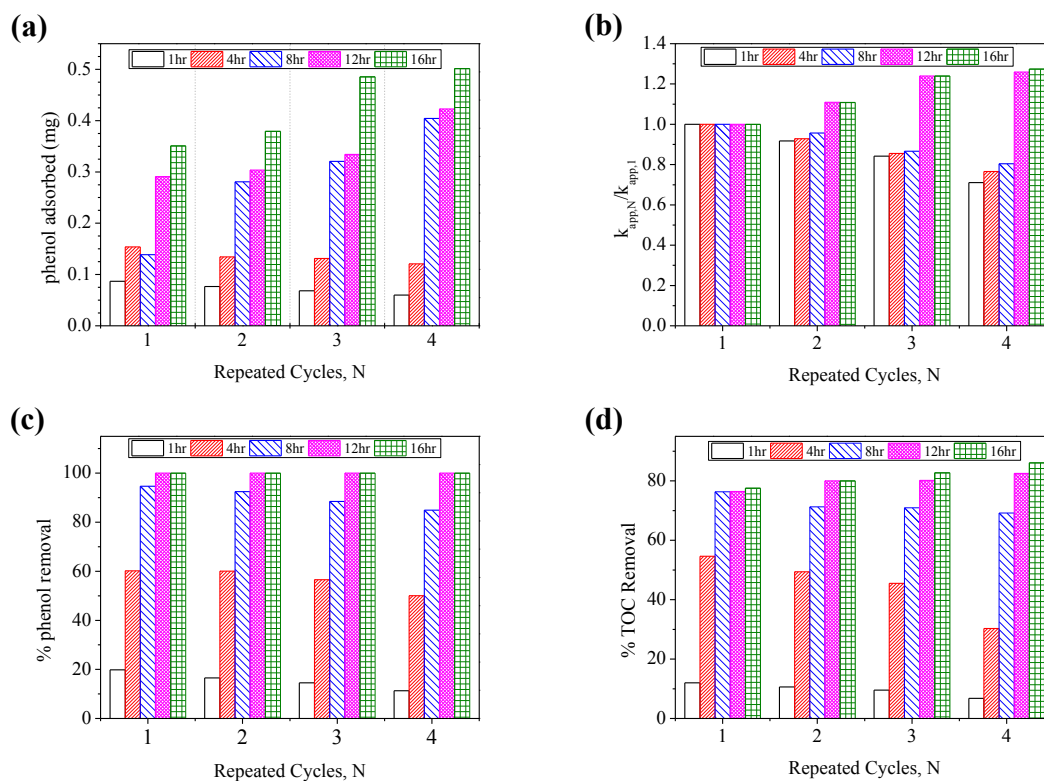


Figure 5-11: Effect of irradiation duration on in-situ regeneration efficiencies, (a) phenol adsorption capacity recovered, (b) phenol in solution disappearance kinetics, (c) percentage of total amount of phenol removed from solution and (d) percentage of TOC removal from the solution

It can be found from Figure 5-11(a) that the longer the irradiation duration, the better adsorption capacity recovery. When short irradiation duration were used (1 hour and 4 hours), only limited adsorption capacities were recovered, and the recovery efficiencies gradually decreased after each irradiation-adsorption cycle. The regeneration during the short irradiation durations was assumed to be due to the rapid degradation of adsorbate bound to exterior surface of composite photocatalysts (Yap and Lim, 2012), but no degradation of the adsorbed substances in the inner pores. However, due to the insufficient irradiation duration, incomplete degradation of the adsorbed organic molecules may occur for the composite photocatalysts, which resulted in the deactivation of the photocatalysts by the adsorbed molecules, reduced the photocatalytic activity and total percentage removal of phenol and TOC from the solution (Chen et al., 2012). When the irradiation duration extended to 8 hours and

above, the re-adsorption capacities gradually increased after each cycle. The longer the irradiation duration, the higher adsorption capacity recovered, indicating that the regeneration process was limited by the rate of diffusion of adsorbates from the interior surface of the adsorbent to the exterior where photocatalytic reaction took place (Crittenden et al., 1997; Tao et al., 2006; Yap and Lim, 2012; Zhu and Zou, 2009). Photocatalytic degradation happened on free phenol molecules in the solution first, but when the concentration gradient between the composite photocatalysts and bulk solution reached certain level, the adsorbed substances on the adsorbent would be slowly desorbed from the adsorptive site and transferred to the photoactive site for degradation. Furthermore, it is noticed that the relative photocatalytic activity, $k_{app,N}/k_{app,1}$ increased beyond 1.00 after extended UV irradiations in *Figure 5-11(b)*. The increased photocatalytic activity indicates that the adsorbed intermediates were also degraded after long irradiation durations, and the photocatalytic activity was recovered by recovering the synergistic effect of the PAC/P25 combination. Lastly, it should be noticed that the TOC removal (*Figure 5-11(d)*) is always slower than phenol removal (*Figure 5-11(c)*) under all cases tested. The complete mineralization was never reached, even after 16 hours of irradiation. Moreover, full phenol removal was obtained within 12 hours, but extending the irradiation hours to 16 hours did not result in much improvement of TOC removal, indicating that some of the degradation intermediates, possibility short aliphatic acids, are hard to be degraded by photocatalysis.

5.4. Conclusions

The performance of the buoyant composite photocatalyst prepared by the two-layered configuration approach was examined in more details. Buoyant composite photocatalysts of different compositions (P25: PAC ratios) were prepared with different number of the soak-dry-cure cycles, from 1 cycle up to 6 cycles. All the obtained composite photocatalysts were buoyant and can float on water. The TGA analysis revealed that the P25 loading on the PPG-PAC intermediate increased with increasing coating cycles, so as the P25: PAC ratio. The adsorptivity and photocatalytic performances of the obtained composite photocatalysts were evaluated by phenol removals under various conditions. The adsorption capacity of the PAC was not affected by the thermal immobilization process on PPG-PAC, but the uptake rate was greatly reduced. The adsorption uptake amount decreased significantly after the coating of P25 and the capacity continued to decrease with the increase of the coating cycles indicating that the immobilization of P25 on PPG-PAC caused the physical blockages of the adsorption sites of PAC. The photocatalytic activity of the composite photocatalysts with PAC was significantly higher than that of 100%P25-PPG (without PAC), and it is especially true for the PPG-PAC-P25(2), suggesting that the co-adsorbent could synergistically enhance the photocatalytic degradation performance. The photocatalytic degradation performances were further analyzed with the modified Langmuir-Hinshelwood kinetic model under different initial phenol concentrations. PPG-PAC-P25(2) achieved the highest rate constant of k_r and adsorption equilibrium constant of K_C , and it also achieved the highest apparent rate constants (k_{app}) under all concentrations. Therefore, it could be implied that for the composite photocatalysts to show high photocatalytic activity, they should have enough and well dispersed TiO_2 particles on the surface, but at the same time, retain

the adsorption strength of the PAC as much as possible to bring sufficient organic molecules to the vicinity of the composite photocatalysts. 12.3g of PPG-PAC-P25(2) was found to be adequate for the photocatalytic degradation setup used in this study, which was about 1.5 times of the amount of photocatalyst required to cover the entire irradiation area. The photocatalytic activity of P25 slurry photocatalytic degradation system was largely reduced due to the scattering effect of the silica gel particles, but only small decrease in the photocatalytic activity was observed with PPG-PAC-P25(2), suggesting that the “floating” mechanism of PPG-PAC-P25(2) can largely avoid the scattering effect of the suspended solids by forming a blanket to conceal the shielding effect of the solids. The quenching effect of IPA on the PPG-PAC-P25(2) composite photocatalysts was more severe than that of KI. This may be due to the co-adsorbent component used, because PAC is a good organic adsorbent and hence its concentrating effect applies to both phenol and IPA. However, KI is inorganic scavenger which does not respond to the adsorptive property of PAC, thus showing no significant negative effect of the inorganic ions present in the solution on photocatalytic degradation efficiency towards phenol removal by PPG-PAC-P25(2). Lastly, the in-situ regeneration experiment with pre-saturated phenol on PPG-PAC-P25(2) revealed that the longer the irradiation duration, the better adsorption capacity recovery, confirming that the regeneration process was limited by the rate of diffusion of adsorbates from the interior surface of the adsorbent to the exterior where photocatalytic reaction took place.

Chapter 6: Conclusions and Recommendations

6.1. Conclusions

This research attempted to prepare a desired composite photocatalyst with both the adsorption and photocatalytic degradation components on a relatively cheap substrate that incurs the composite with buoyant property.

The composite photocatalyst was first developed by a direct thermal immobilization method by loading P25 and PAC from a mixture simultaneously onto PPG at temperature slightly higher than the melting temperature of PPG. All the prepared composite photocatalysts were in millimeter size and truly floating on water surface. The FESEM observation confirmed that both P25 and PAC were well-distributed on the PPG surface. The actual compositions of the obtained composite photocatalysts were analyzed with TGA by the two-stage method. The percentage of PAC loaded on the composite photocatalysts varied with the relative percentage of the PAC content in the powder mixture. Higher amount of PAC immobilization was achieved with higher PAC percentage in the powder mixture. Whereas, the dependence of the amount of P25 immobilized on the composite photocatalyst on the percentage of P25 in the powder mixture was not significant, possibly due to the large difference in the particle sizes of P25 and PAC. The adsorption activity of the obtained composite photocatalysts can be well described by the Langmuir isotherm model. The photocatalytic activity of the PAC-containing composite photocatalysts was found to be higher than that of the 100%P25-PPG that contained P25 but without PAC, confirmed the hypothesis that combining the adsorptive and photocatalytic components on the solid supporting material would have an enhancing effect on the overall pollutant removal efficiency. The kinetics of phenol degradation by the

composite photocatalysts can be well-fitted with the Langmuir–Hinshelwood model, with a pseudo-first-order reaction constant. The study successfully confirmed the hypothesis that the PAC component in the composite photocatalysts helped concentrating the organic pollutants in the bulk solution to the vicinity of the photocatalyst particles and thus made the photocatalytic degradation process less dependent on the organic concentration in the bulk solution, which enhanced the photocatalytic degradation process efficiency. Among all the 3 composite photocatalysts, 50%P25-PPG was found to be the most efficient composite photocatalysts with both high adsorptivity and high photocatalytic activity. The 50%P25-PPG composite photocatalysts was also found to works better under acidic conditions.

However, the buoyant composite photocatalysts prepared by the direct thermal immobilization of PAC and P25 together showed some detachment of the P25 nanoparticles and thus unstable performance after extended long periods of usage, attributed to the slow photocatalytic degradation of the PPG substrate immobilized with the P25 particles in the photocatalytic degradation process of phenol. Therefore, a modified method to prepare the buoyant composite photocatalysts with a novel two-layered configuration was developed to improve the photocatalytic degradation stability of the composite photocatalyst for its potential use in long term practical applications for organic pollutant removal. Taking the advantage of the physical inertness of PAC, an entire PAC layer was first anchored onto the PPG surface by the direct thermal immobilization method. Then, another layer of P25 nanoparticles was loaded onto the PAC-immobilized PPG by a new suspension hydrothermal deposition method. Experiments showed that PPG-PAC-P25 had good mechanical and chemical stability against normal mechanical attrition in the process and possible photocatalytic

degradation under UV irradiation. The thermally immobilized PAC layer was found to be tightly anchored on the PPG substrate, serving as a good platform for the loading of P25 nanoparticles in addition to its function as a protection barrier for the PPG substrate from being photocatalytically degraded. PPG-PAC-P25 was also found to have enhanced photocatalytic performance for phenol removal than 25%P25-PPG or 100%P25-PPG, due to the well-dispersed deposition of P25 on the PPG-PAC intermediate that formed a micro-porous structure that appeared desirable to retain some of the adsorption function of the PAC. The photocatalytic degradation kinetics of phenol by the composite photocatalysts can be well fitted to a pseudo-first-order kinetic model. The recyclability test of PPG-PAC-P25 was carried out with 20 cycles in a batch feed process, and the phenol removal efficiency was found to be decreased by only 7% after the 20th cycle, demonstrating that the newly developed two-layer configuration composite photocatalysts is a potentially very promising composite photocatalyst for the degradation of organic pollutants in aqueous solutions for practical applications. However, the performance of the PPG-PAC-P25 may be further examined for the optimum combination of the adsorbent and the photocatalyst components in the obtained composite photocatalyst and its suitable operation parameters.

The composition of the buoyant composite photocatalysts with the two-layered configuration was varied with different number of the soak-dry-cure cycles for different P25 loadings, from 1 cycle up to 6 cycles. The P25 loading on the PPG-PAC intermediate increased with increasing the coating cycles. The adsorption capacity decreased greatly after the coating of P25 as compared to that of the PPG-PAC intermediate, and continued to decrease as the number of coating cycles increased, indicating that the immobilization of P25 on PPG-PAC caused the physical blockages

of the adsorption sites on the PAC layer. The photocatalytic activity of all the prepared composite photocatalysts was significantly higher than that of 100%P25-PPG, especially true for the PPG-PAC-P25(2), suggesting that the PAC layer could synergistically enhance the photocatalytic degradation performance. The photocatalytic degradation performances were further analyzed with the modified Langmuir-Hinshelwood kinetic model under different initial phenol concentrations. PPG-PAC-P25(2) achieved the highest photocatalytic reaction rate constant (k_r) and adsorption equilibrium constant (K_C), and it also achieved the highest apparent rate constants (k_{app}) under all concentrations. Therefore, it could be implied that adsorptivity of the composite photocatalysts is detrimental to the overall performance of the photocatalysts. Not only there need to have enough and well dispersed TiO₂ nanoparticles on the surface, but the adsorption strength of the PAC need to be retained as much as possible to make a highly efficient composite photocatalysts. 12.3g of PPG-PAC-P25(2) was found to be the adequate amount for the photocatalytic degradation setup used in this study, which was about 1.5 times of the photocatalyst amount required to cover the entire irradiation area. Too few photocatalysts would reduce the UV light utilization efficiency, whereas too much photocatalysts would make the floating layer too thick and crowded and reduce the efficiency of the composite photocatalysts. The photocatalytic activity of P25 slurry photocatalytic degradation system was largely reduced due to the scattering effect of the silica gel particles, but only small decrease in the photocatalytic activity was observed with PPG-PAC-P25(2), suggesting that the “floating” mechanism of PPG-PAC-P25(2) can largely avoid the scattering effect of the suspended solids on UV light irradiation. The quenching effect of IPA on the PPG-PAC-P25(2) composite photocatalysts was more severe than that of KI. This was due to the co-adsorbent

component used, because PAC is a good organic adsorbent and its concentrating effect applies to both phenol and IPA. However, KI is an inorganic salt which does not respond to the adsorptive force of PAC. Thus the PAC only concentrated phenol to the photocatalysts and largely shielded of the negative effect of the inorganic ions present in the solution on photocatalytic degradation efficiency towards phenol removal by PPG-PAC-P25(2). Lastly, the in-situ regeneration experiment for PPG-PAC-P25(2) pre-saturated with phenol revealed that the longer the irradiation duration, the better adsorption capacity recovery, indicating that the regeneration process was limited by the rate of diffusion of adsorbates from the interior surface of the adsorbent to the exterior where photocatalytic reaction took place.

6.2. Suggested future studies

An easy and economic method for preparing the novel composite photocatalysts has been investigated in this thesis. The preparation method utilized the available materials, of PPG, PAC and P25, at a relatively low temperature. The challenge of photocatalytic degradation of the polymeric support used by the composite photocatalysts has been successfully solved by the use of the intermediate barrier layer of PAC in the two-layered configuration. However, the prepared composite photocatalysts were only active under UV irradiation. Considering the natural sunlight only containing the UV light at as low as 3 - 5%, but the visible light up to 45-50% (Han and Bai, 2009), it would be more cost-effective if the composite photocatalysts could be made active under both the UV and visible light range (Singh et al., 2013). Most of the modification studies have been carried out by doping TiO₂ with precious metals, metal oxides, or inorganic components so as to reduce the band gap energy of the photocatalyst. Some of the successful modification method reported on P25 nanoparticles involved metal doping by photo-induced reduction process (Chen et al., 2013), dye sensation (Subash et al., 2013) and carbon and nitrogen doping at evaluated pressure (Janus and Morawski, 2007). Beside doping, the addition of conductive component, such as carbon nanotubes (CNT), fullerenes (C60) and graphene oxide (GO) was also the possible method for obtaining photocatalysts of visible light activity (Pastrana-Martínez et al., 2013).

In this thesis, only phenol was used as the target pollutant in the photocatalytic degradation reaction. However, as already been proven, the adsorptivity of organic pollutants towards both TiO₂ (Linsebigler et al., 1995) and activated carbon (Cheremisinoff and Ellerbusch, 1978) were found to be strongly pollutant dependent. The adsorptivity of TiO₂ towards phenol was very low. But it was noticed in our trial

experiments that the adsorption of methyl orange (MO) dye was comparatively better. The photocatalytic degradation of MO dye showed different level of synergism, depending on the P25 to PAC ratio. Although this difference may be partially attributed to the different photocatalytic degradability of MO dye and phenol, the differences in the adsorption and desorption strengths of MO dye and phenol to the composite buoyant photocatalysts may also play an important role in the reaction performance. According to the photocatalytic reaction steps mentioned in Chapter 2, the photoreactions are generally believed to occur on the surface of TiO_2 . Hence, the photocatalytic activity of the buoyant composite photocatalyst to certain organic pollutants may be improved through modifying the adsorptivity of the buoyant composite photocatalyst, leading to the possibility of enhancing the selectivity of the composite photocatalysts by surface modification. Possible routes to modify the surface adsorptivity include surface treatment such as acid surface treatment (Boehm, 2002) and plasma surface treatment (Şahin et al., 2013).

Last but not least, the recyclability of the prepared composite photocatalysts in Chapter 4 and 5 clearly revealed that the designed buoyant composite photocatalysts can be considered for large scale industrial wastewater applications. Hence, an efficient photocatalytic reactors design is required for large-scale usage as demanded by the industrial and commercial applications (Alfano and Cassano, 2009; Ray, 2009). The major issues in the development of a photocatalytic reactor, include the proper light distribution inside the reactor and realize high surface areas for the catalyst per unit volume of the reactor. The fixed-bed reactor system is a widely used reactor design in the heterogeneous photocatalysis systems. The fixed-bed reactor design offers much higher surface to volume ratio than the traditional immersion type of reactor design and is flexible to be scaled-up for commercial applications (Mukherjee

and Ray, 1999). However, in order to fulfill the ultimate purpose of the large-scale applications on photocatalytic treatment of industrial wastewater, in-depth studies on the reactor design are necessary.

Reference

Aarathi, T. and Madras, G. Photocatalytic degradation of rhodamine dyes with nano-TiO₂, *Ind. Eng. Chem. Res.*, *46*, pp. 7-14. 2006.

Aarathi, T. and Madras, G. Photocatalytic reduction of metals in presence of combustion synthesized nano-TiO₂, *Catal. Commun.*, *9*, pp. 630-634. 2008.

Aguedach, A., Brosillon, S., Morvan, J. and Lhadi, E. K. Photocatalytic degradation of azo-dyes reactive black 5 and reactive yellow 145 in water over a newly deposited titanium dioxide, *Appl. Catal., B*, *57*, pp. 55-62. 2005.

Ahmed, S. Impact of operating conditions and recent developments in heterogeneous photocatalytic water purification process, *Crit. Rev. Env. Sci. Technol.*, *42*, pp. 601-675. 2011.

Ahmed, S., E. Jones, C., J. Kemp, T. and R. Unwin, P. The role of mass transfer in solution photocatalysis at a supported titanium dioxide surface, *Phys. Chem. Chem. Phys.*, *1*, pp. 5229-5233. 1999.

Ahmed, S., Rasul, M., Martens, W., Brown, R. and Hashib, M. Advances in heterogeneous photocatalytic degradation of phenols and dyes in wastewater: A review, *Water Air Soil Pollut*, *215*, pp. 1-27. 2010a.

Ahmed, S., Rasul, M. G., Brown, R. and Hashib, M. A. Influence of parameters on the heterogeneous photocatalytic degradation of pesticides and phenolic contaminants in wastewater: A short review, *J. Environ. Manage.*, *92*, pp. 311-330. 2011.

Ahmed, S., Rasul, M. G., Martens, W. N., Brown, R. and Hashib, M. A. Heterogeneous photocatalytic degradation of phenols in wastewater: A review on current status and developments, *Desalination*, *261*, pp. 3-18. 2010b.

Al-Rasheed, R. and Cardin, D. J. Photocatalytic degradation of humic acid in saline waters. Part 1. Artificial seawater: influence of TiO₂, temperature, pH, and air-flow, *Chemosphere*, *51*, pp. 925-933. 2003a.

Al-Rasheed, R. and Cardin, D. J. Photocatalytic degradation of humic acid in saline waters: Part 2. Effects of various photocatalytic materials, *Appl. Catal., A*, *246*, pp. 39-48. 2003b.

Al-Sayyed, G., D'oliveira, J.-C. and Pichat, P. Semiconductor-sensitized photodegradation of 4-chlorophenol in water, *J. Photochem. Photobiol. A*, *58*, pp. 99-114. 1991.

Alam, M. Z., Ameen, E. S., Muyibi, S. A. and Kabbashi, N. A. The factors affecting the performance of activated carbon prepared from oil palm empty fruit bunches for adsorption of phenol, *Chem. Eng. J.*, *155*, pp. 191-198. 2009.

Alfano, O. M. and Cassano, A. E. Scaling-up of photoreactors: Applications to advanced oxidation processes. In *Advances in Chemical Engineering*, Volume 36, ed by Hugo, I. D. L. & Benito Serrano, R., pp. 229-287: Academic Press. 2009

Ameta, R., Benjamin, S., Ameta, A. and Ameta, S. C. Photocatalytic degradation of organic pollutants: A review. Paper presented at the Materials Science Forum. 2013.

Anderson, C. and Bard, A. J. An Improved Photocatalyst of TiO₂/SiO₂ Prepared by a Sol-Gel Synthesis, *J. Chem. Phys.*, *99*, pp. 9882-9885. 1995.

Ao, Y., Xu, J., Fu, D., Shen, X. and Yuan, C. A novel magnetically separable composite photocatalyst: Titania-coated magnetic activated carbon, *Sep. Purif. Technol.*, *61*, pp. 436-441. 2008.

Araña, J., Doña-Rodríguez, J. M., Cabo, C. G. I., González-Díaz, O., Herrera-Melián, J. A. and Pérez-Peña, J. FTIR study of gas-phase alcohols photocatalytic degradation with TiO₂ and AC-TiO₂, *Appl. Catal., B*, *53*, pp. 221-232. 2004.

Araña, J., Doña-Rodríguez, J. M., Tello Rendón, E., Garriga I Cabo, C., González-Díaz, O., Herrera-Melián, J. A., Pérez-Peña, J., Colón, G. and Navío, J. A. TiO₂ activation by using activated carbon as a support: Part I. Surface characterisation and decantability study, *Appl. Catal., B*, *44*, pp. 161-172. 2003a.

Araña, J., Doña-Rodríguez, J. M., Tello Rendón, E., Garriga I Cabo, C., González-Díaz, O., Herrera-Melián, J. A., Pérez-Peña, J., Colón, G. and Navío, J. A. TiO₂ activation by using activated carbon as a support: Part II. Photoreactivity and FTIR study, *Appl. Catal., B*, *44*, pp. 153-160. 2003b.

Araña, J., Herrera Melián, J. A., Doña Rodríguez, J. M., González Díaz, O., Viera, A., Pérez Peña, J., Marrero Sosa, P. M. and Espino Jiménez, V. TiO₂-photocatalysis as a tertiary treatment of naturally treated wastewater, *Catal. Today*, *76*, pp. 279-289. 2002.

Aruldoss, U., Kennedy, L. J., Judith Vijaya, J. and Sekaran, G. Photocatalytic degradation of phenolic sytan using TiO₂ impregnated activated carbon, *J. Colloid Interface Sci.*, *355*, pp. 204-209. 2011.

Augugliaro, V., Palmisano, L., Schiavello, M., Sclafani, A., Marchese, L., Martra, G. and Miano, F. Photocatalytic degradation of nitrophenols in aqueous titanium dioxide dispersion, *Applied Catalysis*, *69*, pp. 323-340. 1991.

Bahnemann, D. Photocatalytic water treatment: solar energy applications, *Sol. Energy.*, *77*, pp. 445-459. 2004.

Balasubramanian, G., Dionysiou, D. D., Suidan, M. T., Baudin, I. and Lainé, J.-M. Evaluating the activities of immobilized TiO₂ powder films for the photocatalytic degradation of organic contaminants in water, *Appl. Catal., B*, *47*, pp. 73-84. 2004.

Balasubramanian, G., Dionysiou, D. D., Suidan, M. T., Subramanian, V., Baudin, I. and Laîné, J. M. Titania powder modified sol-gel process for photocatalytic applications, *J. Mater. Sci.*, *38*, pp. 823-831. 2003.

Ballari, M. D. L. M., Brandi, R., Alfano, O. and Cassano, A. Mass transfer limitations in photocatalytic reactors employing titanium dioxide suspensions: II. External and internal particle constrains for the reaction, *Chem. Eng. J.*, *136*, pp. 242-255. 2008.

Bandala, E. R., Peláez, M. A., García-López, A. J., Salgado, M. D. J. and Moeller, G. Photocatalytic decolourisation of synthetic and real textile wastewater containing benzidine-based azo dyes, *Chemical Engineering and Processing: Process Intensification*, *47*, pp. 169-176. 2008.

Bansal, R. C. and Goyal, M. Activated carbon adsorption. pp. 497 425 cm., Boca Raton: Dekker/CRC Press. 2005

Bard, A. J. Photoelectrochemistry and heterogeneous photo-catalysis at semiconductors, *Journal of Photochemistry*, *10*, pp. 59-75. 1979.

Bard, A. J. Photoelectrochemistry, *Science*, *207*, pp. 139-144. 1980.

Benestad, C., Hagen, I., Jebens, A., Oehme, M. and Ramdahl, T. Emissions of organic micropollutants from discontinuously operated municipal waste incinerators, *Waste Management & Research*, *8*, pp. 193-201. 1990.

Berry, R. J. and Mueller, M. R. Photocatalytic decomposition of crude oil slicks using TiO₂ on a floating substrate, *Microchem. J.*, *50*, pp. 28-32. 1994.

Bhatkhande, D. S., Pangarkar, V. G. and Beenackers, A. a. C. M. Photocatalytic degradation for environmental applications – a review, *Journal of Chemical Technology & Biotechnology*, *77*, pp. 102-116. 2002.

Bideau, M., Claudel, B., Dubien, C., Faure, L. and Kazouan, H. On the "immobilization" of titanium dioxide in the photocatalytic oxidation of spent waters, *J. Photochem. Photobiol. A*, *91*, pp. 137-144. 1995.

Boehm, H. P. Surface oxides on carbon and their analysis: a critical assessment, *Carbon*, *40*, pp. 145-149. 2002.

Borges, M. E., Hernández, T. and Esparza, P. Photocatalysis as a potential tertiary treatment of urban wastewater: new photocatalytic materials, *Clean Techn Environ Policy*, pp. 1-6. 2013.

Braslavsky, S. E., Braun, A. M., Cassano, A. E., Emeline, A. V., Litter, M. I., Palmisano, L., Parmon, V. N., Serpone, N., Alfano, O. M., Anpo, M., Augugliaro, V., Bohne, C., Esplugas, S., Oliveros, E., Von Sonntag, C., Weiss, R. G. and Schiavello, M. Glossary of terms used in photocatalysis and radiation catalysis (IUPAC Recommendations 2011), *Pure Appl. Chem.*, *83*, pp. 931-1014. 2011.

Brezova, V., Blazkova, A., Breznan, M., Kottas, P. and Ceppan, M. Phenol degradation on glass-fibers with immobilized titanium-dioxide particles, *Collect. Czech. Chem. Commun.*, *60*, pp. 788-794. 1995.

Busca, G., Berardinelli, S., Resini, C. and Arrighi, L. Technologies for the removal of phenol from fluid streams: A short review of recent developments, *J. Hazard. Mater.*, *160*, pp. 265-288. 2008.

Byrappa, K., Rai, K. M. L. and Yoshimura, M. Hydrothermal preparation of TiO₂ and photocatalytic degradation of hexachlorocyclohexane and dichlorodiphenyltrichloromethane, *Environ. Technol.*, *21*, pp. 1085 - 1090. 2000.

Calza, P. and Pelizzetti, E. Photocatalytic transformation of organic compounds in the presence of inorganic ions, *Pure Appl. Chem.*, *73*, pp. 1839-1848. 2001.

Carp, O., Huisman, C. L. and Reller, A. Photoinduced reactivity of titanium dioxide, *Prog. Solid State Chem.*, *32*, pp. 33-177. 2004.

Carpio, E., Zúñiga, P., Ponce, S., Solis, J., Rodriguez, J. and Estrada, W. Photocatalytic degradation of phenol using TiO₂ nanocrystals supported on activated carbon, *J. Mol. Catal. A: Chem.*, *228*, pp. 293-298. 2005.

Chen, D., Chen, Q., Ge, L., Yin, L., Fan, B., Wang, H., Lu, H., Xu, H., Zhang, R. and Shao, G. Synthesis and Ag-loading-density-dependent photocatalytic activity of Ag@TiO₂ hybrid nanocrystals, *Appl. Surf. Sci.*, *284*, pp. 921-929. 2013.

Chen, D., Li, F. and Ray, A. K. Effect of mass transfer and catalyst layer thickness on photocatalytic reaction, *AIChE J.*, *46*, pp. 1034-1045. 2000a.

Chen, D., Li, F. and Ray, A. K. External and internal mass transfer effect on photocatalytic degradation, *Catal. Today*, *66*, pp. 475-485. 2001.

Chen, D. and Ray, A. K. Photocatalytic kinetics of phenol and its derivatives over UV irradiated TiO₂, *Appl. Catal., B*, *23*, pp. 143-157. 1999.

Chen, D., Sivakumar, M. and Ray, A. K. Heterogeneous Photocatalysis in Environmental Remediation, *Developments in Chemical Engineering and Mineral Processing*, *8*, pp. 505-550. 2000b.

Chen, F., Fang, P., Gao, Y., Liu, Z., Liu, Y. and Dai, Y. Effective removal of high-chroma crystal violet over TiO₂-based nanosheet by adsorption-photocatalytic degradation, *Chem. Eng. J.*, *204-206*, pp. 107-113. 2012.

Chen, H. Y., Zahraa, O. and Bouchy, M. Inhibition of the adsorption and photocatalytic degradation of an organic contaminant in an aqueous suspension of TiO₂ by inorganic ions, *J. Photochem. Photobiol. A*, *108*, pp. 37-44. 1997.

Chen, L. C. and Chou, T. C. Kinetics of photodecolorization of methyl orange using titanium dioxide as catalyst, *Ind. Eng. Chem. Res.*, *32*, pp. 1520-1527. 1993.

Chen, X. and Mao, S. S. Titanium dioxide nanomaterials: Synthesis, properties, modifications, and applications, *Chem. Rev.*, *107*, pp. 2891-2959. 2007.

Chen, Y. and Dionysiou, D. D. TiO₂ photocatalytic films on stainless steel: The role of Degussa P-25 in modified sol-gel methods, *Appl. Catal., B*, *62*, pp. 255-264. 2006.

Chen, Y., Yang, S., Wang, K. and Lou, L. Role of primary active species and TiO₂ surface characteristic in UV-illuminated photodegradation of Acid Orange 7, *J. Photochem. Photobiol. A*, *172*, pp. 47-54. 2005.

Cheremisinoff, P. N. and Ellerbusch, F. Carbon adsorption handbook. pp.: Ann Arbor Science Publishers. 1978

Cho, S. and Choi, W. Solid-phase photocatalytic degradation of PVC-TiO₂ polymer composites, *J. Photochem. Photobiol. A*, *143*, pp. 221-228. 2001.

Choi, W. Pure and modified TiO₂ photocatalysts and their environmental applications, *Catalysis Surveys from Asia*, *10*, pp. 16-28. 2006.

Chong, M. N., Jin, B., Chow, C. W. K. and Saint, C. Recent developments in photocatalytic water treatment technology: A review, *Water. Res.*, *44*, pp. 2997-3027. 2010.

Collins-Martinez, V., Ortiz, A. L. and Elguezabal, A. A. Influence of the anatase/rutile ratio on the TiO₂ photocatalytic activity for the photodegradation of light hydrocarbons, *International Journal of Chemical Reactor Engineering*, *5*. 2007.

Cordero, T., Chovelon, J.-M., Duchamp, C., Ferronato, C. and Matos, J. Surface nano-aggregation and photocatalytic activity of TiO₂ on H-type activated carbons, *Appl. Catal., B*, *73*, pp. 227-235. 2007a.

Cordero, T., Duchamp, C., Chovelon, J.-M., Ferronato, C. and Matos, J. Influence of L-type activated carbons on photocatalytic activity of TiO₂ in 4-chlorophenol photodegradation, *J. Photochem. Photobiol. A*, *191*, pp. 122-131. 2007b.

Crittenden, J. C., Suri, R. P. S., Perram, D. L. and Hand, D. W. Decontamination of water using adsorption and photocatalysis, *Water. Res.*, *31*, pp. 411-418. 1997.

D'oliveira, J. C., Al-Sayyed, G. and Pichat, P. Photodegradation of 2- and 3-chlorophenol in titanium dioxide aqueous suspensions, *Environ. Sci. Technol.*, *24*, pp. 990-996. 1990.

Da Silva, C. G. and Faria, J. L. S. Photochemical and photocatalytic degradation of an azo dye in aqueous solution by UV irradiation, *J. Photochem. Photobiol. A*, *155*, pp. 133-143. 2003.

Damodar, R. A. and Swaminathan, T. Performance evaluation of a continuous flow immobilized rotating tube photocatalytic reactor (IRTPR) immobilized with TiO₂ catalyst for azo dye degradation, *Chem. Eng. J.*, *144*, pp. 59-66. 2008.

Decher, G. Fuzzy nanoassemblies: Toward layered polymeric multicomposites, *Science*, *277*, pp. 1232-1237. 1997.

Decher, G., Hong, J. D. and Schmitt, J. Buildup of ultrathin multilayer films by a self-assembly process: III. Consecutively alternating adsorption of anionic and cationic

polyelectrolytes on charged surfaces, *Thin Solid Films*, 210–211, Part 2, pp. 831-835. 1992.

Dhananjeyan, M. R., Kiwi, J. and Thampi, K. R. Photocatalytic performance of TiO and FeO immobilized on derivatized polymer films for mineralisation of pollutants, *Chem. Commun.*, pp. 1443-1444. 2000.

Ding, Z., Hu, X., Lu, G. Q., Yue, P.-L. and Greenfield, P. F. Novel silica gel supported TiO₂ photocatalyst synthesized by cvd method, *Langmuir*, 16, pp. 6216-6222. 2000.

Ding, Z., Hu, X., Yue, P. L., Lu, G. Q. and Greenfield, P. F. Synthesis of anatase TiO₂ supported on porous solids by chemical vapor deposition, *Catal. Today*, 68, pp. 173-182. 2001.

Diya'uddeen, B. H., Daud, W. M. a. W. and Abdul Aziz, A. R. Treatment technologies for petroleum refinery effluents: A review, *Process Saf. Environ. Prot.*, 89, pp. 95-105. 2011.

Dontsova, D., Keller, V., Keller, N., Steffanut, P., Félix, O. and Decher, G. Photocatalytically active polyelectrolyte/nanoparticle films for the elimination of a model odorous gas, *Macromol. Rapid Commun.*, 32, pp. 1145-1149. 2011.

Dor, S., Rühle, S., Ofir, A., Adler, M., Grinis, L. and Zaban, A. The influence of suspension composition and deposition mode on the electrophoretic deposition of TiO₂ nanoparticle agglomerates, *Colloids Surf., A*, 342, pp. 70-75. 2009.

El-Sheikh, A. H., Al-Degs, Y. S., Newman, A. P. and Lynch, D. E. Oxidized activated carbon as support for titanium dioxide in UV-assisted degradation of 3-chlorophenol, *Sep. Purif. Technol.*, 54, pp. 117-123. 2007.

Epling, G. A. and Lin, C. Investigation of retardation effects on the titanium dioxide photodegradation system, *Chemosphere*, 46, pp. 937-944. 2002.

Esplugas, S., Gimenez, J., Contreras, S., Pascual, E. and Rodriguez, M. Comparison of different advanced oxidation processes for phenol degradation, *Water. Res.*, 36, pp. 1034-1042. 2002.

Fabiyi, M. E. and Skelton, R. L. Photocatalytic mineralisation of methylene blue using buoyant TiO₂-coated polystyrene beads, *J. Photochem. Photobiol. A*, 132, pp. 121-128. 2000.

Faramarzpour, M., Vossoughi, M. and Borghei, M. Photocatalytic degradation of furfural by titania nanoparticles in a floating-bed photoreactor, *Chem. Eng. J.*, *146*, pp. 79-85. 2009.

Fateh, R., Dilert, R. and Bahnemann, D. Transparent hydrophilic photocatalytic thin films on polycarbonate substrates prepared by a sol-gel process. In *Proceedings of the 1st Wseas International Conference on Materials Science*, ed by Yfantis, D. K., Iliescu, M., Simian, D., Mastorakis, N. & Vladareanu, L., pp. 95-100. 2008

Fernández, A., Lassaletta, G., Jiménez, V. M., Justo, A., González-Elipe, A. R., Herrmann, J. M., Tahiri, H. and Ait-Ichou, Y. Preparation and characterization of TiO₂ photocatalysts supported on various rigid supports (glass, quartz and stainless steel). Comparative studies of photocatalytic activity in water purification, *Appl. Catal., B*, *7*, pp. 49-63. 1995.

Folli, A., Campbell, S. B., Anderson, J. A. and Macphee, D. E. Role of TiO₂ surface hydration on NO oxidation photo-activity, *Journal of Photochemistry and Photobiology A: Chemistry*, *In Press, Accepted Manuscript*.

Foo, K. Y. and Hameed, B. H. Decontamination of textile wastewater via TiO₂/activated carbon composite materials, *Adv. Colloid Interface Sci.*, *159*, pp. 130-143. 2010.

Fostier, A. H., Pereira, M. D. S. S., Rath, S. and Guimarães, J. R. Arsenic removal from water employing heterogeneous photocatalysis with TiO₂ immobilized in PET bottles, *Chemosphere*, *72*, pp. 319-324. 2008.

Fox, M. A. and Dulay, M. T. Heterogeneous photocatalysis, *Chem. Rev.*, *93*, pp. 341-357. 1993.

Fu, P., Luan, Y. and Dai, X. Preparation of activated carbon fibers supported TiO₂ photocatalyst and evaluation of its photocatalytic reactivity, *J. Mol. Catal. A: Chem.*, *221*, pp. 81-88. 2004.

Fujishima, A. and Honda, K. Electrochemical photolysis of water at a semiconductor electrode, *Nature*, *238*, pp. 37-38. 1972.

Gao, X. and Wachs, I. E. Titania-silica as catalysts: molecular structural characteristics and physico-chemical properties, *Catal. Today*, *51*, pp. 233-254. 1999.

Gao, Y. M., Shen, H. S., Dwight, K. and Wold, A. Preparation and photocatalytic properties of titanium(IV) oxide films, *Mater. Res. Bull.*, *27*, pp. 1023-1030. 1992.

Garcia, J. C., Simionato, J. I., Silva, A. E. C. D., Nozaki, J. and Souza, N. E. D. Solar photocatalytic degradation of real textile effluents by associated titanium dioxide and hydrogen peroxide, *Sol. Energy.*, *83*, pp. 316-322. 2009.

Gaya, U. I. and Abdullah, A. H. Heterogeneous photocatalytic degradation of organic contaminants over titanium dioxide: A review of fundamentals, progress and problems, *J. Photochem. Photobiol. C: Photochem. Rev.*, *9*, pp. 1-12. 2008.

Gibbs, T. S. Optimization of titanium dioxide photocatalysis for sanitary wastewater treatment. M.S. Thesis 1403438, The University of Alabama in Huntsville, 2001

Gimeno, O., Carbajo, M., Beltrán, F. J. and Rivas, F. J. Phenol and substituted phenols AOPs remediation, *J. Hazard. Mater.*, *119*, pp. 99-108. 2005.

Giri, R. R., Ozaki, H., Ota, S., Taniguchi, S. and Takanami, R. Influence of inorganic solids on photocatalytic oxidation of 2,4-dichlorophenoxyacetic acid with UV and TiO₂ fiber in aqueous solution, *Desalination*, *255*, pp. 9-14. 2010.

Goslich, R., Dillert, R. and Bahnemann, D. Solar water treatment: Principles and reactors, *Water Sci. Technol.*, *35*, pp. 137-148. 1997.

Haarstrick, A., Kut, O. M. and Heinzle, E. TiO₂-assisted degradation of environmentally relevant organic compounds in wastewater using a novel fluidized bed photoreactor, *Environ. Sci. Technol.*, *30*, pp. 817-824. 1996.

Han, H. and Bai, R. Buoyant photocatalyst with greatly enhanced visible-light activity prepared through a low temperature hydrothermal method, *Ind. Eng. Chem. Res.*, *48*, pp. 2891-2898. 2009.

Han, H. and Bai, R. Highly effective buoyant photocatalyst prepared with a novel layered-TiO₂ configuration on polypropylene fabric and the degradation performance for methyl orange dye under UV-Vis and Vis lights, *Sep. Purif. Technol.*, *73*, pp. 142-150. 2010.

Han, H. and Bai, R. Effect of thickness of photocatalyst film immobilized on a buoyant substrate on the degradation of methyl orange dye in aqueous solutions under different light irradiations, *Ind. Eng. Chem. Res.*, *50*, pp. 11922-11929. 2011.

Heller, A. Conversion of sunlight into electrical power and photoassisted electrolysis of water in photoelectrochemical cells, *Acc. Chem. Res.*, *14*, pp. 154-162. 1981.

Herrmann, J.-M. Heterogeneous photocatalysis: fundamentals and applications to the removal of various types of aqueous pollutants, *Catal. Today*, *53*, pp. 115-129. 1999.

Herrmann, J.-M., Matos, J., Disdier, J., Guillard, C., Laine, J., Malato, S. and Blanco, J. Solar photocatalytic degradation of 4-chlorophenol using the synergistic effect between titania and activated carbon in aqueous suspension, *Catal. Today*, *54*, pp. 255-265. 1999.

Ho, Y. S. and McKay, G. Sorption of dye from aqueous solution by peat, *Chem. Eng. J.*, *70*, pp. 115-124. 1998.

Hoffmann, M. R., Martin, S. T., Choi, W. and Bahnemann, D. W. Environmental applications of semiconductor photocatalysis, *Chem. Rev.*, *95*, pp. 69-96. 1995.

Hosseini, S. N., Borghei, S. M., Vossoughi, M. and Taghavinia, N. Immobilization of TiO₂ on perlite granules for photocatalytic degradation of phenol, *Appl. Catal., B*, *74*, pp. 53-62. 2007.

Hsiao, C. Y., Lee, C. L. and Ollis, D. F. Heterogeneous photocatalysis - degradation of dilute-solutions of dichloromethane (CH₂Cl₂), chloroform (CHCl₃), and carbon-tetrachloride (CCl₄) with illuminated TiO₂ photocatalyst, *J. Catal.*, *82*, pp. 418-423. 1983.

Iketani, K., Sun, R.-D., Toki, M., Hirota, K. and Yamaguchi, O. Sol-gel-derived TiO₂/poly(dimethylsiloxane) hybrid films and their photocatalytic activities, *J. Phys. Chem. Solids*, *64*, pp. 507-513. 2003.

Ilisz, I. and Dombi, A. Investigation of the photodecomposition of phenol in near-UV-irradiated aqueous TiO₂ suspensions. II. Effect of charge-trapping species on product distribution, *Appl. Catal., A*, *180*, pp. 35-45. 1999.

Jackson, N. B., Wang, C. M., Luo, Z., Schwitzgebel, J., Ekerdt, J. G., Brock, J. R. and Heller, A. Attachment of TiO₂ powders to hollow glass microbeads: Activity of the TiO₂ - coated beads in the photoassisted oxidation of ethanol to acetaldehyde, *J. Electrochem. Soc.*, *138*, pp. 3660-3664. 1991.

Jaeger, C. D. and Bard, A. J. Spin trapping and electron spin resonance detection of radical intermediates in the photodecomposition of water at titanium dioxide particulate systems, *J. Chem. Phys.*, *83*, pp. 3146-3152. 1979.

Jamil, T. S., Ghaly, M. Y., Fathy, N. A., Abd El-Halim, T. A. and Österlund, L. Enhancement of TiO₂ behavior on photocatalytic oxidation of MO dye using TiO₂/AC

under visible irradiation and sunlight radiation, *Sep. Purif. Technol.*, *98*, pp. 270-279. 2012.

Janus, M. and Morawski, A. W. New method of improving photocatalytic activity of commercial Degussa P25 for azo dyes decomposition, *Appl. Catal., B*, *75*, pp. 118-123. 2007.

Kamegawa, T., Suzuki, N. and Yamashita, H. Design of macroporous TiO₂ thin film photocatalysts with enhanced photofunctional properties, *Energy & Environmental Science*, *4*, pp. 1411-1416. 2011.

Kasanen, J., Salstela, J., Suvanto, M. and Pakkanen, T. T. Photocatalytic degradation of methylene blue in water solution by multilayer TiO₂ coating on HDPE, *Appl. Surf. Sci.*, *258*, pp. 1738-1743. 2011a.

Kasanen, J., Suvanto, M. and Pakkanen, T. T. Improved adhesion of TiO₂-based multilayer coating on HDPE and characterization of photocatalysis, *J. Appl. Polym. Sci.*, *119*, pp. 2235-2245. 2011b.

Keane, D., Basha, S., Nolan, K., Morrissey, A., Oelgemöller, M. and Tobin, J. Photodegradation of famotidine by integrated photocatalytic adsorbent (IPCA) and kinetic study, *Catal. Lett.*, *141*, pp. 300-308. 2011.

Khataee, A. R., Zarei, M. and Ordikhani-Seyedlar, R. Heterogeneous photocatalysis of a dye solution using supported TiO₂ nanoparticles combined with homogeneous photoelectrochemical process: Molecular degradation products, *J. Mol. Catal. A: Chem.*, *338*, pp. 84-91. 2011.

Kim, H. J., Shul, Y. G. and Han, H. S. Photocatalytic properties of silica-supported TiO₂, *Top. Catal.*, *35*, pp. 287-293. 2005.

Kim, S.-H., Ngo, H. H., Shon, H. K. and Vigneswaran, S. Adsorption and photocatalysis kinetics of herbicide onto titanium oxide and powdered activated carbon, *Sep. Purif. Technol.*, *58*, pp. 335-342. 2008.

Koopman, M. Titania coated hollow glass microspheres for environmental applications. Ph.D. Thesis 3301385, The University of Alabama at Birmingham, 2007

Krogman, K. C., Zacharia, N. S., Grillo, D. M. and Hammond, P. T. Photocatalytic layer-by-layer coatings for degradation of acutely toxic agents, *Chem. Mater.*, *20*, pp. 1924-1930. 2008.

Krýsa, J., Keppert, M., Waldner, G. and Jirkovský, J. Immobilized particulate TiO₂ photocatalysts for degradation of organic pollutants: Effect of layer thickness, *Electrochim. Acta*, *50*, pp. 5255-5260. 2005.

Kusiak-Nejman, E., Janus, M., Grzmil, B. and Morawski, A. W. Methylene Blue decomposition under visible light irradiation in the presence of carbon-modified TiO₂ photocatalysts, *J. Photochem. Photobiol. A*, *226*, pp. 68-72. 2011.

Lam, S.-M., Sin, J.-C. and Mohamed, A. Parameter effect on photocatalytic degradation of phenol using TiO₂-P25/activated carbon (AC), *Korean J. Chem. Eng.*, *27*, pp. 1109-1116. 2010.

Leary, R. and Westwood, A. Carbonaceous nanomaterials for the enhancement of TiO₂ photocatalysis, *Carbon*, *49*, pp. 741-772. 2011.

Lee, D.-K., Kim, S.-C., Cho, I.-C., Kim, S.-J. and Kim, S.-W. Photocatalytic oxidation of microcystin-LR in a fluidized bed reactor having TiO₂-coated activated carbon, *Sep. Purif. Technol.*, *34*, pp. 59-66. 2004.

Lee, M. K., Uhm, Y. R., Rhee, C. K. and Lee, Y. B. Organic suspension behavior of rutile TiO₂ nanoparticles with high specific surface area, *Mater. Trans.*, *51*, pp. 2157-2161. 2010.

Lei, L., Chu, H. P., Hu, X. and Yue, P.-L. Preparation of heterogeneous photocatalyst (TiO₂/alumina) by metallo-organic chemical vapor deposition, *Ind. Eng. Chem. Res.*, *38*, pp. 3381-3385. 1999.

Leon Y Leon, C. A., Solar, J. M., Calemma, V. and Radovic, L. R. Evidence for the protonation of basal plane sites on carbon, *Carbon*, *30*, pp. 797-811. 1992.

Li, G., Bai, R. and Zhao, X. S. Coating of TiO₂ thin films on the surface of SiO₂ microspheres: Toward industrial photocatalysis, *Ind. Eng. Chem. Res.*, *47*, pp. 8228-8232. 2008.

Li Puma, G., Bono, A., Krishnaiah, D. and Collin, J. G. Preparation of titanium dioxide photocatalyst loaded onto activated carbon support using chemical vapor deposition: A review paper, *J. Hazard. Mater.*, *157*, pp. 209-219. 2008.

Li, W. and Liu, S. Bifunctional activated carbon with dual photocatalysis and adsorption capabilities for efficient phenol removal, *Adsorption*, *18*, pp. 67-74. 2012.

Li, Y., Li, X., Li, J. and Yin, J. Photocatalytic degradation of methyl orange by TiO₂-coated activated carbon and kinetic study, *Water. Res.*, *40*, pp. 1119-1126. 2006.

Lim, T.-T., Yap, P.-S., Srinivasan, M. and Fane, A. G. TiO₂/AC composites for synergistic adsorption-photocatalysis processes: Present challenges and further developments for water treatment and reclamation, *Crit. Rev. Env. Sci. Technol.*, *41*, pp. 1173 - 1230. 2011.

Lin, H. F., Ravikrishna, R. and Valsaraj, K. T. Reusable adsorbents for dilute solution separation. 6. Batch and continuous reactors for the adsorption and degradation of 1,2-dichlorobenzene from dilute wastewater streams using titania as a photocatalyst, *Sep. Purif. Technol.*, *28*, pp. 87-102. 2002.

Ling, C. M., Mohamed, A. R. and Bhatia, S. Performance of photocatalytic reactors using immobilized TiO₂ film for the degradation of phenol and methylene blue dye present in water stream, *Chemosphere*, *57*, pp. 547-554. 2004.

Linsebigler, A. L., Lu, G. and Yates, J. T. Photocatalysis on tio₂ surfaces: Principles, mechanisms, and selected results, *Chem. Rev.*, *95*, pp. 735-758. 1995.

Liotta, L. F., Gruttadauria, M., Di Carlo, G., Perrini, G. and Librando, V. Heterogeneous catalytic degradation of phenolic substrates: Catalysts activity, *J. Hazard. Mater.*, *162*, pp. 588-606. 2009.

Litter, M. I. Heterogeneous photocatalysis: Transition metal ions in photocatalytic systems, *Appl. Catal.*, *B*, *23*, pp. 89-114. 1999.

Liu, J., Crittenden, J. C., Hand, D. W. and Perram, D. L. Regeneration of adsorbents using heterogeneous photocatalytic oxidation, *Journal of Environmental Engineering*, *122*, pp. 707-713. 1996.

Liu, S., Lim, M. and Amal, R. Photocatalysis of natural organic matter in water: Characterization and treatment integration. In *Photocatalysis and Water Purification*, ed by pp. 271-294: Wiley-VCH Verlag GmbH & Co. KGaA. 2013

Liu, S. X., Chen, X. Y. and Chen, X. A TiO₂/AC composite photocatalyst with high activity and easy separation prepared by a hydrothermal method, *J. Hazard. Mater.*, *143*, pp. 257-263. 2007.

Liu, S. X., Sun, C. L. and Zhang, S. R. Photocatalytic regeneration of coal-based activated carbon, *Chinese Journal of Catalysis*, *24*, pp. 355-358. 2003.

Ljubas, D. Solar photocatalysis--a possible step in drinking water treatment, *Energy*, *30*, pp. 1699-1710. 2005.

López-Muñoz, M.-J., Grieken, R. V., Aguado, J. and Marugán, J. Role of the support on the activity of silica-supported TiO₂ photocatalysts: Structure of the TiO₂/SBA-15 photocatalysts, *Catal. Today*, *101*, pp. 307-314. 2005.

Luck, F. Wet air oxidation: past, present and future, *Catal. Today*, *53*, pp. 81-91. 1999.

Magalhães, F. and Lago, R. M. Floating photocatalysts based on TiO₂ grafted on expanded polystyrene beads for the solar degradation of dyes, *Sol. Energy.*, *83*, pp. 1521-1526. 2009.

Magalhães, F., Moura, F. C. C. and Lago, R. M. TiO₂/LDPE composites: A new floating photocatalyst for solar degradation of organic contaminants, *Desalination*, *276*, pp. 266-271. 2011.

Malik, S. A. Treatment of the oil refinery wastewater using photocatalysis. M.S. Thesis 1429523, King Fahd University of Petroleum and Minerals (Saudi Arabia), 2005

Marin, M. L., Lhiaubet-Vallet, V., Santos-Juanes, L., Soler, J., Gomis, J., Arques, A., Amat, A. M. and Miranda, M. A. A photophysical approach to investigate the photooxidation mechanism of pesticides: Hydroxyl radical versus electron transfer, *Appl. Catal., B*, *103*, pp. 48-53. 2011.

Marsh, H. Activated carbon. pp. xvii, 536 , ports, charts 525 cm., Oxford: Elsevier Ltd. 2006

Martinez-Huitle, C. A. and Ferro, S. Electrochemical oxidation of organic pollutants for the wastewater treatment: direct and indirect processes, *Chem. Soc. Rev.*, *35*, pp. 1324-1340. 2006.

Matos, J., García, A. and Poon, P. Environmental green chemistry applications of nanoporous carbons, *J. Mater. Sci.*, *45*, pp. 4934-4944. 2010.

Matos, J., Laine, J. and Herrman, J. Association of activated carbons of different origins with titania with the photocatalytic purification of water, *Carbon*, *37*, pp. 1870-1872. 1999.

Matos, J., Laine, J. and Herrmann, J.-M. Synergy effect in the photocatalytic degradation of phenol on a suspended mixture of titania and activated carbon, *Appl. Catal., B*, *18*, pp. 281-291. 1998.

Matos, J., Laine, J. and Herrmann, J. M. Effect of the type of activated carbons on the photocatalytic degradation of aqueous organic pollutants by UV-irradiated titania, *J. Catal.*, *200*, pp. 10-20. 2001.

Matos, J., Laine, J., Herrmann, J. M., Uzcategui, D. and Brito, J. L. Influence of activated carbon upon titania on aqueous photocatalytic consecutive runs of phenol photodegradation, *Appl. Catal., B*, *70*, pp. 461-469. 2007.

Matsuzawa, S., Maneerat, C., Hayata, Y., Hirakawa, T., Negishi, N. and Sano, T. Immobilization of TiO₂ nanoparticles on polymeric substrates by using electrostatic interaction in the aqueous phase, *Appl. Catal., B*, *83*, pp. 39-45. 2008.

Matthews, R. W. Hydroxylation reactions induced by near-ultraviolet photolysis of aqueous titanium dioxide suspensions, *Journal of the Chemical Society, Faraday Transactions 1: Physical Chemistry in Condensed Phases*, *80*, pp. 457-471. 1984.

Matthews, R. W. Response to the comment. "Photocatalytic reactor design: an example of mass-transfer limitations with an immobilized catalyst", *J. Chem. Phys.*, *92*, pp. 6853-6854. 1988.

Mcnaught, A. D. *Compendium of chemical terminology : IUPAC recommendations*. pp. vii, 450, Oxford: Blackwell Science. 1997

Meichtry, J. M., Lin, H. J., De La Fuente, L., Levy, I. K., Gautier, E. A., Blesa, M. A. and Litter, M. I. Low-cost TiO₂ photocatalytic technology for water potabilization in plastic bottles for isolated regions. Photocatalyst fixation, *Journal of Solar Energy Engineering*, *129*, pp. 119-126. 2007.

Mijangos, F., Varona, F. and Villota, N. Changes in solution color during phenol oxidation by fenton reagent, *Environ. Sci. Technol.*, *40*, pp. 5538-5543. 2006.

Mills, A. and Le Hunte, S. An overview of semiconductor photocatalysis, *J. Photochem. Photobiol. A*, *108*, pp. 1-35. 1997.

Mills, A. and Morris, S. Photomineralization of 4-chlorophenol sensitized by titanium dioxide: a study of the initial kinetics of carbon dioxide photogeneration, *J. Photochem. Photobiol. A*, *71*, pp. 75-83. 1993.

Minero, C., Catozzo, F. and Pelizzetti, E. Role of adsorption in photocatalyzed reactions of organic molecules in aqueous titania suspensions, *Langmuir*, *8*, pp. 481-486. 1992.

Minero, C., Mariella, G., Maurino, V., Vione, D. and Pelizzetti, E. Photocatalytic Transformation of Organic Compounds in the Presence of Inorganic Ions. 2. Competitive Reactions of Phenol and Alcohols on a Titanium Dioxide–Fluoride System†, *Langmuir*, *16*, pp. 8964-8972. 2000.

Modestov, A., Glezer, V., Marjasin, I. and Lev, O. Photocatalytic degradation of chlorinated phenoxyacetic acids by a new buoyant titania-exfoliated graphite composite photocatalyst, *The Journal of Physical Chemistry B*, *101*, pp. 4623-4629. 1997.

Mukherjee, P. S. and Ray, A. K. Major challenges in the design of a large-scale photocatalytic reactor for water treatment, *Chemical Engineering & Technology*, *22*, pp. 253-260. 1999.

Nair, M., Luo, Z. and Heller, A. Rates of photocatalytic oxidation of crude oil on salt water on buoyant, cenosphere-attached titanium dioxide, *Ind. Eng. Chem. Res.*, *32*, pp. 2318-2323. 1993.

Nakata, K. and Fujishima, A. TiO₂ photocatalysis: Design and applications, *J. Photochem. Photobiol. C: Photochem. Rev.*, *13*, pp. 169-189. 2012.

Nakhla, G., Abuzaid, N. and Farooq, S. Activated carbon adsorption of phenolics in oxic systems: Effect of pH and temperature variations, *Water Environ. Res*, *66*, pp. 842-850. 1994.

Naskar, S., Arumugom Pillay, S. and Chanda, M. Photocatalytic degradation of organic dyes in aqueous solution with TiO₂ nanoparticles immobilized on foamed polyethylene sheet, *J. Photochem. Photobiol. A*, *113*, pp. 257-264. 1998.

Nawi, M. A. and Zain, S. M. Enhancing the surface properties of the immobilized Degussa P-25 TiO₂ for the efficient photocatalytic removal of methylene blue from aqueous solution, *Appl. Surf. Sci.*, *258*, pp. 6148-6157. 2012.

Neti, N. and Joshi, P. Cellulose reinforced-TiO₂ photocatalyst coating on acrylic plastic for degradation of reactive dyes, *J. Coat. Technol. Res.*, *7*, pp. 643-650. 2010.

Ochiai, T. and Fujishima, A. Photoelectrochemical properties of TiO₂ photocatalyst and its applications for environmental purification, *J. Photochem. Photobiol. C: Photochem. Rev.*, *13*, pp. 247-262. 2012.

Palominos, R., Freer, J., Mondaca, M. A. and Mansilla, H. D. Evidence for hole participation during the photocatalytic oxidation of the antibiotic flumequine, *J. Photochem. Photobiol. A*, *193*, pp. 139-145. 2008.

Pantopoulos, K. and Schipper, H. M. Principles of free radical biomedicine: Glutathione. pp.: Nova Science Publishers, Incorporated. 2011

Parent, Y., Blake, D., Magrini-Bair, K., Lyons, C., Turchi, C., Watt, A., Wolfrum, E. and Prairie, M. Solar photocatalytic processes for the purification of water: State of development and barriers to commercialization, *Sol. Energy.*, *56*, pp. 429-437. 1996.

Pastrana-Martínez, L. M., Morales-Torres, S., Papageorgiou, S. K., Katsaros, F. K., Romanos, G. E., Figueiredo, J. L., Faria, J. L., Falaras, P. and Silva, A. M. T. Photocatalytic behaviour of nanocarbon–TiO₂ composites and immobilization into hollow fibres, *Appl. Catal., B*, *142–143*, pp. 101-111. 2013.

Pelton, R., Geng, X. and Brook, M. Photocatalytic paper from colloidal TiO₂--fact or fantasy, *Adv. Colloid Interface Sci.*, *127*, pp. 43-53. 2006.

Pirkanniemi, K. and Sillanpää, M. Heterogeneous water phase catalysis as an environmental application: a review, *Chemosphere*, *48*, pp. 1047-1060. 2002.

Portjanskaja, E., Krichevskaya, M., Preis, S. and Kallas, J. Photocatalytic oxidation of humic substances with TiO₂-coated glass micro-spheres, *Environ. Chem. Lett.*, *2*, pp. 123-127. 2004.

Pozzo, R. L., Baltanás, M. A. and Cassano, A. E. Supported titanium oxide as photocatalyst in water decontamination: State of the art, *Catal. Today*, *39*, pp. 219-231. 1997.

Pozzo, R. L., Giombi, J. L., Baltanás, M. A. and Cassano, A. E. The performance in a fluidized bed reactor of photocatalysts immobilized onto inert supports, *Catal. Today*, *62*, pp. 175-187. 2000.

Pruden, A. L. and Ollis, D. F. Degradation of chloroform by photoassisted heterogeneous catalysis in dilute aqueous suspensions of titanium dioxide, *Environ. Sci. Technol.*, *17*, pp. 628-631. 1983.

Qamar, M., Muneer, M. and Bahnemann, D. Heterogeneous photocatalysed degradation of two selected pesticide derivatives, triclopyr and daminozid in aqueous suspensions of titanium dioxide, *J. Environ. Manage.*, *80*, pp. 99-106. 2006.

Qiu, W. and Zheng, Y. A comprehensive assessment of supported titania photocatalysts in a fluidized bed photoreactor: Photocatalytic activity and adherence stability, *Appl. Catal., B*, *71*, pp. 151-162. 2007.

Qourzal, S., Assabbane, A. and Ait-Ichou, Y. Synthesis of TiO₂ via hydrolysis of titanium tetraisopropoxide and its photocatalytic activity on a suspended mixture with activated carbon in the degradation of 2-naphthol, *J. Photochem. Photobiol. A*, *163*, pp. 317-321. 2004.

Rajeshwar, K., Osugi, M. E., Chanmanee, W., Chenthamarakshan, C. R., Zaroni, M. V. B., Kajitvichyanukul, P. and Krishnan-Ayer, R. Heterogeneous photocatalytic treatment of organic dyes in air and aqueous media, *J. Photochem. Photobiol. C: Photochem. Rev.*, *9*, pp. 171-192. 2008.

Ray, A. K. Photocatalytic Reactor Configurations for Water Purification: Experimentation and Modeling. In *Advances in Chemical Engineering, Volume 36*, ed by Hugo, I. D. L. & Benito Serrano, R., pp. 145-184: Academic Press. 2009

Robert, D., Keller, V. and Keller, N. Immobilization of a semiconductor photocatalyst on solid supports: Methods, materials, and applications. In *Photocatalysis and Water Purification*, ed by pp. 145-178: Wiley-VCH Verlag GmbH & Co. KGaA. 2013

Robert, D., Parra, S., Pulgarin, C., Krzton, A. and Weber, J. V. Chemisorption of phenols and acids on TiO₂ surface, *Appl. Surf. Sci.*, *167*, pp. 51-58. 2000.

Rodríguez-Reinoso, F. The role of carbon materials in heterogeneous catalysis, *Carbon*, *36*, pp. 159-175. 1998.

Rosenberg, I., Brock, J. R. and Heller, A. Collection optics of titanium dioxide photocatalyst on hollow glass microbeads floating on oil slicks, *J. Chem. Phys.*, *96*, pp. 3423-3428. 1992.

S. H. Abdul Kaleel, Bijal. Kottukkal Bahuleyan, J. Masihullah and Al-Harhi, M. Thermal and mechanical properties of polyethylene/doped-TiO₂ nanocomposites synthesized using in situ polymerization, *J. Nano Mat.*, *2011*. 2011.

Şahin, Ö., Saka, C. and Kutluay, S. Cold plasma and microwave radiation applications on almond shell surface and its effects on the adsorption of Eriochrome Black T, *Journal of Industrial and Engineering Chemistry*, *19*, pp. 1617-1623. 2013.

Salvador, F. and Merchán, M. D. Study of the desorption of phenol and phenolic compounds from activated carbon by liquid-phase temperature-programmed desorption, *Carbon*, *34*, pp. 1543-1551. 1996.

Sánchez, B., Coronado, J. M., Candal, R., Portela, R., Tejedor, I., Anderson, M. A., Tompkins, D. and Lee, T. Preparation of TiO₂ coatings on PET monoliths for the photocatalytic elimination of trichloroethylene in the gas phase, *Appl. Catal., B*, *66*, pp. 295-301. 2006.

Schmelling, D. C., Gray, K. A. and Kamat, P. V. The influence of solution matrix on the photocatalytic degradation of TNT in TiO₂ slurries, *Water. Res.*, *31*, pp. 1439-1447. 1997.

Sellappan, R., Zhu, J., Fredriksson, H., Martins, R. S., Zäch, M. and Chakarov, D. Preparation and characterization of TiO₂/carbon composite thin films with enhanced photocatalytic activity, *J. Mol. Catal. A: Chem.*, *335*, pp. 136-144. 2011.

Serpone, N., Borgarello, E., Harris, R., Cahill, P., Borgarello, M. and Pelizzetti, E. Photocatalysis over TiO₂ supported on a glass substrate, *Solar Energy Materials*, *14*, pp. 121-127. 1986.

Serpone, N. and Pelizzetti, E. *Photocatalysis : fundamentals and applications.* pp. x, 650 p. : ill. ; 625 cm., New York: : Wiley. 1989

Shan, A. Y., Ghazi, T. I. M. and Rashid, S. A. Immobilisation of titanium dioxide onto supporting materials in heterogeneous photocatalysis: A review, *Appl. Catal., A*, *389*, pp. 1-8. 2010.

Shi, J.-W., Chen, S.-H., Wang, S.-M., Wu, P. and Xu, G.-H. Favorable recycling photocatalyst TiO₂/CFA: Effects of loading method on the structural property and photocatalytic activity, *J. Mol. Catal. A: Chem.*, *303*, pp. 141-147. 2009.

Shironita, S., Mori, K., Shimizu, T., Ohmichi, T., Mimura, N. and Yamashita, H. Preparation of nano-sized platinum metal catalyst using photo-assisted deposition method on mesoporous silica including single-site photocatalyst, *Appl. Surf. Sci.*, *254*, pp. 7604-7607. 2008.

Siffert, B. and Metzger, J.-M. Study of the interaction of titanium dioxide with cellulose fibers in an aqueous medium, *Colloids and Surfaces*, *53*, pp. 79-99. 1991.

Singh, H. K., Saquib, M., Haque, M. M., Muneer, M. and Bahnemann, D. W. Titanium dioxide mediated photocatalysed degradation of phenoxyacetic acid and 2,4,5-trichlorophenoxyacetic acid, in aqueous suspensions, *J. Mol. Catal. A: Chem.*, *264*, pp. 66-72. 2007.

Singh, S., Mahalingam, H. and Singh, P. K. Polymer-supported titanium dioxide photocatalysts for environmental remediation: A review, *Appl. Catal., A*, *462-463*, pp. 178-195. 2013.

Sriwong, C., Wongnawa, S. and Patarapaiboolchai, O. Photocatalytic activity of rubber sheet impregnated with TiO₂ particles and its recyclability, *Catal. Commun.*, *9*, pp. 213-218. 2008.

Subash, B., Senthilraja, A., Dhatshanamurthi, P., Swaminathan, M. and Shanthi, M. Solar active photocatalyst for effective degradation of RR 120 with dye sensitized mechanism, *Spectrochimica Acta Part A: Molecular and Biomolecular Spectroscopy*, *115*, pp. 175-182. 2013.

Subrahmanyam, M., Boule, P., Durga Kumari, V., Naveen Kumar, D., Sancelme, M. and Rachel, A. Pumice stone supported titanium dioxide for removal of pathogen in drinking water and recalcitrant in wastewater, *Sol. Energy.*, *82*, pp. 1099-1106. 2008.

Suda, Y. and Morimoto, T. Molecularly adsorbed water on the bare surface of titania (rutile), *Langmuir*, *3*, pp. 786-788. 1987.

Takahashi, K. and Yui, H. Analysis of surface oh groups on tio₂ single crystal with polarization modulation infrared external reflection spectroscopy, *The Journal of Physical Chemistry C*, *113*, pp. 20322-20327. 2009.

Takeda, N., Torimoto, T., Sampath, S., Kuwabata, S. and Yoneyama, H. Effect of inert supports for titanium dioxide loading on enhancement of photodecomposition rate of gaseous propionaldehyde, *J. Chem. Phys.*, *99*, pp. 9986-9991. 1995.

Tang, H. L., Chen, Y.-C., Regan, J. M. and Xie, Y. F. Disinfection by-product formation potentials in wastewater effluents and their reductions in a wastewater treatment plant, *J. Environ. Monit.*, *14*, pp. 1515-1522. 2012.

Tanveer, M. and Tezcanli Guyer, G. Solar assisted photo degradation of wastewater by compound parabolic collectors: Review of design and operational parameters, *Renewable and Sustainable Energy Reviews*, 24, pp. 534-543. 2013.

Tao, Y., Wu, C.-Y. and Mazyck, D. W. Removal of methanol from pulp and paper mills using combined activated carbon adsorption and photocatalytic regeneration, *Chemosphere*, 65, pp. 35-42. 2006.

Teekateerawej, S., Nishino, J. and Nosaka, Y. Design and evaluation of photocatalytic micro-channel reactors using TiO₂-coated porous ceramics, *J. Photochem. Photobiol. A*, 179, pp. 263-268. 2006.

Tennakone, K. and Kottegoda, I. R. M. Photocatalytic mineralization of paraquat dissolved in water by TiO₂ supported on polythene and polypropylene films, *J. Photochem. Photobiol. A*, 93, pp. 79-81. 1996.

Tennakone, K., Tilakaratne, C. T. K. and Kottegoda, I. R. M. Photocatalytic degradation of organic contaminants in water with TiO₂ supported on polythene films, *J. Photochem. Photobiol. A*, 87, pp. 177-179. 1995.

Terzyk, A. P. Further insights into the role of carbon surface functionalities in the mechanism of phenol adsorption, *J. Colloid Interface Sci.*, 268, pp. 301-329. 2003.

Thomas, R. T., Nair, V. and Sandhyarani, N. Journal of Environment Management TiO₂ nanoparticle assisted solid phase photocatalytic degradation of polythene film: A mechanistic investigation, *Colloids Surf., A*, 422, pp. 1-9. 2013.

Torimoto, T., Ito, S., Kuwabata, S. and Yoneyama, H. Effects of adsorbents used as supports for titanium dioxide loading on photocatalytic degradation of propylamide, *Environ. Sci. Technol.*, 30, pp. 1275-1281. 1996.

Torimoto, T., Okawa, Y., Takeda, N. and Yoneyama, H. Effect of activated carbon content in TiO₂-loaded activated carbon on photodegradation behaviors of dichloromethane, *J. Photochem. Photobiol. A*, 103, pp. 153-157. 1997.

Tromholt, T., Manceau, M., Helgesen, M., Carlé, J. E. and Krebs, F. C. Degradation of semiconducting polymers by concentrated sunlight, *Sol. Energy Mater. Sol. Cells*, 95, pp. 1308-1314. 2011.

Tryba, B., Morawski, A. W. and Inagaki, M. Application of TiO₂-mounted activated carbon to the removal of phenol from water, *Appl. Catal., B*, 41, pp. 427-433. 2003.

Tu, W., Lin, Y.-P. and Bai, R. Removal of phenol in aqueous solutions by novel buoyant Composite photocatalysts and the kinetics, *Sep. Purif. Technol.*, *115*, pp. 180-189. 2013.

Turchi, C. S. and Ollis, D. F. Comment. Photocatalytic reactor design: an example of mass-transfer limitations with an immobilized catalyst, *J. Chem. Phys.*, *92*, pp. 6852-6853. 1988.

Turchi, C. S. and Ollis, D. F. Photocatalytic degradation of organic water contaminants: Mechanisms involving hydroxyl radical attack, *J. Catal.*, *122*, pp. 178-192. 1990.

Vaccaro, R. F. Estimation of adsorbable solutes in sea water with carbon-14 labeled phenol and activated carbon, *Environ. Sci. Technol.*, *5*, pp. 134-138. 1971.

Valente, J. P. S., Padilha, P. M. and Florentino, A. O. Studies on the adsorption and kinetics of photodegradation of a model compound for heterogeneous photocatalysis onto TiO₂, *Chemosphere*, *64*, pp. 1128-1133. 2006.

Van Doorslaer, X., Heynderickx, P. M., Demeestere, K., Debevere, K., Van Langenhove, H. and Dewulf, J. TiO₂ mediated heterogeneous photocatalytic degradation of moxifloxacin: Operational variables and scavenger study, *Appl. Catal., B*, *111-112*, pp. 150-156. 2012.

Velásquez, J., Valencia, S., Rios, L., Restrepo, G. and Marín, J. Characterization and photocatalytic evaluation of polypropylene and polyethylene pellets coated with P25 TiO₂ using the controlled-temperature embedding method, *Chem. Eng. J.*, *203*, pp. 398-405. 2012.

Vimonses, V., Jin, B., Chow, C. W. K. and Saint, C. An adsorption-photocatalysis hybrid process using multi-functional-nanoporous materials for wastewater reclamation, *Water. Res.*, *44*, pp. 5385-5397. 2010.

Wang, C. M., Heller, A. and Gerischer, H. Palladium catalysis of O₂ reduction by electrons accumulated on TiO₂ particles during photoassisted oxidation of organic compounds, *J. Am. Chem. Soc.*, *114*, pp. 5230-5234. 1992.

Wang, X., Hu, Z., Chen, Y., Zhao, G., Liu, Y. and Wen, Z. A novel approach towards high-performance composite photocatalyst of TiO₂ deposited on activated carbon, *Appl. Surf. Sci.*, *255*, pp. 3953-3958. 2009a.

Wang, X., Liu, Y., Hu, Z., Chen, Y., Liu, W. and Zhao, G. Degradation of methyl orange by composite photocatalysts nano-TiO₂ immobilized on activated carbons of different porosities, *J. Hazard. Mater.*, *169*, pp. 1061-1067. 2009b.

Wu, R.-J., Chen, C.-C., Chen, M.-H. and Lu, C.-S. Titanium dioxide-mediated heterogeneous photocatalytic degradation of terbufos: Parameter study and reaction pathways, *J. Hazard. Mater.*, *162*, pp. 945-953. 2009.

Wu, R.-J., Chen, C.-C., Lu, C.-S., Hsu, P.-Y. and Chen, M.-H. Phorate degradation by TiO₂ photocatalysis: Parameter and reaction pathway investigations, *Desalination*, *250*, pp. 869-875. 2010.

Xing, Z., Li, J., Wang, Q., Zhou, W., Tian, G., Pan, K., Tian, C., Zou, J. and Fu, H. A floating porous crystalline TiO₂ ceramic with enhanced photocatalytic performance for wastewater decontamination, *Eur. J. Inorg. Chem.*, *2013*, pp. 2411-2417. 2013.

Xu, Y. and Langford, C. H. Enhanced Photoactivity of a Titanium(IV) Oxide Supported on ZSM5 and Zeolite A at Low Coverage, *J. Chem. Phys.*, *99*, pp. 11501-11507. 1995.

Xu, Y. M. Photocatalytic degradation of environmental pollutants: The active species and reaction mechanism, *Progress in Chemistry*, *21*, pp. 524-533. 2009.

Xue, G., Liu, H., Chen, Q., Hills, C., Tyrer, M. and Innocent, F. Synergy between surface adsorption and photocatalysis during degradation of humic acid on TiO₂/activated carbon composites, *J. Hazard. Mater.*, *186*, pp. 765-772. 2011.

Yang, R. T. (2003). *Adsorbents : fundamentals and applications*. 410.

Yao, S., Li, J. and Shi, Z. Immobilization of TiO₂ nanoparticles on activated carbon fiber and its photodegradation performance for organic pollutants, *Particuology*, *8*, pp. 272-278. 2010.

Yap, P.-S. and Lim, T.-T. Solar regeneration of powdered activated carbon impregnated with visible-light responsive photocatalyst: Factors affecting performances and predictive model, *Water. Res.*, *46*, pp. 3054-3064. 2012.

Yaroshenko, A., Savos'kin, M., Mochalin, V. and Lazareva, N. New floating photocatalysts based on expanded graphite and anatase, *Russ. J. Appl. Chem.*, *80*, pp. 754-756. 2007.

Yoneyama, H. and Torimoto, T. Titanium dioxide/adsorbent hybrid photocatalysts for photodestruction of organic substances of dilute concentrations, *Catal. Today*, *58*, pp. 133-140. 2000.

Yu, C., Wu, R., Fu, Y., Dong, X. and Ma, H. (2012a) Preparation of polyaniline supported TiO₂ photocatalyst and its photocatalytic property. *Vol. 356-360* (pp. 524-528).

Yu, C. L., Wu, R. X., Fu, Y. H., Dong, X. L. and Ma, H. C. Preparation of polyaniline supported TiO₂ photocatalyst and its photocatalytic property, *Advanced Materials Research*, *356*, pp. 524-528. 2012b.

Yu, Y., Yu, J. C., Yu, J.-G., Kwok, Y.-C., Che, Y.-K., Zhao, J.-C., Ding, L., Ge, W.-K. and Wong, P.-K. Enhancement of photocatalytic activity of mesoporous TiO₂ by using carbon nanotubes, *Appl. Catal., A*, *289*, pp. 186-196. 2005.

Yuan, R., Guan, R., Liu, P. and Zheng, J. Photocatalytic treatment of wastewater from paper mill by TiO₂ loaded on activated carbon fibers, *Colloids Surf., A*, *293*, pp. 80-86. 2007.

Yuan, R., Zheng, J., Guan, R. and Zhao, Y. Surface characteristics and photocatalytic activity of TiO₂ loaded on activated carbon fibers, *Colloids Surf., A*, *254*, pp. 131-136. 2005.

Yuen, F. K. and Hameed, B. H. Recent developments in the preparation and regeneration of activated carbons by microwaves, *Adv. Colloid Interface Sci.*, *149*, pp. 19-27. 2009.

Yuranova, T., Mosteo, R., Bandara, J., Laub, D. and Kiwi, J. Self-cleaning cotton textiles surfaces modified by photoactive SiO₂/TiO₂ coating, *J. Mol. Catal. A: Chem.*, *244*, pp. 160-167. 2006.

Zaleska, A., Hupka, J., Wierowski, M. and Biziuk, M. Photocatalytic degradation of lindane, p,p'-DDT and methoxychlor in an aqueous environment, *Journal of Photochemistry and Photobiology A: Chemistry*, *135*, pp. 213-220. 2000.

Zhang, F.-S., Nriagu, J. O. and Itoh, H. Photocatalytic removal and recovery of mercury from water using TiO₂-modified sewage sludge carbon, *J. Photochem. Photobiol. A*, *167*, pp. 223-228. 2004.

Zhang, W., Zou, L. and Wang, L. Photocatalytic TiO₂/adsorbent nanocomposites prepared via wet chemical impregnation for wastewater treatment: A review, *Appl. Catal., A*, *371*, pp. 1-9. 2009.

Zhang, W., Zou, L. D. and Wang, L. Z. Visible-light assisted methylene blue (MB) removal by novel TiO₂/adsorbent nanocomposites, *Water Sci. Technol.*, *61*, pp. 2863-2871. 2010.

Zhang, X. and Lei, L. Effect of preparation methods on the structure and catalytic performance of TiO₂/AC photocatalysts, *J. Hazard. Mater.*, *153*, pp. 827-833. 2008.

Zhang, X., Sun, D. D., Li, G. and Wang, Y. Investigation of the roles of active oxygen species in photodegradation of azo dye AO7 in TiO₂ photocatalysis illuminated by microwave electrodeless lamp, *J. Photochem. Photobiol. A*, *199*, pp. 311-315. 2008.

Zhang, X., Zhou, M. and Lei, L. Enhancing the concentration of TiO₂ photocatalyst on the external surface of activated carbon by MOCVD, *Mater. Res. Bull.*, *40*, pp. 1899-1904. 2005.

Zhao, X., Lv, L., Pan, B., Zhang, W., Zhang, S. and Zhang, Q. Polymer-supported nanocomposites for environmental application: A review, *Chem. Eng. J.*, *170*, pp. 381-394. 2011.

Zhou, J., Cheng, Y. and Yu, J. Preparation and characterization of visible-light-driven plasmonic photocatalyst Ag/AgCl/TiO₂ nanocomposite thin films, *J. Photochem. Photobiol. A*, *223*, pp. 82-87. 2011.

Zhu, B. and Zou, L. Trapping and decomposing of color compounds from recycled water by TiO₂ coated activated carbon, *J. Environ. Manage.*, *90*, pp. 3217-3225. 2009.

Publications

Journal Paper:

Tu, W., Lin, Y.-P. and Bai, R. Removal of phenol in aqueous solutions by novel buoyant Composite photocatalysts and the kinetics, *Sep. Purif. Technol.*, 115, pp. 180-189. 2013.

Zhu, X., Tu, W., Wee, K.-H. and Bai, R. Effective and low fouling oil/water separation by a novel hollow fiber membrane with both hydrophilic and oleophobic surface properties, *J. Membr. Sci.*, 466, pp. 36-44. 2014.

Tu, W., Lin, Y.-P. and Bai, R. A buoyant composite photocatalysts prepared by a two-layered configuration and its enhanced performances in phenol removal from aqueous solutions. (in preparation).

Tu, W., Lin, Y.-P. and Bai, R. Phenol removal by two-layered buoyant composite photocatalyst and its in-situ regeneration. (in preparation)

Conference Presentation:

Wenting Tu, Yi-Pin Lin, Renbi Bai, “Development of Buoyant Composite Photocatalysts for the Removal of Phenol in Saline Media and the Kinetic Study”, presented at the Photocatalytic and Advanced Oxidation Technologies for the Treatment of Water, Air, Soil and Surfaces, Gdansk University of Technology, July 4-8, 2011